INTEGRATING SPATIAL AND TEMPORAL DISTRIBUTION OF SNOW DYNAMICS INTO MULE DEER WINTER RANGE HABITAT SELECTION

by

Zoltán K. Mityók

B.Sc., The University of British Columbia, 2016

A THESIS SUBMITTED IN PARTIAL FULFILLMENT OF

THE REQUIREMENTS FOR THE DEGREE OF

MASTER OF SCIENCE

in

THE FACULTY OF GRADUATE AND POSTDOCTORAL STUDIES

(Forestry)

THE UNIVERSITY OF BRITISH COLUMBIA

(Vancouver)

March 2019

The following individuals certify that they have read, and recommend to the Faculty of Graduate and Postdoctoral Studies for acceptance, a thesis/dissertation entitled:

Integrating spatial and temporal distribution of snow dynamics into mule deer winter range habitat selection

submitted by Zoltán K. Mityók in partial fulfillment of the requirements for

the degree of Master of Science

in Forestry

Examining Committee:

Dr. Nicholas C. Coops
Supervisor

Dr. Cole Burton
Supervisory Committee Member

Dr. Sue Senger
Supervisory Committee Member

Dr. Tara Martin
Additional Examiner

Additional Supervisory Committee Members:

Supervisory Committee Member

Supervisory Committee Member

Abstract

Many migratory terrestrial mammal species within North America rely on particular habitat characteristics to provide shelter from snow cover in order to assure inter-annual survivorship. Mule deer (*Odocoileus hemionus*) in particular, are reported to be in decline across South-central British Columbia, likely due to reductions in adequate winter range habitat, limiting the degree of shelter that can be utilized to avoid snow and low temperatures. This thesis sought to evaluate predictions from multiple step selection functions (SSF) by considering both mule deer responses to the timing and distribution of snow cover as well as forest stand attributes including canopy cover and forest edge. In order to generate such SSFs, increasing spatial and temporal information regarding snow timing and distribution across the landscape was required. Previously however, predictions of fine-scale snow dynamics across the landscape suitable for analysis with hourly telemetry data were limited. Therefore, the first component of this thesis was to utilize the strengths of both medium spatial resolution and high temporal resolution satellite imagery and develop a data fusion algorithm to predict snow cover dynamics at a 30m spatial resolution daily, since 2000 using Landsat data with MODIS (Moderate Resolution Imaging Spectroradiometer) snow map data as inputs. The final fused snow map product (MODSAT-NDSI) achieved an overall accuracy of 90% using 33 validation test sites, which included government snow pillow data and an installed camera network. Environmental covariates from MODSAT-NDSI snow maps and 77 deer's GPS telemetry data in the mule deer SSFs were used to produce predictions of relative probability of use for population-level estimates of habitat selection patterns. The top-ranked SSF models (based on AIC) indicated that mule deer avoided areas with greater, and more persistent, snow cover, and selected areas closer to forest edge. Key thesis outcomes include generated snow cover maps that can be updated and utilized in further studies, a data fusion algorithm that can be replicated for other remote sensing metrics, and habitat selection models that may help to inform future mule deer habitat management.

Lay Summary

Snow cover influences the natural environment in many ways. For example, melt water from snow affects flood timing, and snow pack protects the Earth from solar radiation. Snow cover also affects the health of many wildlife populations. Previous studies indicate that snow cover affects the health of mule deer (*Odocoileus hemionus*), that migrate to winter range habitats in order to survive the winter. To explore this relationship, this thesis develops and then uses new snow cover maps to predict habitat types selected by deer. The research found that mule deer avoid areas with early snowfall, late snowmelt, and remain close to the forest edge during winter. Future applications include using the new snow maps in climate change research, and using the habitat predictions to help inform land management.

Preface

My supervisory committee and I developed the objectives of this dissertation through a series of discussions. The research presented in this dissertation has been published or submitted to scientific journals for publication as listed below. For the two manuscripts, I, with support from my supervisory committee, developed the specific approaches to data processing and analysis, interpreted the results, and wrote and prepared the manuscripts for publication. Co-authors provided critical feedback and ideas for each manuscript and in certain cases provided important data inputs.

Chapter 2: Zoltán K. Mityók, Douglas K. Bolton, Nicholas C. Coops, Ethan E. Berman & Sue Senger (2018): Snow cover mapped daily at 30 meters resolution using a fusion of multitemporal MODIS NDSI data and Landsat surface reflectance, Canadian Journal of Remote Sensing, DOI: 10.1080/07038992.2018.1538775

Chapter 3: Zoltán K. Mityók **,** Nicholas C. Coops, Sue Senger, Cole Burton, Txomin Hermosilla, Sean P. Kearney and Brandon Prehn. (2019). Integrating spatial and temporal distribution of snow dynamics into mule deer winter range habitat selection. Submitted.

I have also contributed to additional snow cover research during my thesis which informed the developed approached, warranting co-authorship:

Berman, E. E., Bolton, D. K., Coops, N. C., Mityok, Z. K., Stenhouse, G. B., & Moore, R. D. (2018). Daily estimates of Landsat fractional snow cover driven by MODIS and dynamic time-warping. Remote Sensing of Environment, 216, 635-646.

Table of Contents

List of Tables

List of Figures

List of Abbreviations

AAC – annually-derived accumulation/winter start date

AIC – Akaike Information Criterion

ASP – Automated Snow Pillow

AveACC – time-averaged winter start/accumulation date

AveMELT – time-averaged winter end/melt date

AveSUM – time-averaged total number of snow-covered days

AveSW – time-averaged snow cover rank

AveVAR – time-averaged snow pack variability index

BBMM – Brownian Bridge Movement Model

CC – Canopy Cover (as a percentage)

CWD – Chronic Wasting Disease

DEM – Digital Elevation Model

DFE – Distance to Forest Edge

DOY – Day of Year

ETM – Enhanced Thematic Mapper

fSCA – Fractional Snow Covered Area

GIS – Geographic Information Systems

GLM – Generalised Linear Models

GPS – Global Positioning System

IRSS- Integrated Remote Sensing Studio

LIDAR – Light Detection and Ranging

MDWR – Mule Deer Winter Range

MELT – annually-derived winter end/melt date

MODIS – Moderate Resolution Imaging Spectroradiometer

MODSCAG – MODIS Snow-Covered Area and Grain size

NDSI – Normalized Difference Snow Index

NDVI – Normalized Difference Vegetation Index

NIR – Near Infrared

NTV – Non-Treed Vegetation

OLI – Operational Land Imager

RMSE – Root Mean Squared Error

RSA – Resource Selection Analysis

RSF – Resource Selection Function

SDM – Species Distribution Models

SGS- St'át'imc Government Services

SSA – Step Selection Analysis

SSF – Step Selection Function

STARFM – Spatial and Temporal Adaptive Reflectance Fusion Models

SUM – annually-derived total number of snow-covered days

SW – annually-derived snow cover rank

SWI – Snow Water Equivalent

SWIR – Short-wave Infrared

TEK – Traditional Ecological Knowledge

TM – Thematic Mapper

TMSCAG – Thematic Mapper Snow-Covered Area and Grain Size

UBC – University of British Columbia

UD – Utilization Distribution

USGS – United States Geological Survey

VAR – annually-derived snow pack variability index

VHF – Very High Frequency

Acknowledgements

Funding for this research was generously provided by MITACS, and St'át'imc Government Services (SGS) facilitated this project through many collaborative efforts, which included providing equipment, feedback, and assistance in the field (for more information, visit http://statimc.ca/programs/sgs-environment/). Lenora Starr (SGS), Darwyn John (SGS), Denise Antione (SGS), and Nora Billy (SGS) have particularly helped a great deal in this project through feedback, fieldwork, and guided tours that allowed me to familiarize myself with the worlds and environments that the mule deer inhabit. SGS staff were also the most welcoming in terms of inclusivity, going so far as to include me in ceremonies and provide personal tours through historical and artistic museums that have allowed me to learn much about their culture. For these experiences and more, I am eternally grateful. Dr. Sue Senger offered much support throughout the project with honest and real advice, opportunities to network, and help with logistics. She has also become an admirable friend whom I look up to and whom I could share personal hopes, dreams and disappointments. Dr. Cole Burton (UBC) has also been an advisor and supporter of this project, offering invaluable guidance and providing patient and thoughtful answers to any questions I had for him. Scott Taylor is the Lillooet Base Manager and pilot for Black Comb Helicopters (blackcombhelicopters.com), whose assistance, enthusiasm and positivity has made this project possible by accessing remote locations for validation sites. I want to thank everyone in the Integrated Remote Sensing Studio (IRSS) for being the best friends/collaborators/support group that I have ever had the pleasure of working with side-by-side. I recognize and thank Matt Manual, Lillooet Tribal Council, for his passion and for the access to the GPS collar data for Mule deer. I would like to thank all of the individuals who allowed cameras to be installed on their private properties: Linda and Tom Hancock, Eckhard and Deanne Zeidler, and Jacquie and Verne Rasmussen. And finally, I thank Dr. Nicholas Coops. Even after more than two years I am still shocked and amazed and eternally thankful for that fateful email that I received from you seemingly out of nowhere. It was an email that brought with it an incredible opportunity and a personal dream of mine that I am forever grateful for. Thank you so much for believing in and forever encouraging me, through both the difficult and incredibly fun times. Thank you for being who you are, which is someone who managed to father a lab environment that is loving, connected and supportive of each other.

Dedication

To my family, they make me so proud and I hope to make them feel the same way towards me. Thank you dad, mom, (Zoltán S.R. and Erzsebet Mityók) my brothers Michael and Andrew Mityók, and my closest friend Attila Mityók, for all of the help and support that you have given me during my life, including these last two and a half years as a graduate student.

And to my love, Priyanka Joshi. Your love has been the source of my strength, determination and happiness. Thank you for being exactly as you are.

Chapter 1: Introduction

1.1 Background and motivation

Both the public, and land managers, are increasingly recognizing the importance of ecosystem services in regional and local land management plans (Bennett, Peterson, & Gordon, 2009; B. Fisher, Turner, & Morling, 2009). However, much of the provisional, supporting, regulating and cultural services are globally declining in terms of abundance and quality (Assembly, 2015; Carpenter et al., 2006; Foley et al., 2005; Sachs & Reid, 2006). Whether an anthropocentric or biocentric philosophy is considered, the maintenance and/or recovery of these goods and services is critical to our survival. Ecology and wildlife research has helped drive the impetus to conserve not only material goods and services, but also the systems and organisms that are fundamentally connected with those goods and services (Collins et al., 2011; Gustafsson, 2013; Haila, 1999).

Land managers and the public have the responsibility to uphold the United Nations Sustainable Development Goals, which include taking urgent action to combat climate change, and to protect, restore and promote sustainable use of terrestrial ecosystems while halting biodiversity loss (Assembly, 2015). However, habitat loss and degradation continues to occur due to industrial development, resource extraction, and climate change, complicating efforts to recover wildlife populations (Arthur, Manly, Mcdonald, & Garner, 1996; Bergman, Bishop, Freddy, White, & Doherty, 2014; Beschta et al., 2013; Boyce, Meyer, & Irwin, 1994; Mladenoff & Sickley, 1998; Sawyer, Nielson, Lindzey, & Mcdonald, 2006).

Migratory ungulate species have been impacted by habitat loss and climate change as well, and land managers have particular difficulty managing for these mobile populations that change and adapt behavior according to altered environments. Characteristically, migration is the relatively long-distance movement of individuals, usually on a seasonal basis, between regions that are optimized for seasonal needs (Dingle & Drake, 2007). The regions may be alternatively habitable and inhabitable – as in the case of alpine meadows that become snow packed in winter – or otherwise less conducive in particular months to providing quality shelter and food. Migration is a consequence of mobile populations, and is required for certain organism to complete their life cycle (Dingle and Drake, 2007). Changes in temperature and land cover can alter environmental cues – and therefore subsequent migratory ungulate responses to those cues – or may be occurring at such a rate as to prevent adaptation by creating a lag between new environmental cues and the affected species' responses. Animal migration therefore is a significant ecological dynamic, and an understanding of migration patterns is a critical component in many wildlife studies (Bohrer, Beck, Ngene, Skidmore, & Douglas-Hamilton, 2014; Dodge et al., 2013; Gavashelishvili, McGrady, Ghasabian, & Bildstein, 2012; Gillespie, 2001; Jonsen, Myers, & Flemming, 2003; Moore, 2011; Puckett, Delaney, & Antonios, 2006; Schick et al., 2013).

Industrial development and other human-caused disturbances have impacted one migratory ungulate species in particular within southern interior British Columbia: the mule deer (*Odocoileus hemionus*) (Armleder, Waterhouse, Keisker, & Dawson, 1994; Poole & Wright, 2010; Procter, 2013). The status of mule deer across their native but scattered habitat range throughout western North America is of least concern according to the International Union for the Conservation of Nature (IUCN, 2016). However, a large body of literature has grown to include many cases where particular mule deer populations have declined due to several context-dependent factors, including habitat loss, overhunting, and predation (Ballard et al., 2001; Innes, 2013). This thesis was motivated by the perceived declines in mule deer populations that have been documented in British Columbia as well as by several other studies, from Montana to California, and Alberta to British Columbia (Anthony, 1977; Cullingham et al., 2011; Mackie, 1970; Pierce et al., 2009; Poole & Wright, 2010; Sawyer et al., 2006). In these studies, habitat loss was most often found to be the likely cause of such population declines. In addition, chronic wasting disease (CWD), which continues to increase mule deer and other ungulate species' mortality throughout western North America (Nobert, Merrill, Pybus, Bollinger, & Hwang, 2016; Russell, Gude, Anderson, & Ramsey, 2015; Salazar, Waldner, Stookey, & Bollinger, 2016) is becoming more prevalent. The variation between particular populations' reductions in terms of rate and cause is the result of the specie's far-reaching but often isolated and scattered dispersal and occupancy, where populations are separated by major desert regions including the Sonoran desert and cold deserts of northeastern Arizona (Innes, 2013). For example, desert mule deer populations within their southern-most range in central Mexico are likely affected by drought (Olivas-Sánchez, Vital-García, Flores-Margez, Mora-Covarrubias, & Clemente-Sánchez, 2018). Concurrently, recent declines in mule deer populations within Southern Interior British Columbia are likely due to habitat loss, eliciting news coverage and the large-scale B.C. Interior Mule Deer Project ("BCWF- Southern Interior Mule Deer Project," n.d.; Lowe, 2018; Zeman, n.d.). Mule deer also occupy tundra environments within Alaska, the great plains within northern United States and southern Canada, and the Canadian boreal forest where quaking aspen (*Populus tremuloides*) parkland, with many populations remaining stable or increasing (Innes, 2013).

Within my study area, St’át’imc First Nations communities and their government organization St’át’imc Government Services (SGS) greatly influenced and motivated this thesis research due to their concerns for particular mule deer populations within their territory. Habitat loss due to flooding, logging, road development and fire has been attributed to be the cause of observed and notable population declines (Senger, Hamiton, & McLellan, 2008). St’át’imc concern for many different wildlife species (including grizzly bear, ungulates, and fish) resulted in this thesis’ final study area boundary (see Chapter 2, section 2.2), which reflects a buffered version of the threatened grizzly bear population units for southwestern British Columbia (Ministry of Environment, 2012).

Adequate quality and availability of mule deer winter range (MDWR) habitat has been found to be a particularly critical factor in ungulate wildlife survivorship (Doerr, Degayner, & Ith, 2005; Poole & Wright, 2010), and therefore may be one of the most critical habitat types to conserve in order to facilitate population maintenance or recovery. MDWR is characterized by areas occupied by mule deer during the winter in order to obtain food and shelter. It’s policy definition in BC considers those areas that contain the winter habitat requirements of mule deer, and special management practices must be conducted in order to maintain those habitat requirements (Government of British Columbia, 2004). Mule deer thrive in higher elevations during spring and summer, where continental weather patterns ensure warm temperatures even at these higher elevations. Vegetation green up during these periods then allows for plentiful forage. However, previous studies indicate that snow processes have a direct effect on mule deer species survivorship as they relocate to winter range areas in order to survive the winter (Armleder et al., 1994; Doerr et al., 2005; Gilbert, Hundertmark, Person, Lindberg, & Boyce, 2017; Parker, Robbins, & Hanley, 1984). Snow cover within topographically variable landscapes force migratory species to lower elevations, limiting the range over which forage can be located. Simultaneously, greater energy is expended via locomotion through deep snowpack that can result in starvation and exhaustion (Parker et al., 1984), or prevent deer from escaping predators. Therefore, quality MDWR habitat would provide enough sustenance, cover from predators, and thermal cover from the cold while allowing for low-energy-cost movement. In order to ensure the continued survival of a species that provides humans with revenue, protein, and cultural identity from hiking, hunting and other activities, a greater understanding of winter range habitat selection and snow cover dynamics effects on selection is vital.

Beyond its effects on MDWR habitat selection, snow dynamics are an important determinant in many environmental, meteorological and ecological systems (Liston, 1999). The importance of modelling snow dynamics is well known, due in part to the onset of global climate change (Onstott, 1997). Climate change research continues to monitor how anthropogenic activities may affect environmental processes of varying scale (Assembly, 2015) while the timing of spring habitat release and location of snow refugia may be more accurately predicted using snow maps for Grizzly bear *(Ursus arctos ssp.)* and wolverine *(Gulo gulo)* studies (Kelly and Reynolds, 2015; Pigeon, Stenhouse, & Côté, 2016). Water flow from snow melt can be derived from snow cover maps, and may better inform local hydro facilities and fish management (Nolin, 2010). Snow processes have thus been shown to also improve our understanding of wildlife populations when snow cover is mapped at the appropriate temporal and spatial scale (Beniston & Stoffel, 2016; Kelly & Reynolds, 2015; Manning & Garton, 2012). Therefore, mapping snow distribution patterns through time in order to research MDWR habitat selection may contribute to a number of future research fields and topics.

1.2 Remote sensing of snow

MODerate-resolution Imaging Spectroradiometer (MODIS) and Landsat satellite sensors are widely used by Earth scientists to map, monitor and geospatially analyze terrestrial, atmospheric and oceanic processes. MODIS captures daily imagery at 250, 500 and 1000 m spatial resolution while Landsat sensors generates 30 m by 30 m imagery with a revisit time of 16 days. The highly variable and practical use of datasets derived from these satellite instruments have generated great interest in procedures to download, distribute, further process and analyze these imagery datasets (Barnes et al., 2003; Beck, Atzberger, Høgda, Johansen, & Skidmore, 2006; Hansen et al., 2003; Justice et al., 2002).

The monitoring of snow cover and albedo has helped researchers to obtain information on the extent and timing of snow cover within remote, expansive and hard-to-reach areas (Crawford, 2015; Czyzowska-Wisniewski, van Leeuwen, Hirschboeck, Marsh, & Wisniewski, 2015; Nolin, 2011; Selkowitz & Forster, 2015). Snow cover maps and Geographic Information System (GIS) layers produced from MODIS and Landsat sensors have undergone various evolutions in light of their conceptual and mathematical bases. The Normalized Difference Snow Index (NDSI) can be calculated from data from both sensors to estimate the fractional Snow Covered Area (fSCA), where an fSCA value between 0 and 100 indicates the percentage of the pixel area covered by snow. NDSI utilizes particular bandwidths of the electromagnetic spectrum, which have been designed to isolate various spectral signals linked to particular land cover surface types or features (Hall et al., 1998). Differences in NDSI reflectivity are known to change as a function of the age of snow (Hall & Martinec, 1985; Salomonson & Appel, 2004). Overtime, snow accumulates moisture, measured as the snow water equivalent (SWE). Before melting occurs, the moisture in snow alters the crystalline structure and thus greater scattering of Near Infrared (NIR) reflectance occurs, resulting in an attenuated response detected by the satellite sensor (Hall & Riggs, 2007).

One of the current versions of daily snow cover products available is MODIS Snow-Covered Area and Grain size (MODSCAG), and at longer time step intervals the Landsat's Thematic Mapper Snow-Covered Area and Grain size (TMSCAG). These snow detection algorithms were developed as an alternative to NDSI whereby spectral mixture analysis is used to calculate fSCA (Painter et al., 2009; Rittger et al., 2013). Both MODSCAG and TMSCAG apply spectral mixture analysis by incorporating the pure surface reflectance signatures of snow which change as a function of the size of snow grains. These reflectance signatures are called endmembers, obtained from extensive imaging spectrometer libraries. Along with the endmembers of rock, soil, vegetation and ice, the algorithm can detect the percentage of snow cover present within a single pixel by linearly weighting the respective proportion of each endmembers reflectance (Nolin, 2010). The algorithm accounts for the spatial variability of mountainous terrain by solving for grain size in conjunction with fSCA. Solving for both parameters allows for differing slopes and aspects and their effect on snow grain size to alter the spectral reflectance of snow, resulting in a spectral mixture analysis tailored to each pixel undergoing the analysis (Painter el al., 2009).

TMSCAG has the appropriate spatial resolution, but can only track changes in snow cover distribution in 16-day time step intervals. These intervals are often greatly extended due to cloud cover severely reducing the quality of images. Such large gaps in temporal resolution prevent the monitoring of snow conditions during critical time periods where snow cover and depth can change daily (Garvelmann et al., 2013). Such critical periods affecting the timing of mule deer migration include melt and green up phases that elicit winter to spring migration, as well as initial snowfall periods that initiate the transition from rut to winter season migration (Poole and Wright, 2010).

Although the MODSCAG and TMSCAG algorithms have been shown to be better at capturing the spatial heterogeneity of snow cover compared to NDSI (Rittger et al., 2009), MODSCAG is still only able to estimate fSCA for a 500 m by 500 m area. Mule deer movement occurs at much finer spatial scales than 500 m, which has necessitated the generation of 30 m by 30 m landcover data sets (Gilbert et al., 2017). Even still, the research area utilized by Gilbert et al. (2017) in Southeast Alaska is much less heterogeneous in terms of topography and elevation compared to the coastal mountain range of British Columbia, where this thesis' research takes place (Poole and Wright, 2010). Elevation only increases up to approximately 1000 m in the Alaskan study, with large stretches of beach and coastline while the Coast Mountains within southern British Columbia reach elevations of nearly 3000 meters; large extents within the south-central and south-western BC having severely scoured terrain and river systems.

1.2.1 Remote sensing data fusion

A possible solution to the aforementioned trade-offs between temporal and spatial resolution is the use of data fusion, specifically the consolidation of data from a number of satellites with other geospatial datasets such as climate and terrain. In this thesis, I address this disparity between spatial and temporal resolution by applying a novel data fusion technique for a new region, since wildlife telemetry research often requires environmental data sets to be both spatially and temporally fine-scaled.

In previous studies, Terra and Aqua's MODIS have been data fused with Landsat's Thematic Mapper (TM), Enhanced Thematic Mapper Plus (ETM+), and Operational Land Imager (OLI) (Gao et al., 2006a; Hilker et al., 2009; Hwang et al., 2011; Walker et al., 2012; Wu et al., 2012). Data from sensors of varying spatial and temporal resolution require novel algorithms to be developed in order to concurrently utilize the strengths of both, known as data fusion techniques. For example, the MODIS sensor has a low spatial resolution with a single pixel covering an area of 250,000 m^2 (Hall and Riggs, 2016) whereas Landsat detects moderate spatial detail of 900 m^2, accounting for much more of the heterogeneity within a landscape. The disadvantage of high spatial resolution relates to the tradeoff between spatial versus temporal resolution (Coops et al., 2012; Gao et al., 2006b). Landsat satellites orbit sun-synchronously, scanning the entirety of the Earth every 16 days, resulting in a revisit time once during this period. Analysis or monitoring of ecological events and changes that occur more frequently than every 16 days are thereby greatly hindered by such low temporal density of Landsat (Coops et al., 2012). Alternatively, MODIS has a daily repeat coverage but less detail.

A number of research projects that monitor land cover change at a temporal resolution greater than every 16 days have incorporated MODIS or other coarse spatial resolution instruments into their research. There are differing approaches to data fusion in the literature many of which are focused on phenology (Hilker et al., 2009). Phenology concerns the study of the relationship between recurring biotic and abiotic events (Lieth, 2013) which include the budding and eventual senescing of deciduous foliage (Fisher, Mustard, & Vadeboncoeur, 2006) and by this definition, would also include snow events in relation to wildlife habitat selection. The technique developed by Fisher et al. (2006) and adapted by others (Melaas, Friedl, & Zhu, 2013; Nijland, Bolton, Coops, & Stenhouse, 2016) uses the entire Landsat record to generate a curve-fitting formula segmented into a 2-part sigmoid curve, charting the average season length and reflective magnitude of all Landsat observations via pixel-by-pixel based analysis. For snow, the first part of this sigmoid curve represents the rise of snow reflectance at the onset of the winter season, while the second sigmoid signals the decrease in snow cover reflectance towards the end of the season.

Initially, this averaged phenology curve technique was able to accurately describe phenological variability only within relatively homogenous deciduous forest (Fisher et al., 2006). Interannual variability was addressed by weighting anomalous land surface temperatures while considering a time lag between the curve-fitted average and a specific year's uni-modal green-up and/or senescing signal. Nijland et al., (2016) adapted the technique to mixed and coniferous forest stands, while also building on validation techniques utilizing phenocamera networks within their respective study area. The yearly adjusted phase shift of the averaged phenology curves produced good agreement with day of the year (DOY) environmental cues observed from plot based camera networks, especially green up with a RMSE of 7 days (Nijland et al., 2016).

1.2.2 Field validation and snow depth measurement techniques

Conditions at the plot level such as snow depth and/or snow presence/absence using near-surface remote sensing generates detailed and useful information, but such datasets have been difficult to apply to heterogeneous landscapes across broad scales (Casey & Kelly, 2010; Marty & Meister, 2012; Juraj Parajka, Haas, Kirnbauer, Jansa, & Blöschl, 2012b; Ryan, Doesken, & Fassnacht, 2008; Singh et al., 2011; Varhola, Coops, Weiler, & Moore, 2010). Snow stakes with measured markings indicating depth along have been a cost effective and reliable method of monitoring snow cover (Marty and Meister, 2012), while snow depth ultra-sonic sensors and radar are able to log highly accurate measurements, as much as within 1 cm or less (Ryan and Doesken, 2008; Singh et al., 2011).

Cameras determine snow, no-snow conditions visually, rather than through a calibrated measure of distance as in the case of sensors, which have a known ground level, and then emit an active pulse. Depth is determined by the time it takes for the pulse to return to the sensor. The lack of visual confirmation from sensors can be prone to error once snow cover is only 1 or 2 centimeters thick (Ryan and Doesken, 2008). Cost and maintenance of various snow depth sensors has additionally limited the wide spread use of the technology (Varhola et al., 2010). The stake method allows for the monitoring of depth at a particular point in the foreground while also potentially observing spatio-temporal changes in snow cover over the greater landscape in the background (Parajka et al., 2012a).

The study by Gilbert et al. (2017) used a combination of snow stakes and temperature loggers to derive daily averages of snow depth across the northern portion of Prince of Wales Island, Southeast Alaska. This study was able to interpolate snow depth across the region using inverse distance weighting across field station measurements, followed by raster-based, cell-by-cell regressions of the 30 m by 30 m snow depth raster against a vegetation species composition raster dataset.

In situ monitoring of snow cover using camera traps may readily distinguish snow from snow free conditions. However, the current literature highlight difficulties in measuring snow depth using near-surface remote sensing and then applying measurements to broader scales (Casey and Kelly; 2010; Marty and Meister, 2012; Parajka et al., 2012a; Ryan and Doesken, 2008; Singh et al., 2011). Therefore, snow cover and snow depth continues to be a challenge to monitor and represents an important topic of research in remote sensing.

1.3 Telemetry tracking of animal movement

Remote sensing technologies can provide useful data to better understand the effects of climate change and habitat loss on mule deer migration and habitat selection. These technologies can reduce costs by remotely collecting large amounts of quantifiable data over larger spatial scales compared to *in situ* observations, with ground-based data collection often requiring both more time and labor (Neumann et al., 2015). Remote sensing allows for greater detail and insight to be gained from individual movement patterns in remote/isolated areas, as well as the environmental variables influencing migration such as primary productivity or snow cover and depth (Gilbert et al., 2017; Neumann et al., 2015).

Concurrent with advances in remote sensing technologies, animal tracking has progressed from coarse Doppler radar technologies – with greatly attenuated signals within moist environments in the 1950s – to very high frequency (VHF) radio tracking, which allowed for periodic relocation of animals. Global positioning systems (GPS) have subsequently been developed for animal tracking that specifically allows for the most consistent collection of location data with the highest volumes through automated tracking (Zschille, Stier, & Roth, 2008), allowing for nearly limitless access to observing animal locations. Remote sensing technologies are therefore able to track animal movements while simultaneously informing researchers of the state of, and the pressures on landscape biodiversity at multiple scales (Pettorelli et al., 2014). Statistically verifiable relationships between animal movements and multiple environmental factors derived from remote sensing products can act as proxies for animal movements when extrapolation is necessary for wildlife management decisions. Some limitations of GPS tracking include the fact that it remains difficult to determine what activity an individual was performing when relocated (Macdonald, 1978). In addition, older VHF telemetry data has shown to be less reliable compared to satellite data (Johansson, Simms, & McCarthy, 2016), while canopy cover and limited number of satellites continue to affect the accuracy of satellite data (Moen, Pastor, & Cohen, 1997)

1.4 Modelling migration and habitat selection

The final component linking environmental observations with GPS location data is the analytical techniques and species distribution models (SDMs) used to describe relationships between organisms and their environment. Such an endeavor has become increasingly important following the proliferation of new statistical methods, developments in information technology and rapid advances in GIS and remote sensing (Elith & Leathwick, 2009; Lele, Merrill, Keim, & Boyce, 2013). After the gathering of data rich information such as remote sensing imagery for an entire region, these advances have translated into the increased use of model-based interpolation in order to map suitable habitat in unsampled sites for conservation and land management (Elith and Leathwick, 2009). Austin (2002) as well as Elith and Leathwick (2009) noted the need for statistical models to continually undergo scrutiny and increased sophistication in order to utilize ecological concepts and the growing volume of data available to modelers. While traditional SDMs were more static and limited to what field data can be obtained, many current modelling methods account for potentially erroneous linear assumptions, spatial autocorrelation and/or lack of ecological concepts and proximal indicators. Such models include resource selection functions (RSFs), generalised linear models (GLMs) and step-selection functions (SSFs). SSF and RSF are associated with approaches of SDM termed step selection analysis (SSA) and resource selection analysis (RSA) respectively (Avgar, Potts, Lewis, & Boyce, 2016).

SDMs which are explicitly proportional to the probability of use of a resource by a species are defined as RSFs (Boyce and McDonald, 1999; Lele et al., 2013). RSFs can account for some of the disparities mentioned by Austin (2002) by quantitatively characterizing resource use and by being intrinsically accommodating of spatial structure (Boyce and McDonald, 1999). Such models have been adapted to make strong predictions of polar bear *(Ursus maritimus)* seasonal habitat selection based on pack ice concentration and the variables affecting its temporal and spatial distribution (Arthur et al., 1996). Spotted owl *(Strix occidentalis caurina)* nest site distributions were accurately mapped according to old growth habitat (Boyce et al., 1994; Manly et al., 2007) and timber wolf *(Canis lupus)* populations were projected using prey density estimates and several other variables within the Great Lakes and New England Regions of the United States (Mladenoff et al., 1998).

The SSF is another type of RSF that focuses on steps, or the consecutive relocations from telemetry points, and is a method of investigating the correlation between biotic and abiotic processes as well (Thurfjell, Ciuti, & Boyce, 2014). Each GPS point is denoted as a location, while every interval between locations is a step, and use is associated with the steps and locations observed by the individual. Available steps and locations are determined by generating any number of random steps using animal movement patterns such as the distance between locations, the angle of trajectory from one step to the next, and/or speed. RSF can then be applied in a conditional logistic regression model comparing either used and available steps or used versus available locations in order to generate utilization distributions (UDs).

The Brownian bridge movement model (BBMM) developed by Horne et al. (2007) is another model developed specifically for the application of GPS relocation data. The technique explicitly incorporates the time interval between relocation points, thereby permitting speed to be implemented as a parameter in predictive modelling. This has been proven to be important in stochastic modelling since it predicts that slower organisms travelling greater distances will have more uncertain (i.e., flatter) utilization distributions (Horne, Garton, Krone, & Lewis, 2007) compared to faster organisms travelling shorter distances. The added parameter and resulting refinement in the model offers the potential to utilize BBMM probabilities in regressions against any number of environmental covariates to build relationships between movements/habitat range and abiotic characteristics (Rickbeil, Coops, & Adamczewski, 2015).

Specific to mule deer, modelling and statistical techniques have ranged in approaches. They have included selectivity indices to determine mule deer food selection within a home range (Doerr et al., 2005), resource use and availability analysis (Armleder et al., 1994; Byers, Steinhorst, & Krausman, 1984), and fixed-kernel density estimators that utilize observations from neighboring locations to generate filters representing the probability density of wildlife observations (Seaman & Powell, 1996). In the aforementioned study conducted by Gilbert et al. (2017), SSFs as well as an ecological understanding of mule deer calorie intake requirements were used to identify used and available habitat locations. RSF was then adapted to represent the relative probability of a location being selected using a 2-step modelling approach utilizing conditional logistic and mixed-effects regressions. The work by Gilbert et al. (2017) is an important step in mule deer modelling as snow depth became a time-varying predictor variable that allowed for dynamic geographic factors to influence models that may have otherwise remained static.

1.5 Research objectives

Remote sensing data was utilized in this research in order to generate spatially explicit information regarding spatial and temporal snow distribution. Such information was generated at the ecologically relevant spatial and temporal scales (30 m x 30 m, daily to weekly temporal resolution). While snow dynamics has been monitored and well researched at the global scale using sensors of low/coarse spatial resolution, local and regional snow dynamic assessment has proven to be more difficult due to trade-offs between sensors' spatial and temporal resolution (Coops et al., 2012; Gao et al., 2006b; Kelly and Reynolds, 2015; Onstott, 1997).

The aim of my MSc research is to integrate spatial and temporal dynamics of snow cover data over an 18-year period with GPS telemetry data of mule deer locations from 2007 – 2014 (Mitchell and Wilton, 2012; Poole and Wright, 2010; Procter and Iredale, 2013). In doing so, I aim to better predict where priority winter range conservation areas may be located, based on particular habitat characteristics including snow cover. To do so, the most current remote sensing technologies were used to map snow cover timing and distribution over an 18-year period in order to analyze snow cover patterns and dynamics. I used previously acquired radio collar and GPS data from over 80 mule deer from three different studies to calculate step selection functions related to different seasons of the year. Finally, the relative probability of selection for winter range areas are analyzed against snow cover maps according to temporal and spatial snow dynamics and resource selectivity analysis, an approach similarly conducted by Gilbert et al. (2017).

The overall thesis objective is to answer the question:

How can the understanding of mule deer winter habitat use be improved by remotely sensed snow cover dynamics?

1) How can snow cover temporal and spatial dynamics be mapped using a combination of satellite remote sensing datasets to produce information relevant for wildlife studies?

2) Will mule deer preferentially select locations with decreased snow cover and of greater canopy interception (i.e., areas providing shelter and forage)?

1.6 Dissertation overview

The format of this dissertation is four chapters: this introduction, two research chapters which address the main research objectives and a final concluding chapter.

Chapter 2 describes the novel algorithm for data fusion and assesses the accuracy of the snow maps using field validation data and is published in Canadian Journal of Remote Sensing.

Chapter 3 is the submitted article which utilizes the newly produced snow map data along with other core covariate data sets to generate step selection function models of mule deer movement and habitat selection using GPS telemetry data from previous studies. This paper is submitted to Journal of Applied Ecology.

In Chapter 4, conclusions are drawn which highlight the main findings from each of the two aforementioned chapters and discuss insights gained in this dissertation. I also detail limitations of the thesis project as a whole and consider directions for future research.

Chapter 2: How can snow cover temporal and spatial dynamics be mapped using a combination of satellite remote sensing datasets to produce information relevant for wildlife studies?

2.1 Introduction

The timing and distribution of snow cover through accumulation and melt cycles impacts many of the Earth's biotic and abiotic processes, and are a vital determinant in hydrologic systems, radiation balances, ecological functioning and global climate change (Cohen, Koshida, & Mortsch, 2015; Liston, 1999; Moore, 2011; Onstott, 1997). Snow cover extent, and persistence, have become reliable indicators of shifting climate trends (Lemke et al., 2007; Qin, Liu, & Li, 2006; Shuai, Masek, Gao, & Schaaf, 2011; Whetton, Haylock, & Galloway, 1996) while the modelling and mapping of snow distribution patterns through time can be used to estimate water flow during spring melt seasons (Nolin, 2011). Such information often derived from snow models helps to better inform local hydrological facilities, fish management, and sea ice research (Jost & Weber, 2012; Khadka et al., 2017; Parajka & Blöschl, 2008; Sproles, Roth, & Nolin, 2017; Wegmann et al., 2015). Beyond fresh water systems of fisheries and dams, snow cover also economically impacts communities that require road access during winter, as well as agricultural activities in northern latitude regions (Bokhorst et al., 2016). In addition, there is a growing urgency to understand snow processes and its effects on terrestrial wildlife populations at ecologically relevant temporal and spatial scales (Beniston & Stoffel, 2016; Kelly & Reynolds, 2015; Manning & Garton, 2012). Spring release of habitat from snow (hereafter spring release) is one such process affected by snow dynamics, as it relates to the timing of receding snow cover and its impact on the availability of plant-based food sources. Wildlife populations such as Grizzly bears (Pigeon, Stenhouse, & Côté, 2016) are greatly affected by the timing of spring release, as early emergence from dens due to earlier food availability has been linked to increased numbers of bear-human conflicts (Pigeon, Côté, & Stenhouse, 2016). The location of snow refugia can also be identified and more accurately predicted using spatially explicit models of snow cover in conjunction with other environmental covariates. Species such as wolverine *(Gulo gulo)* and mule deer *(Odocoileus hemionus)* have been shown to rely on winter habitat that provides thermoneutrality and forage respectively, with snow dynamics providing the link between thermoregulation and specific habitat types (Armleder et al., 1994; Bergman et al., 2014; Copeland et al., 2010; Doerr et al., 2005; Poole & Wright, 2010; Robinson & Merrill, 2012). The inherent connection between snow dynamics and the array of complex adaptive systems mentioned speaks to the range of applications for snow modelling. Therefore, the need to continually monitor snow dynamics, while improving the accuracy and predictive power of such maps and models, remains critical to a number of industries, scientific disciplines, and policy objectives.

Imagery acquired by the Moderate Resolution Imaging Spectroradiometer (MODIS) on board TERRA and AQUA has been widely used by scientists to map, monitor and geospatially analyze terrestrial, atmospheric and oceanic processes including snow. The monitoring of snow cover and albedo at daily temporal resolutions from MODIS has provided key insights into the extent and timing of snow cover within remote, expansive areas (Crawford, 2015; Czyzowska-Wisniewski et al., 2015; Nolin, 2011; Selkowitz & Forster, 2015). To do so, the Normalized Difference Snow Index (NDSI) detection algorithm of Hall, Riggs, & Salomonson (1995) is often used which exploits differences in reflectance between spectral bands in order to isolate the particular spectral signature of snow cover. Similar to clouds, the presence of snow corresponds to high surface reflectance of bands within the visible spectrum. However, clouds continue to reflect radiation beyond the visible spectrum including short-wave infrared whereas snow does not. Therefore, the difference between the reflectance of the visible and short-wave bands is able to discriminate snow from cloud while normalizing an index whose ratio represents the degree of radiation reflected back to the sensor. This methodology has produced a range of daily map layer products, including MOD10A1 with a spatial resolution of 500 m (Stroeve, Box, & Haran, 2006), to MOD10C1C with a spatial resolution of 0.25°, or approximately 28 km at the equator (Hall & Riggs, 2007).

The most recent version of the daily snow cover product is the MODIS Snow-Covered Area and Grain size (MODSCAG) product which was developed as an alternative to NDSI and uses spectral mixture analysis to calculate the fractional Snow Covered Area (fSCA) which ranges between 0 - 100 indicating the pixel area covered by snow (Painter et al., 2009; Rittger, Painter, & Dozier, 2013; Salomonson & Appel, 2006). MODSCAG incorporates the pure surface reflectance signatures of snow which change as a function of the size of snow grains. The algorithm accounts for the spatial variability of mountainous terrain by solving for grain size in conjunction with fSCA, allowing differing slope and aspects and their effect on snow grain size to alter the spectral reflectance of snow (Painter et al., 2009). The algorithm’s daily temporal resolution remains as a principal advantage over other methods, while the shortcoming continues to be spatial estimates that are between 500 m to many kilometres wide.

While snow dynamics have been monitored and well researched at the global scale using remote sensing instruments of coarse spatial resolution such as MODIS, local and regional snow dynamic assessment has proven to be more difficult (Coops et al., 2012; Gao, Xu, Zhao, Pal, & Giorgi, 2006; Jönsson & Eklundh, 2004; Kelly & Reynolds, 2015; Onstott, 1997; Sirén, Somos-valenzuela, Callahan, & Kilborn, 2018). Snow grain morphology is one such phenomenon influencing the viability of detection by satellites over complex landscapes (Stroeve et al., 2006). Particular topographic features such as aspect within mountainous terrain heterogeneously affects the metamorphosis of snow crystal structure across the landscape, as solar radiation attenuating at differing intensities and durations results in varying melt rates that impact snow cover and depth. Insulation properties of closed canopies are also a potential source of greater snow cover variability (Armleder et al., 1994) and forest cover has been associated with higher detection errors due to canopy interception and viewing geometry (Crawford, 2015; Hall, Foster, Verbyla, Klein, & Benson, 1998; Parajka, Holko, Kostka, & Blöschl, 2012b). In order to address the most significant sources of detection error, finer spatial resolution data is often desired to more accurately capture and model snow cover dynamics within variable terrain and land cover (Hall et al., 1998; Kostadinov & Lookingbill, 2015; Raleigh et al., 2013; Rittger et al., 2013; Walters, Watson, Marshall, McNamara, & Flores, 2014).

Spatial estimates of snow cover have also been generated from sensor systems on board Landsat satellites (Lauer, Morain, & Salomonson, 1997). Landsat Thematic Mapper to the Operational Land Imager allow for continual coverage of the Earth since 1982, providing vast opportunities for long-term environmental research (Markham, Storey, Williams, & Irons, 2004; Wulder, Masek, Cohen, Loveland, & Woodcock, 2012). Landsat's improved spatial resolution over

MODIS allows generation of the NDSI index at a spatial resolution of 30 m, while Dozier (1989) incorporated additional spectral bands from Thematic Mapper in order to distinguish differing types of snow cover in terms of grain size. The Landsat TM Snow-Covered Area and Grain size (TMSCAG) is another snow detection algorithm utilized by Painter et al. (2009) and Selkowitz & Forster (2015) which employs radiative transfer models and the spectral endmembers representing a range of land cover types spectral endmembers to calculate fSCA for sub-level estimates of the snow cover extent within a pixel. Although satellite-based approaches have shown to be capable of capturing broad scale snow dynamics (Painter et al., 2009), MODIS products remain limited in their spatial resolution, while TMSCAG and other Landsat-derived algorithms are limited in their ability to temporally track changes in snow cover distribution. The Landsat 16-day repeat cycle is a consequence of the trade-off between orbital repeat, size of swath scans, and spatial resolution, and can limit the number of viable observations to one every few months if cloud cover is especially frequent.

A possible solution to the orbital repeat times and/or scanning swaths preventing production of daily, finer scale maps is the use of novel data fusion algorithms. Data fusion algorithms utilize the strengths of different satellite datasets, applied to the monitoring of snow or other phenomenon where fine scale conditions can change daily, including snow cover, depth and albedo (Garvelmann, Pohl, & Weiler, 2013; Shuai et al., 2011). Data fusion techniques include the Spatial and Temporal Adaptive Reflectance Fusion Models (STARFM) developed by Gao, Masek, Schwaller, & Hall (2006) which develops relationships between weighted neighbouring pixels that are relatively homogenous between coarse and fine pixel values (Hilker et al., 2009; Walker, De Beurs, Wynne, & Gao, 2012; Wu, Mingquan, Niu, Zheng, Wang, Changyao, Wu, Chaoyang, Li, 2012). Other examples of data fusion techniques include downscaling common products such as NDVI from MODIS to Landsat (Hwang, Song, Bolstad, & Band, 2011), developing data fusion algorithms using a process related to speech recognition (Baumann, Ozdogan, Richardson, & Radeloff, 2017; Berman et al., 2018) and utilizing the entire long term Landsat record to generate a curve-fitting formula segmented into a 2-part sigmoid curve (Fisher et al., 2006; Nijland et al., 2016). The final example applied the method in a phenology study, charting the average season length and reflective magnitude of all Landsat observations via pixel-by-pixel based analysis, a method which this article has adapted to mapping snow.

The aim of this first phase of my master's thesis is to integrate spatial and temporal dynamics of snow cover data over an 18-year period in order to produce daily imagery of snow cover at a landscape scale of 30 m by 30 m spatial resolution. To do so, the high temporal density of imagery collected from the MODIS satellite was combined with comparatively fine-spatial scale Landsat satellite imagery in the novel dataset fusion algorithm MODSAT-NDSI (MODIS and Landsat's Normalized Difference Snow Index). The MODSAT-NDSI algorithm utilizes NDSI, the metric common to both imagery datasets, in a technique employing the extensive Landsat record to generate long-term-trend NDSI curves for each pixel. The Landsat NDSI values are then resampled and overlaid with daily MODIS NDSI imagery to calculate the final NDSI values. The resulting snow distribution predictions have a range of applications including forestry, conservation and land management groups. Ultimately this research could provide greater certainty in land use decisions by improving our understanding of snow timing and distribution throughout the landscape, and be utilized for a number of other applications relating to hydrology and wildlife studies.

2.2 Materials and methods

2.2.1 Study area for chapter 2

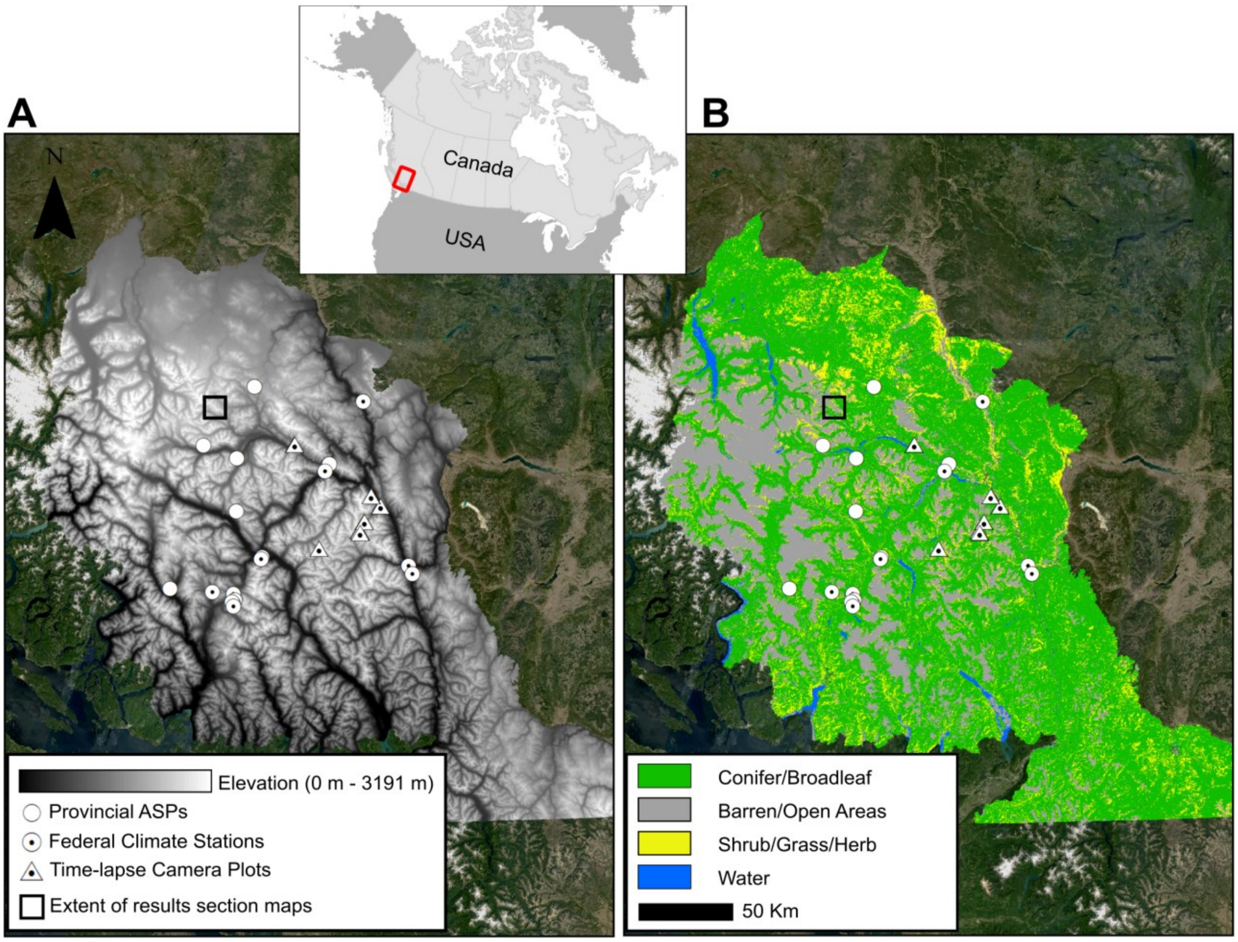

Figure 1: (A) Focus area extent represented as a digital elevation model (DEM) layer and (B) 4 land cover classes. Validation sites are distributed throughout varying elevations and land cover types, which include: provincial automated snow pillows (ASPs), federal climate monitoring stations, and time-lapse camera networks installed for this project. In addition, frame A and B preview the extent of the maps shown in the results section of the paper.

This MSC project is supported by the St’át’imc Government Services (SGS), Lillooet, BC with a focus area comprising the St’át’imc First Nations territory (Figure 1). The St’át’imc are an Interior Salish people, occupying 2.2 million ha of the 5.6 million ha research area; governed by an independent and united Chiefs Council. SGS has several departments including the SGS Environment Program, which is engaged in many activities including wildlife research and conservation projects (www.statimc.ca). Focus is currently directed towards grizzly bear protection as an umbrella species, as well as salmon and mule deer research and conservation.

The study area includes the Central Interior Ecoprovince, the Pacific Ranges Ecoregion and the Southern Interior Ecoprovince (Province of British Columbia, 2016). Characteristically humid within the Pacific Ranges while east of the Coast Range is dominated by a pronounced rain shadow effect, both the Central and Southern Interior Ecoprovinces experience continental climates much drier than that of the coast. Within the most mountainous areas, climate varies greatly in relation to elevation (Poole and Wright, 2010) while precipitation including snow pack is largely dependent on aspect (Armleder and Waterhouse, 1994; Poole and Wright, 2010).

Approximately 54 % of the study area is forested, and habitat within the area ranges from bunchgrass/sagebrush (*Artemisia tridentata*) bench lands along the Fraser River, through mid-elevation interior Douglas-fir (*Pseudotsuga menziesii*) stands. Higher elevation lodgepole pine (*Pinus contorta*) and Engelmann spruce (*Picea glauca* x *engelmannii*) -subalpine-fir (*Abies lasiocarpa*) plateaus graduate into alpine forests and tundra in central areas (Lloyd et al. 1990). Agricultural land use occurs along the benches of the Fraser River, Pemberton meadows and within valley bottoms in warmer drainages. Cattle ranges are an additional and notable portion of the landscape within the North Cascades area south of Lytton.

The last two decades marks the period where elders and the general public within the St’át’imc Nation began to voice their concerns for the mule deer and other terrestrial wildlife populations. The greater frequency and extent of development and clearcut harvesting during this time likely resulted in less available habitat for wildlife, as discussed in previous studies (Anthony and Smith, 1977; Mackie, 1970; Poole and Wright, 2010; Procter and Iredale, 2013; Sawyer et al., 2006). Beginning in the mid 1950’s, forest harvesting began in the territory and continues to this day. The most rapid increases in harvesting intensity occurred in the 1980’s and 90’s, particularly around the northern extent denoted as the Northern Forestry Plan (NFP) area (St’át’imc Government Services, 2016).

2.2.2 Remotely sensed data sources

Table 1: The MODIS tiles identification number based on grid of horizontal and vertical coordinates, and Landsat paths/rows used in the MODSAT-NDSI algorithm.

Satellite	Tiles / Scenes	Date Range Used in Processing
MODIS	H09/V04, H10/V03, H10/V04	2000-02-24 to 2017-12-31
Landsat	45/26, 46/25, 46/26, 47/24, 47/25, 47/26, 48/24, 48/25, 49/24	Landsat 4-5: 1984-11-16 to 2011-10-23 Landsat 7 ETM+ 1999-07-05 to 2016-12-31 Landsat 8 OLI/TIRS 2013-04-19 to 2017-12-31

2.2.3 Landsat

Landsat Level-2 Surface Reflectance data from November 16, 1984 - December 31, 2017 were downloaded from the United States Geological Survey (USGS) Government Agency (https://landsat.usgs.gov/). A total of 9 Landsat footprints were used from the Thematic Mapper (TM), Enhanced Thematic Mapper Plus (ETM+), and Operational Land Imager (OLI) sensors (Table 1). These products included a pixel quality assessment layer for each image, which was used to filter erroneous observations that were cloud, shadow or water contaminated. A total of 7,138 Landsat images were downloaded. Although Landsat data from 1984 to 2017 were used to develop NDSI median average curves, the results reported span from 2000 to 2017 due to the need to fuse Landsat observations with data from the MODIS instrument on board the TERRA satellite, first launched in 2000.

2.2.4 MODIS

Daily MOD10A1 (V6) snow cover data from TERRA were downloaded from February 24, 2000 - December 31, 2017 from the National Aeronautics and Space Administration Snow and Ice Data Center webpage (http://nsidc.org/data/MOD10A1/versions/6#) (Hall & Riggs, 2016). The product has NDSI values calculated and normalized from 0 – 100. The MOD10A1 algorithm used to obtain the final NDSI values includes procedures to identify the best observation for each day, and several data quality tests used to screen out and/or flag pixels. For example, observations were screened based on: low green band reflectance values of ≤ 10, near infrared ≤ 11, NDSI < 10, solar zenith angles $> 70°$, and finally surface temperature and height are ≥ 281 K and ≤ 1300 m respectively. The final screening accounts for pixels at lower elevations emitting temperatures too warm for there to be snow present. Pixels falling above and below tested thresholds in the screening process are flagged as a lower quality observation due to increased uncertainty, reversed from snow covered to no snow or labelled NA. A total of 19,038 images were downloaded.

2.2.5 Land cover classification map

The study area has recently been mapped by the SGS Environment Program in 2014 through the landcover classification project. The study area was built from Landscape units within the Threatened Grizzly Bear Population Unit map (Ministry of Environment, 2012) (Figure 1). Using remote sensing data and ground truthed validation field data, an ecologically relevant thematic land cover map was generated by Chance et al. (2016). The project was completed in 2015, resulting in a cloudless, seamless mosaic of all 9 Landsat 8 OLI surface reflectance scenes from 2013 and 2014 that were used (Table 2). This map provides land cover information at a resolution of 30 m x 30 m pixels that was used in the ground truthed validation phase for snow cover when identifying areas with tree canopy cover.

Table 2: The path/row and dates of the Landsat 8 Operational Land Imager (OLI) Surface Reflectance (SR) images used in the mosaic. Table from Chance et al., 2016.

LANDSAT OLI PATH/ROW	DATE OF IMAGE
45/26	July 15, 2014
46/25	July 3, 2013
46/26	July 3, 2013
47/24	July 13, 2014
47/25	July 13, 2014

47/26	July 13, 2014
48/24	September 6, 2014
48/25	September 6, 2014
49/24	July 11, 2014

Table 3: The definitions of the 15 land cover/land use classes in the study area. Table from Chance et al., 2016.

Class	Definition
Open coniferous forest	≥50% of tree cover is conifer, 6 - 29% canopy closure
Moderate coniferous forest	≥50% of tree cover is conifer, 30 - 74% crown closure
Dense coniferous forest	≥50% of tree cover is conifer, >75% conifer closure
Grassland	>25% grass cover, <25% shrub cover, <6% tree cover, <25% herb cover OR if 6%<25% of any vegetation cover type but grass cover is most-dominant
Broadleaf forest	>50% tree cover, >50% stems broadleaf
Shrub	>25% shrub cover, <6% tree cover, <25% herb cover, <25% grass cover OR if 6%<25% of any vegetation cover type but shrub is most-dominant
Herbaceous	>25% herb cover, <25% shrub cover, <6% tree cover, <25% grass cover OR if 6%<25% of any vegetation cover type but herbaceous is most-dominant
Cropland/human-maintained grassland	Human-maintained grassland, not including rangeland
Barren land	<6% vegetation cover, including sediment along rivers and lakes, rocks

Developed	Impervious, human-created surface
Ice	
Clear water	
Turbid Water	

2.2.6 Snow camera data

I stratified the focus area into five elevation classes to account for differences in snowpack at 500 meter intervals from 0 to > 2000. Pairs of field cameras (either Bushnell Trophy Game Camera HD, Aggressor No-Glow 14 MP or Moultrie Wingscapes TimelapseCam Digital Camera) were installed at each stratified elevation band, one under canopy cover of 60% or more, the other in an open area. This pairing was designed to account for differences in land cover type. Plots were additionally selected based on having a view of the foreground that is 30 m distance or more from the cameras, reflecting the spatial resolution of Landsat. Proximity to a useable road and accessibility was also a factor in plot selection given the highly variable terrain and often remote areas. Images were acquired every 15 minutes from 11:00 to 15:00 to coincide with the orbital repeat time of the TERRA satellite, as well as to ensure that there are quality observations for each day.

2.2.7 Data fusion technique

I fused MODIS and Landsat data to create daily 30 m NDSI predictions by adapting data fusion techniques originally developed for phenological mapping. Fisher et al. (2006) developed a data fusion approach which combined phenology camera data with Landsat satellite imagery. In the study they accurately described phenological variability within a relatively homogenous deciduous forest. Inter-annual variability was addressed by weighting anomalous land surface temperatures while considering a time lag between the curve-fitted average and a specific year's unimodal green-up and/or senescing signal. Nijland et al. (2016) adapted the technique to mixed and coniferous forest stands, and utilized data from a phenocamera networks to validate the estimates. The yearly adjusted, phase shifted phenology curves, produced good agreement with day of the year (DOY) environmental cues observed from plot based camera networks, especially green up, with a RMSE of 7 days (Nijland et al., 2016).

In this chapter I adapt the approach of Nijland et al. (2016) to map snow cover (rather than greenness) by developing inter-annual trajectories of NDSI at the Landsat resolution on a pixel-by-pixel basis with a moving average binning window. Historical Landsat images were used to obtain the historical snow distribution patterns when computing the median average for each Landsat-sized pixel. The yearly adjusted phase shift is calculated by averaging Landsat NDSI values lying within the larger MODIS pixel area when overlaid, and then applying the difference to each Landsat NDSI value. The general approach is shown in Figure 2 and detailed below.

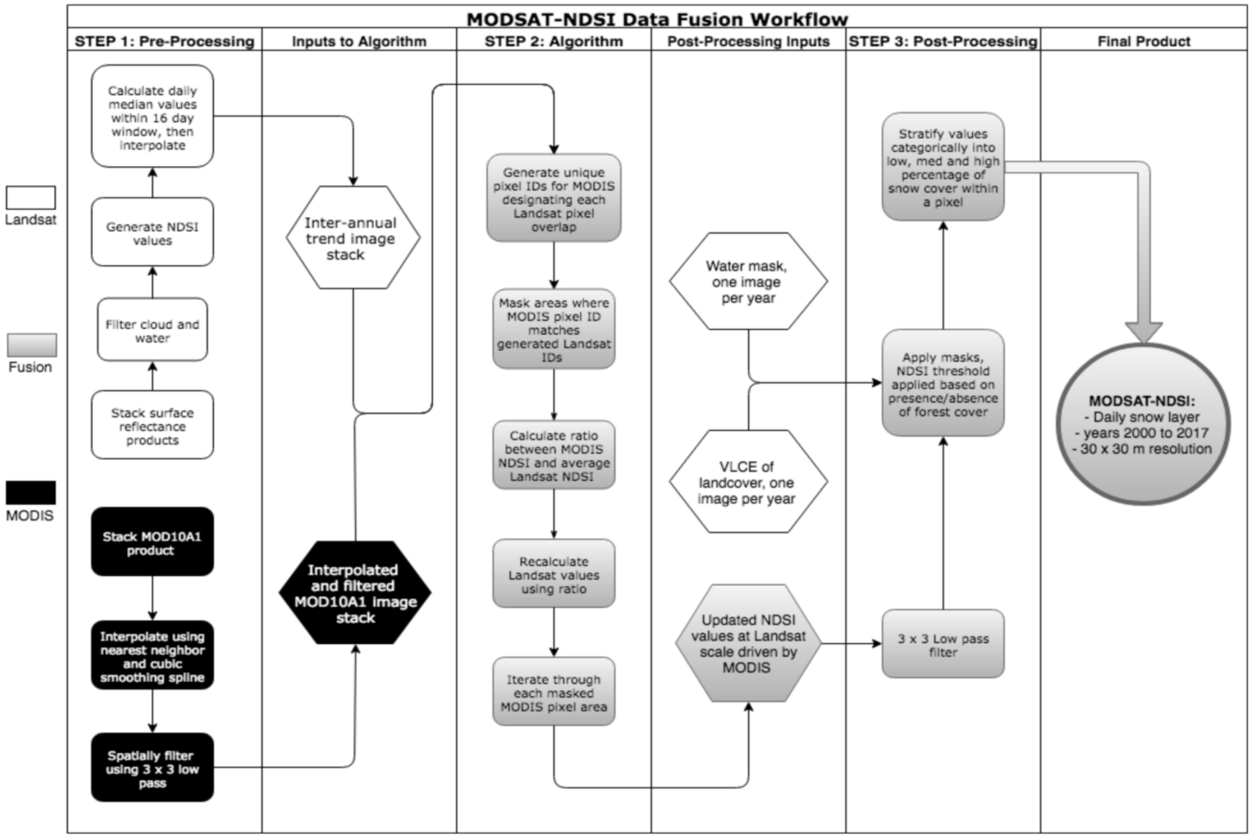

Figure 2: Workflow of MODSAT-NDSI (MODIS and Landsat's Normalized Difference Snow Index) data fusion algorithm. The landcover mask was derived from the Virtual Land Cover Engine (VLCE) developed by Hermosilla et al. (2018).

2.2.7.1 Step 1: Pre-processing

The NDSI snow detection method has been used extensively to assess the variability in snow cover (Hall et al., 1998; Keshri, Shukla, & Gupta, 2009; Shimamura, Izumi, & Matsuyama, 2006; Xiao, Shen, & Qin, 2001) and forms the basis of the data fusion approach. Therefore, NDSI values were calculated for each Landsat image in order to match the processed MOD10A1 NDSI pixel values using the green and short-wave infrared bands (Equation 1).

$$NDSI = (R_{VIS} – R_{SWIR}) / ((R_{VIS} + R_{SWIR}) * 100 \quad (1)$$

Where R_{VIS} is the degree of reflectance in the green visible spectrum (band 2 in Landsat TM and ETM+, band 3 in OLI), and R_{SWIR} denotes the short wave infrared band, being 5 for TM and ETM+ or 6 for OLI. The resultant index from 0 to 100 indicates the degree of a pixel area reflecting the portions of the electromagnetic spectrum associated with snow (i.e., the spectral signature of snow).

On a pixel-by-pixel basis, all downloaded Landsat scenes were used to generate a smoothed median NDSI for each DOY, regardless of year. The median was calculated using a temporal moving window of 16 days, 8 days prior and 8 days after each DOY, generating a single curve of NDSI values for every pixel. Each curve of values thus represents the generalized pattern of how NDSI (i.e., snow cover) changes throughout any given year for every processed Landsat pixel. For both the MODIS MOD10A1 product and the smoothed median Landsat scenes, a similar approach to Dozier, Painter, Rittger, & Frew (2008) was followed in order to interpolate through any missing daily observations. First, nearest neighbour interpolation was applied to the first DOY and last 15 DOYs. The MATLAB functions *csaps* and *imgaussfilt* were then utilized in a cubic spline function. The nearest neighbour step was used to account for the MATLAB function assuming that data begins and ends at zero.

2.2.7.2 Step 2: Algorithm

To facilitate a comparison between the two datasets the Landsat NDSI values were averaged within, and resampled to, the same resolution as the 500 m by 500 m MODIS pixel, as was similarly done by Hwang et al. (2011) when they used Landsat imagery to assess the accuracy of the MODIS snow product. For each DOY (1-365) and year (2000 – 2017), these 500 m average Landsat NDSI values were related to the corresponding MODIS NDSI value using the following equation:

$$\text{Ratio} = \text{MODIS}_{\text{NDSI}} \,/\, \text{Landsat}_{\text{NDSI}(\bar{x})} \qquad (2)$$

Each respective Landsat pixel within the larger 500 x 500 m area was then multiplied by this ratio, thereby adjusting the Landsat NDSI value by the MODIS NDSI value for each DOY and year, resulting in a daily, 30 m NDSI product from 2000-2017.

2.2.7.3 Step 3: Post-processing

As it is well established that canopy cover affects the response of NDSI (Hall et al., 1998; Hall & Riggs, 2007; Liu et al., 2008; Molotch & Margulis, 2008; Parajka et al., 2012b) a Landsat derived canopy cover layer (Hermosilla, Wulder, White, Coops, & Hobart, 2018) was used to generate a mask for forested areas. During data fusion, the forest mask was used to identify forested pixels and alter the NDSI threshold for those pixel areas when classifying snow. Relationships between NDSI and snow cover were derived independently for winter (DOY 1 – DOY 151, & DOY 306 – DOY 365), melt (DOY 152 – DOY 182), summer (DOY 183 – DOY

273), and accumulation periods (DOY 274 – DOY 305) using a series of 16 field sites for training (described below). For both validation and training sites, snow and snow-free days were identified by setting a threshold of depth and snow water equivalent (SWE) for weather stations, and by qualitatively assessing ground cover in camera photos. Thresholds of NDSI were iteratively varied in order to maximize the accuracy of separating snow and snow-free days in the training sites within each time period, using both time-lapse camera and weather station data. This process was conducted independently for both open and forest pixels, with the derived thresholds displayed in Table 2. The training sites used to determine these thresholds were not included in the final validation to ensure that the validation was independent of the training process.

Table 4: Derived seasonal periods and their associated NDSI thresholds based on training validation data

Periods	DOY	Open Areas' NDSI Threshold	Forested Areas' NDSI Threshold
Winter January 1st – May 31st, and November 2nd – December 31st	1 – 151, and 306 – 365	33	8
Melt June 1st – July 1st	152 – 182	28	7
Summer July 2nd – September 30th	183 – 273	33	8
Accumulation October 1st – November 1st	274 – 305	52	13

2.2.8 Field validation using time-lapse photography

Validation of the daily 30m snow cover estimates was undertaken based on snow cover data derived from a field camera network installed within the study area (Figure 1A). Ground based cameras with daily photographs were used to qualitatively estimate snow, similar to methods used by Parajka, Haas, Kirnbauer, Jansa, & Blöschl (2012a). Graduated snow stakes within a camera's field of view is a reliable method to document snow cover change dynamics and other environmental processes in long-term studies (Graham, Hamilton, Mishler, Rundel, & Hansen, 2006; Graham, Riordan, Yuen, Estrin, & Rundel, 2010; Marty & Meister, 2012). Snow cover and depth measurement plots were installed on October 22-24 and December 14-16 2016, and March 16-20, September 29-October 4, and November 8-10 2017. The location of camera installations were based on an elevation stratification as well as degree of forest canopy cover (Table 3). Camera sites were paired with one camera placed in the open, and one in an area of 60% canopy cover or more. Within the foreground, snow stakes were taped with colored tape to indicate graduated 10 cm height intervals. Depth measurement poles were constructed from 2-inch x 10 ft. PVC pipes and 5 ft. tall rebar. Each pole was threaded through 1 rod of rebar to ensure stability. Rods were hammered into soil, submerged around half way (i.e., ~ 0.8 m). Cameras were set to take daily images between 11:00 and 15:00, within the window of the TERRA overpass.

In addition, snow survey data from the automated snow pillow (ASP) stations throughout British Columbia and federal climate data was utilized for validation (British Columbia Ministry of Forests Lands and Natural Resource Operations, 2017; Government of Canada, n.d.).

Table 5: Camera sites: CamA plots = Open/non-forested. CamB plots = Forested, ≥ 60% canopy cover.

Elevation classes 1 – 5 = 0 – 500 m, 500 – 1000 m, 1000 – 1500 m, 1500 – 2000 m, and > 2000 m.

***Provincial snow pillow sites. **Federal climate data sites.**

Plot ID	*Elevation (m) Elevation Class (1-4)*	*Start of data record used in analysis*	*Coordinates (UTM 10N WGS84)*	*Land cover*
Cam1A_older_site	1900 (class 4)	23-OCT-16	X: 0572946 Y: 5586634	
Cam1A_new_site	1855 (class 4)	17-MAR-17	X: 0573109.Y: 5586668	
Cam1B	1880 (class 4)	23-OCT-16	X: 0572942 Y: 5586652	
Cam2A	1702 (class 4)	24-OCT-16	X: 0572440 Y: 5587659	
Cam2B	1683 (class 3)	24-OCT-16	X: 0572510 Y: 5587749	
Cam3A	1428 (class 3)	24-OCT-16	X: 0575007 Y: 5592602	
Cam3B_older_site	1428 (class 3)	24-OCT-16	X: 0575138 Y: 5592728	
Cam3B_new_site	1428 (class 3)	01-OCT-17	X: 0575139 Y: 5592688	
Cam4A	741 (class 2)	15-DEC-16	X: 0579026 Y: 5606733	
Cam4B	790 (class 2)	15-DEC-16	X: 0578912 Y: 5606768	
Cam5A	323 (class 1)	16-DEC-16	X: 0583942 Y: 5601251	
Cam5B	323 (class 1)	16-DEC-16	X: 0583865 Y: 5601363	
Cam6A	1512 (class 4)	16-DEC-16	X: 0550489 Y: 5577942	
Cam6B	1502 (class 4)	17-MAR-17	X: 0550427 Y: 5577996	
Cam7A	1152 (class 3)	18-MAR-17	X: 0536819 Y: 5634731	
Cam7B	1090 (class 3)	18-MAR-17	X: 0537073 Y: 5634761	
*Blackcomb Base Sliding Center***	937 (class 2)	31-APR-07	X: 0504551 Y: 5550026	Forested
*Butcher Creek***	580 (class 2)	01-JAN-00	X: 0574557 Y: 5658212	Open
*Callaghan Valley***	870 (class 2)	06-MAR-07	X: 0537076 Y: 5555006	Forested to Open
*Downton Lake Upper**	1829 (class 4)	29-AUG-15	X: 0442531 Y: 5635316	Forested
*Green Mountain**	1766 (class 4)	01-JAN-00	X: 0435379 Y: 5626131	Forested
*Lytton 2***	174 (class 1)	01-JAN-00	X: 0599242 Y: 5568126	Open
*Lytton RCS***	225 (class 1)	01-MAY-06	X: 0601152 Y: 5564548	Open
*Mission Ridge**	1903 (class 4)	01-JAN-00	X: 0485891 Y: 5622044	Forested
*North Tyaughton**	1969 (class 4)	28-AUG-15	X: 0554788 Y: 5666797	Forested
*Pemberton Airport CS***	204 (class 1)	01-JAN-00	X: 0518936 Y: 5572648	Open
*Pemberton Airport CWS***	204 (class 1)	04-JAN-10	X: 0518674 Y: 5572298	Open
*Shalalth***	243 (class 1)	01-JAN-00	X: 0553600 Y: 5619890	Open
*Tenquille Lake**	1669 (class 4)	31-AUG-00	X: 0505906 Y: 5597935	Open
*Upper Squamish**	1387 (class 3)	01-JAN-00	X: 0469041 Y: 5555398	Forested
*Whistler Mountain High Level***	1640 (class 4)	13-JUN-05	X: 0503855 Y: 5547188	Forested
*Whistler Mountain Mid-Station***	1320 (class 3)	23-JUL-07	X: 0502563 Y: 5548082	Open
*Whistler Nesters***	659 (class 2)	13-JUN-05	X: 0503244 Y: 5552968	Open

Plot ID	Elevation (m) Elevation Class (1-4)	Start of data record used in analysis	Coordinates (UTM 10N WGS84)	Land cover
*Whistler Roundhouse***	1835 (class 4)	01-JAN-00	X: 0503777 Y: 5546168	Open

Validation of the snow mapping algorithm required the use of a combination of data sets (Table 3). A total of 15 camera sites, 6 provincial ASPs, and 12 federal climate stations were used to conduct an accuracy assessment by comparing the presence/absence of snow. Each daily observation was compared between NDSI snow mapped pixels and their associated validation datasets. The snow mapped pixels analyzed were identified by overlaying a point layer dataset, generated using the validation data set's geographic coordinates. Camera observations extended from fall 2016 – winter 2017 while all other sites vary in historical record length, with over 50% of sites having at least 10 years or more of data. A binary validation dataset was developed from each type of site. For the camera network, presence of snow cover was determined by qualitatively assessing whether each photograph showed 15 % or more of snow covered ground. Setting the binary threshold to ≥ 15 % for camera photos was designed to mimic the recommended fSCA threshold used by other authors, who note the limitations of sub-pixel information retrieval from satellite sensors (Cortés, Girotto, & Margulis, 2014; Painter et al., 2009; Rittger et al., 2013). A subset of the government weather station data used for validation recorded snow depth in centimetres, and these records were used to create a binary threshold of snow / no snow using a ≥ 20 cm threshold (Huang, Liang, Zhang, & Guo, 2011). The second set of government data used for validation were British Columbian automated snow pillows, which recorded snow water equivalent data. The threshold for setting snow/no snow for pillow data sets was ≥ 15 cm SWE, based on iterating through multiple trials of the training data set and the uncertainty that is present in these data when examining SI within shallower snowpack (Huang et al., 2011; Ryan et al., 2008; Singh et al., 2011; Varhola, Wawerla, et al., 2010).

The 30 m daily NDSI values were classified into 4 classes in the final snow fusion product (Table 4). Once NDSI thresholds were established for each period, NDSI values below the threshold were considered to represent 0 to 24 % snow cover within a pixel. The remaining pixels with values equal to or greater than the threshold were categorized into low, moderate and high degrees of snow cover by setting 3 evenly spaced intervals between the threshold and 100. The 3 generalized estimations of snow cover within a pixel range from 25 to 100 %. Classes of 25 % snow cover or more were considered snow covered in the binary accuracy assessment.

Table 6: MODSAT-NDSI algorithm's end product classification

Example NDSI Threshold Intervals (Melt Period in open site)	Classified Value	Classification
n/a	0	Unprocessed
< 28	1	0 – 25 % Snow cover (NDSI value lower than threshold)
≥ 28 ≤ 52	2	25 – 50 % Snow cover (low)
> 52 ≤ 76	3	50 – 75 % Snow cover (moderate)
> 76	4	75 – 100 % Snow cover (high)

The overall accuracy of the daily, 30 m Landsat NDSI product was assessed using Equation 3.

$$\text{Accuracy} = (T_p + T_n)/(T_p + T_n + F_p + F_n) \tag{3}$$

T_p are true positive cases of snow being present, validated by comparing predicted and observed values (0 or 1). T_n are true negative cases, and F_p and F_n are false positive and false negative observations respectively. Final accuracy therefore ranged from 0 – 100%.

$$\text{Precision} = (T_p)/(T_p + F_p) \tag{4}$$

$$\text{Recall} = (T_p)/(T_p + F_n) \tag{5}$$

$$\text{Inverse Precision} = (T_n)/(T_n + F_n) \tag{6}$$

$$\text{Inverse Recall} = (T_n)/(T_n + F_p) \tag{7}$$

The four performance measures calculated and shown as equations 4 – 7, identified the proportion of noise (precision and inverse precision) generated in relation to the total number of samples correctly matched (recall and inverse recall).

2.2.9 Inter-annual variability

Once validated, this study demonstrates an application of the MODSAT-NDSI algorithm across 6 forested and 6 open elevation classes. A subset of the resulting NDSI fusion map dataset was used to compare snow melt rates and the total number of snow-present days at different elevations and under forested and open conditions. Randomly sampled pixels for each class were selected across a subset of the focus area (Figure 1, Frame A and/or B) for half the number of years (i.e., 2000 – 2008). The sum of the number of days with snow presence, and the transition DOY of the melt and accumulation periods were calculated using a moving average with a window of 16 days. A thousand pixels were first classified into 1 of the 12 classes, then transition dates were calculated for each pixel. Transition dates from pixels within each class were averaged for each year. The 9 averaged transition DOY values from each of the 9 years were used to generate the final inter annual averages.

2.3 Results

2.3.1 Landsat

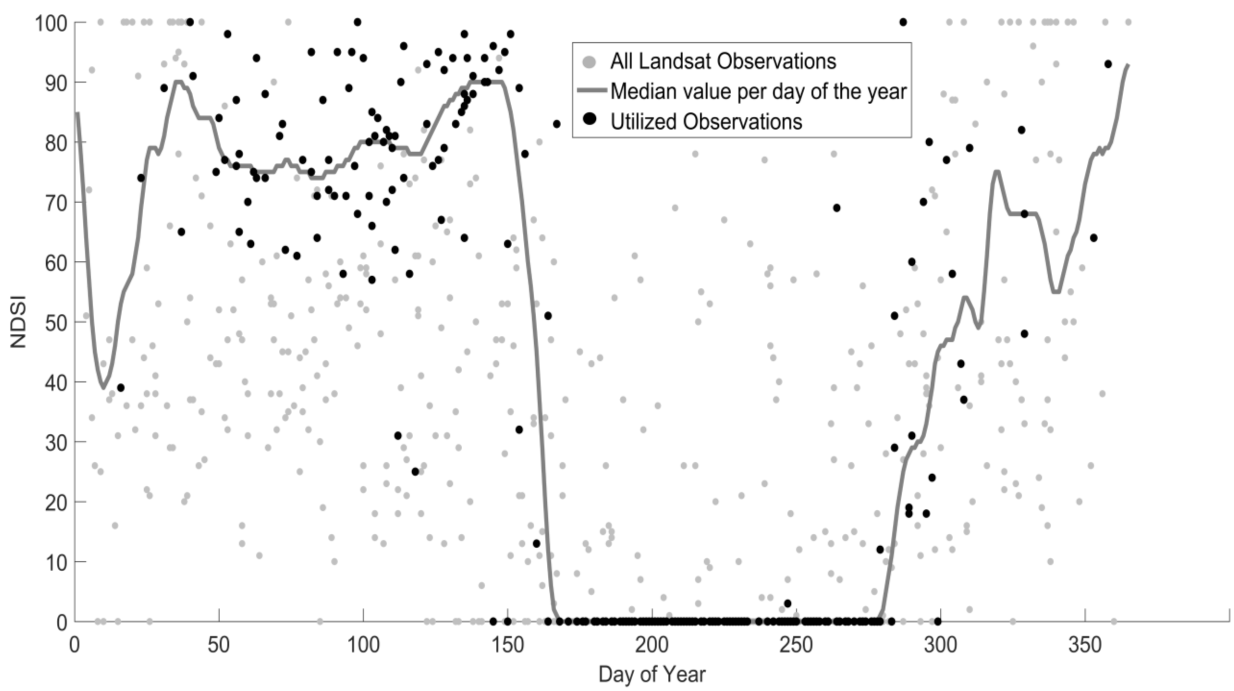

Figure 3: Per pixel processing of median NDSI trend. Median value generated for each day of the year using 16 day moving window, capturing the inter-annual trend of NDSI as it changes throughout any given year from 2000 to 2017. Figure shows the total number of Landsat observations (n = 557), the final observations

used to calculate the median values once pixel quality assessment was applied (n = 266) and the trajectory of change.

Using the 16 day moving window, a resulting image stack for each scene charts the median NDSI value for each day, accounting for the neighbouring spatial relationships that would be present between Landsat-sized pixels throughout the years 2000 to 2017 (Figure 3). The pattern is clear and apparent as snow accumulates in the fall (DOY 270 to 325) and spring melt (DOY 150 to 180).

2.3.2 MODIS

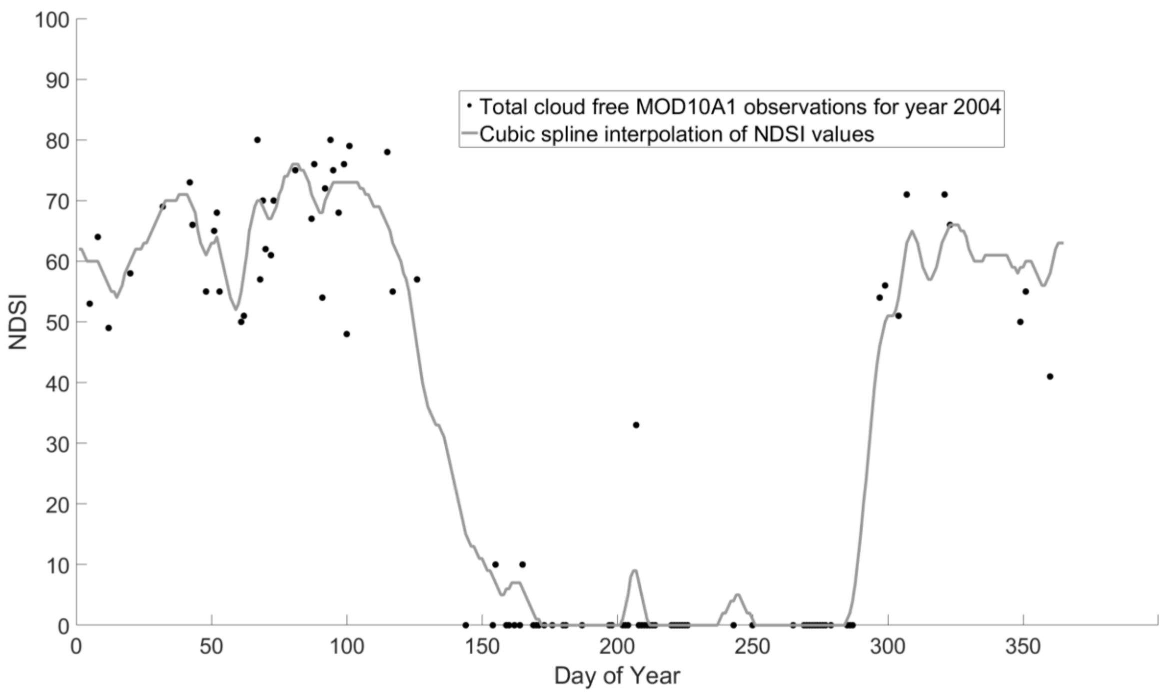

Figure 4: Cubic spline interpolation of MOD10A1 dataset, with additional nearest neighbour interpolations for the start and end periods.

Figure 4 is an example of an interpolated MODIS pixel, where NDSI values initially given by the dataset is often discontinuous due to cloud cover. The daily interpolated values for each pixel was then the input for a spatial low-pass filter which allowed for MODIS-scale pixel values to be smoothed out over the landscape, facilitating more continuous edge-effects once Landsat imagery is applied to the MODIS stacks.

2.3.3 Accuracy

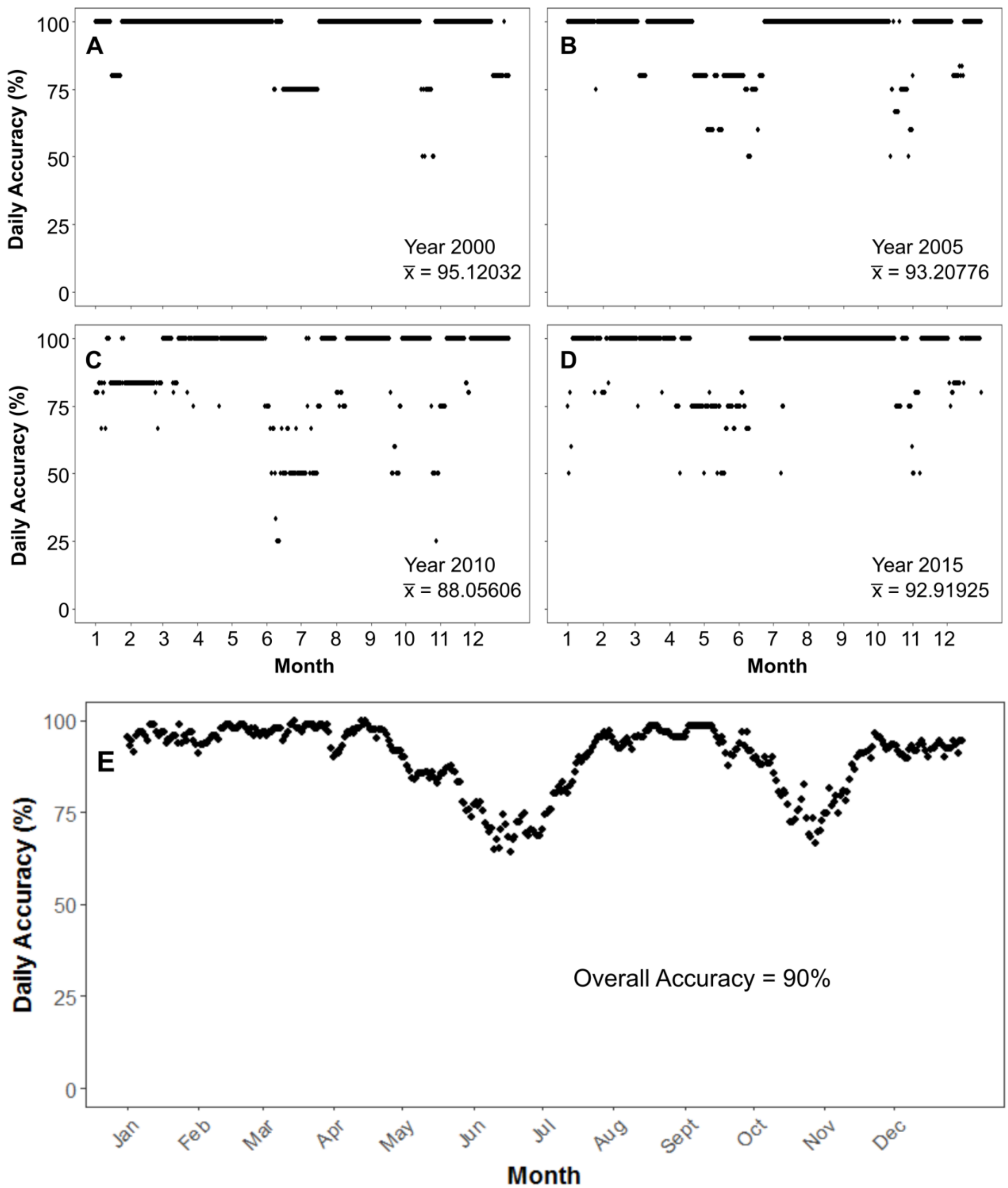

Figure 5: Accuracy assessment of the MODSAT-NDSI algorithm using 17 different validation sites. Frame E: Overall accuracy calculated for each DOY through all years (2000 to 2017). Examples of accuracy

assessments derived from individual years are shown in frames A to D. The validation sites include 15 timelapse camera sites, 6 provincial ASPs, and 12 federal climate stations.

The daily accuracy comparison indicated an overall accuracy of presence of snow of 90% (Figure 5, Frame E). Two distinct troughs in the daily accuracy values indicate an overall decrease in accuracy during the melt and accumulation times of the year.

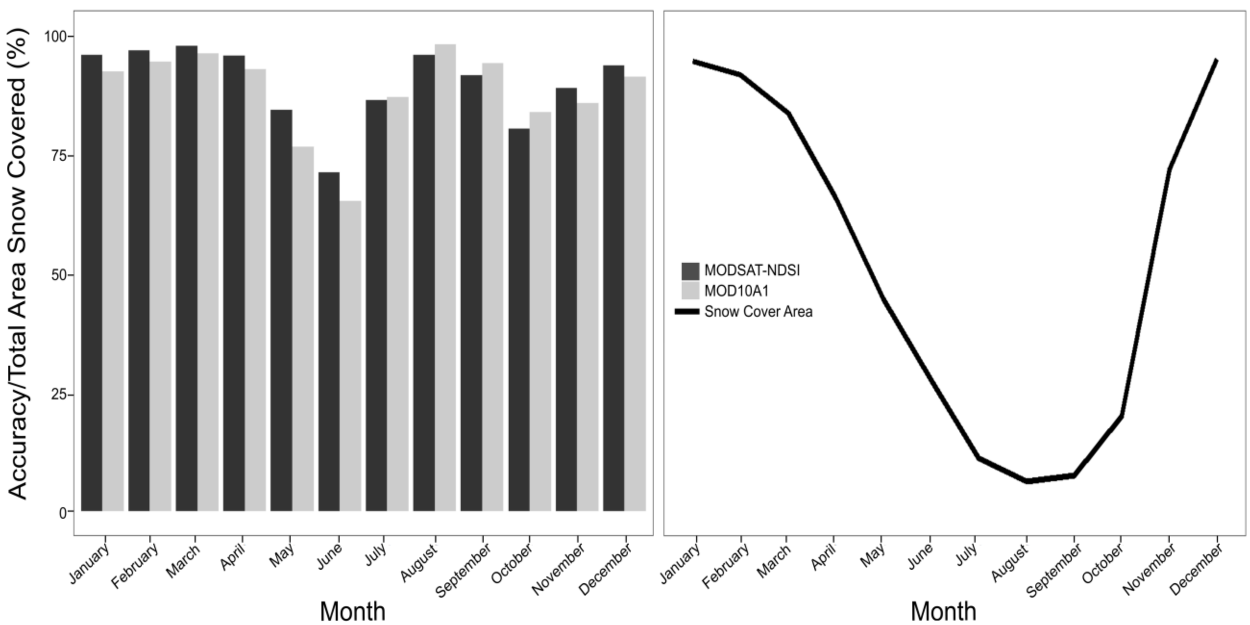

Figure 6: Overall accuracy per month, based on the snow cover algorithms' binary matching of each DOY to test data set comprising of 17 validation sites: they include both camera plots, federal data, and provincial ASPs. Both the fusion algorithm MODSAT-NDSI and MOD10A1 are included for comparison. The interpolated NDSI data values were used when assessing the accuracy of MOD10A1, and the well established method of setting the binary NDSI threshold to 0.4 was used to classify snow. The percentage of area covered in snow each month is also illustrated to exhibit how accuracy may change as snow cover becomes more dynamic throughout the study area.

At a monthly time step, the overall accuracy varied from 71 – 97.6% (Figure 6) with the lowest accuracy between June and October, and the highest accuracy during the winter months, December to April. MODIS' MOD10A1 version 6 algorithm was also tested for accuracy using the interpolated NDSI values that was generated in the pre-processing step. Snow cover was classified using an NDSI threshold of 0.4. The resulting overall accuracy of the MODIS product was 88.51 %. For each month, the proportion of land covered by snow relative to the total area of the study region is also shown in figure 6, demonstrating how accuracy relates to stable versus more dynamic periods of snow cover.

Table 7: Performance measures used to evaluate the MODSAT-NDSI algorithm, each result gives the overall performance measure of all DOYs.

Precision	Recall	F-Score	Inverse Precision	Inverse Recall	Inverse F-Score	**Accuracy**
92.42	90.96	91.68	87.71	89.65	88.67	**90.41**

Comparing precision and recall with the inverse measures of each reveals that the positive identification of snow is more accurate than detecting days when there is no snow, according to the F-measure 91.68, compared to 88.67, calculated as the harmonic mean of precision and recall, and the inverse harmonic mean of precision and recall respectively.

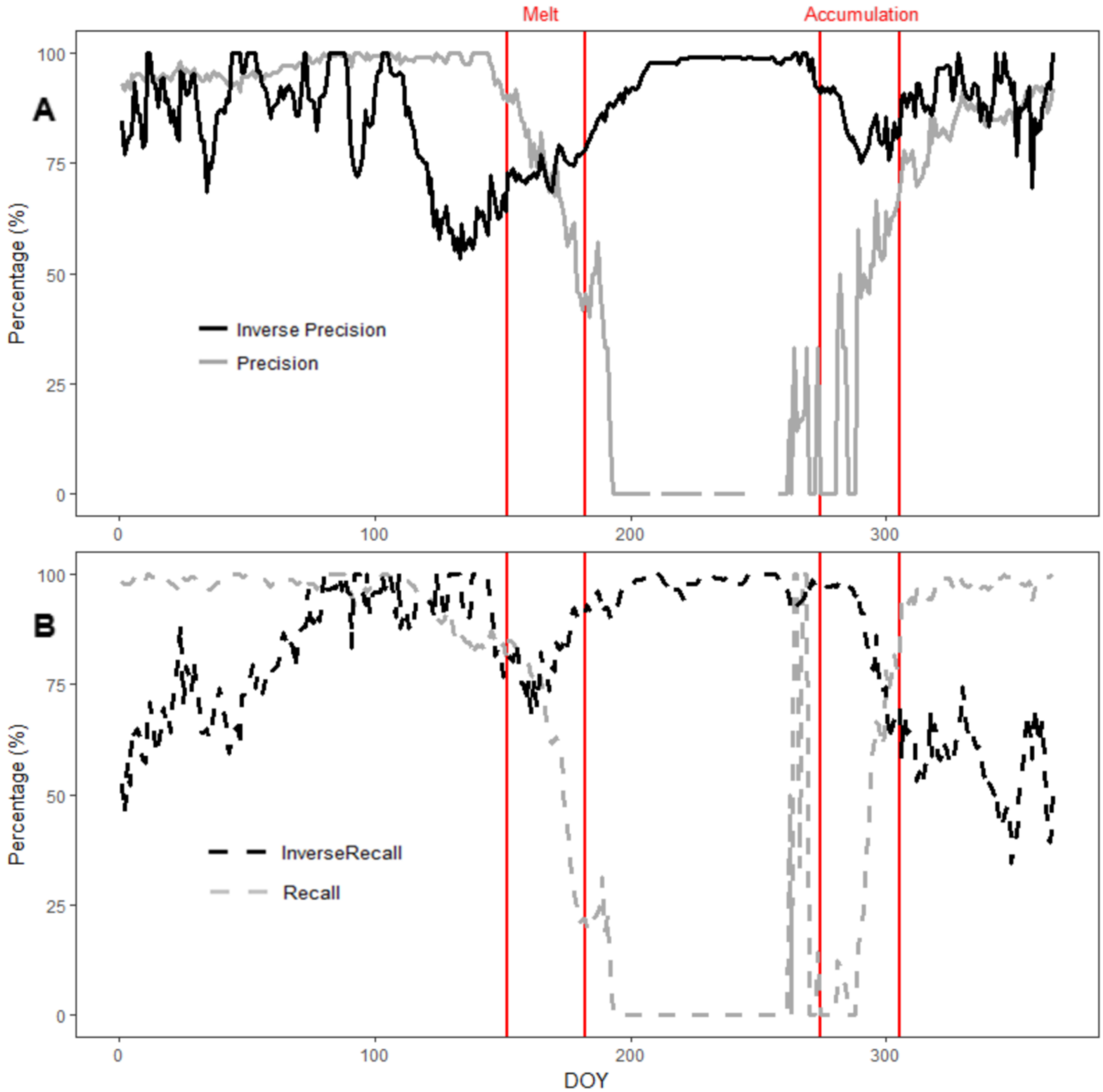

Figure 7: Performance measures of precision and recall, for both positive and negative cases.

The proportion of predictions correctly labelling a pixel area as snow free (i.e., inverse precision) remains high during the accumulation period, shown in figure 7A between DOY 274 and 305 (October 1 to November 1). Within the same period, inverse recall, or the proportion of the model's ability to correctly identify all instances of when snow is free (i.e., not just the correctly predicted observations), continues to decrease (Figure 7B). During melt between DOY 152 to 182 (i.e., June 1 to July 1) both inverse precision and inverse recall increase as precision and recall decrease. The other important feature to note is that, for positive cases (i.e., the detection of snow) the precision and recall curves follow a similar pattern, remaining very high (within 90 – 100%) for most of the year, and between the melt and accumulation periods, it is seen that both performance measures drop to zero percent, signalling that any random snow events during the summer would not be detected by the algorithm. These performance measures can estimate the signal to noise ratio, as it relates to the total number of samples. Specifically within accumulation, the combination of high inverse precision but lower inverse recall means that predictions made concerning the absence of snow remains accurate, but the total number of snow free instances is either greater or less than what is being captured in all predictions (i.e., true negatives and false negatives combined). Precision and recall which describes the degree of true or false positives can help to identify whether the case is the former or latter: increasing precision and recall during approximately the same period of time (Figure 7A and B) is usually due to the total number of real positive cases being very low initially, so a great deal of noise remains in predictions. Over time, the increasing instances of snow events improves recall and precision, meaning that inverse recall was decreasing because there are an increasing number of real negatives not being captured in the model, rather they are being included in an increasing sample size of positive snow events.

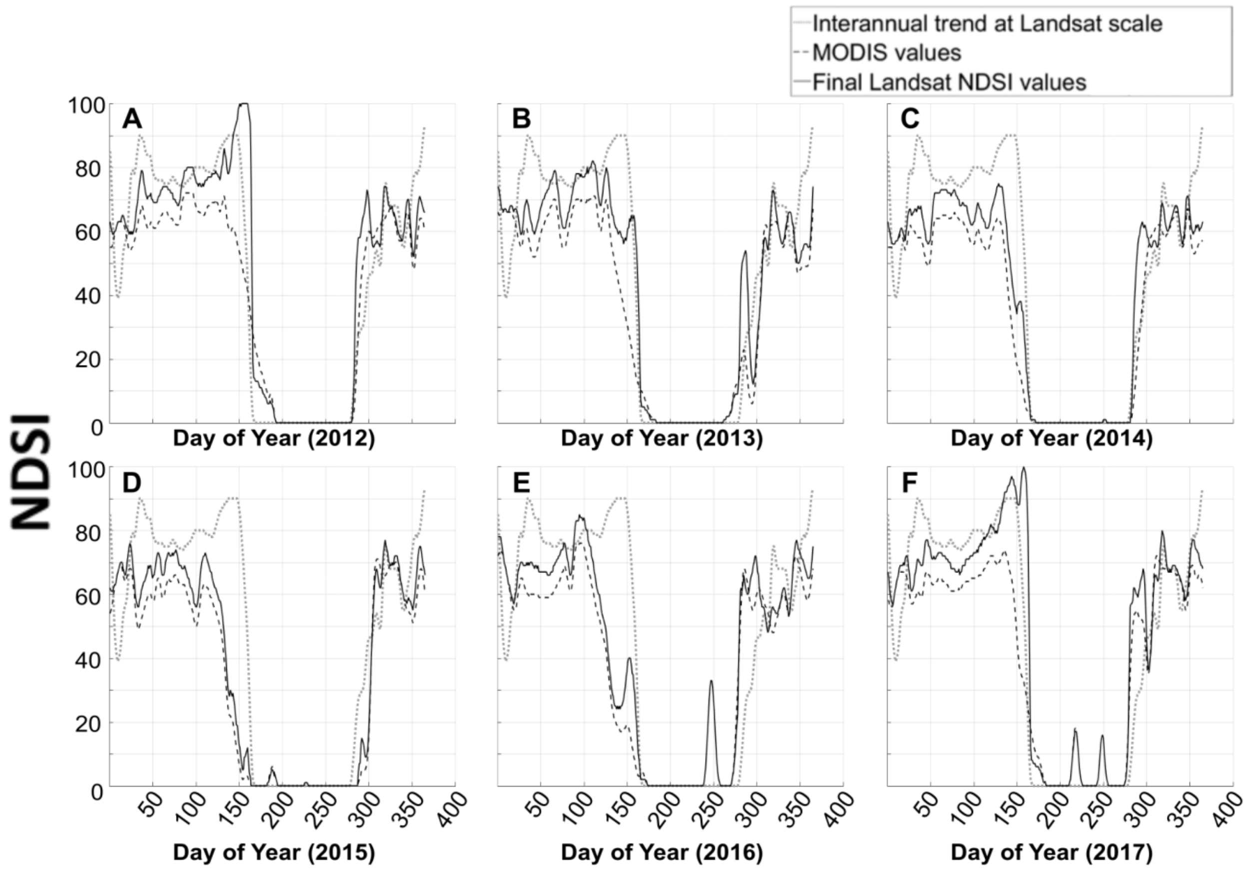

Figure 8: Effect of MODIS' current year observations on Landsat inter-annual trend. Frames A to F: NDSI trajectory through 2012 – 2017 for site Cam1A's associated pixel. Note: NDSI fusion output is affected not only by MODIS, but also by the average of NDSI values generated within each MODIS pixel. The ratio from the difference between MODIS and the Landsat average affects specific Landsat pixels by either increasing or decreasing the median.

Figure 8 shows the trajectory of NDSI values from three different data sets for a given pixel: the inter-annual Landsat median layer stack, the MODIS layer stack from January 1st to December 31st for years 2012 to 2017, and the output of the fusion algorithm for the given 30 x 30 m pixel. The final result is determined by the MODIS dataset as well as the average of all Landsat values falling within the given MODIS pixel, therefore the average was higher than the MODIS NDSI value in different periods in different years, as seen in Figure 8.

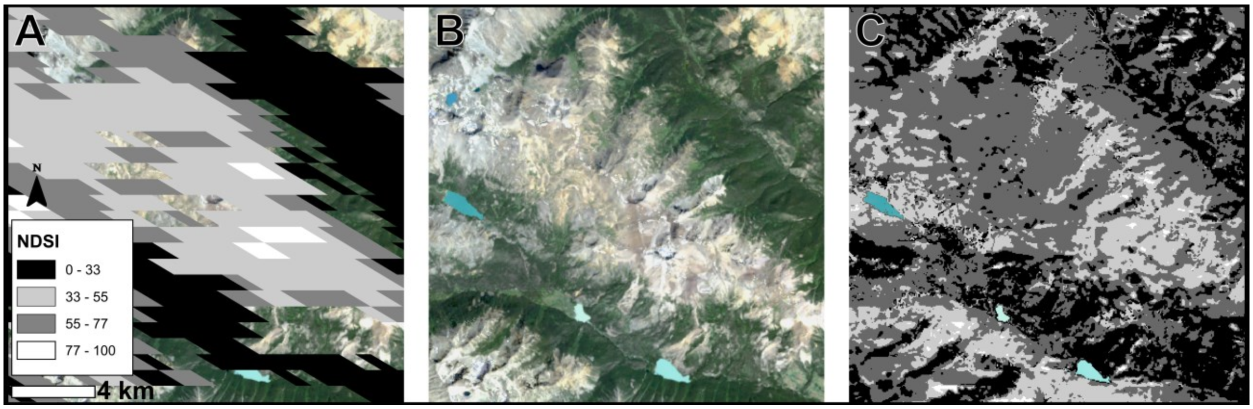

Figure 9: Comparison of map products within study area boundary (see study area map in previous section). Note: no color/transparent areas of snow layer indicate unprocessed areas. Frame A demonstrates the MOD10A1 NDSI snow cover product, labelled according to the classes generated by the new NDSI data fusion algorithm (Frame C). Frame B displays the Landsat resolution true color composite used to overlay snow layer products. Layers from both products are from October 30, 2017.

NDSI values are shown for a subset in figure 9. The fusion layer (Frame C) is compared to the MOD10A1 product (Frame A) for October 30, 2017. Spatially, the NDSI fusion output shows to trace the cover of snow at a much finer spatial resolution, outlining the contours of valleys, avalanche chutes, and higher elevation ridges that can be seen independent of either product in Frame B.

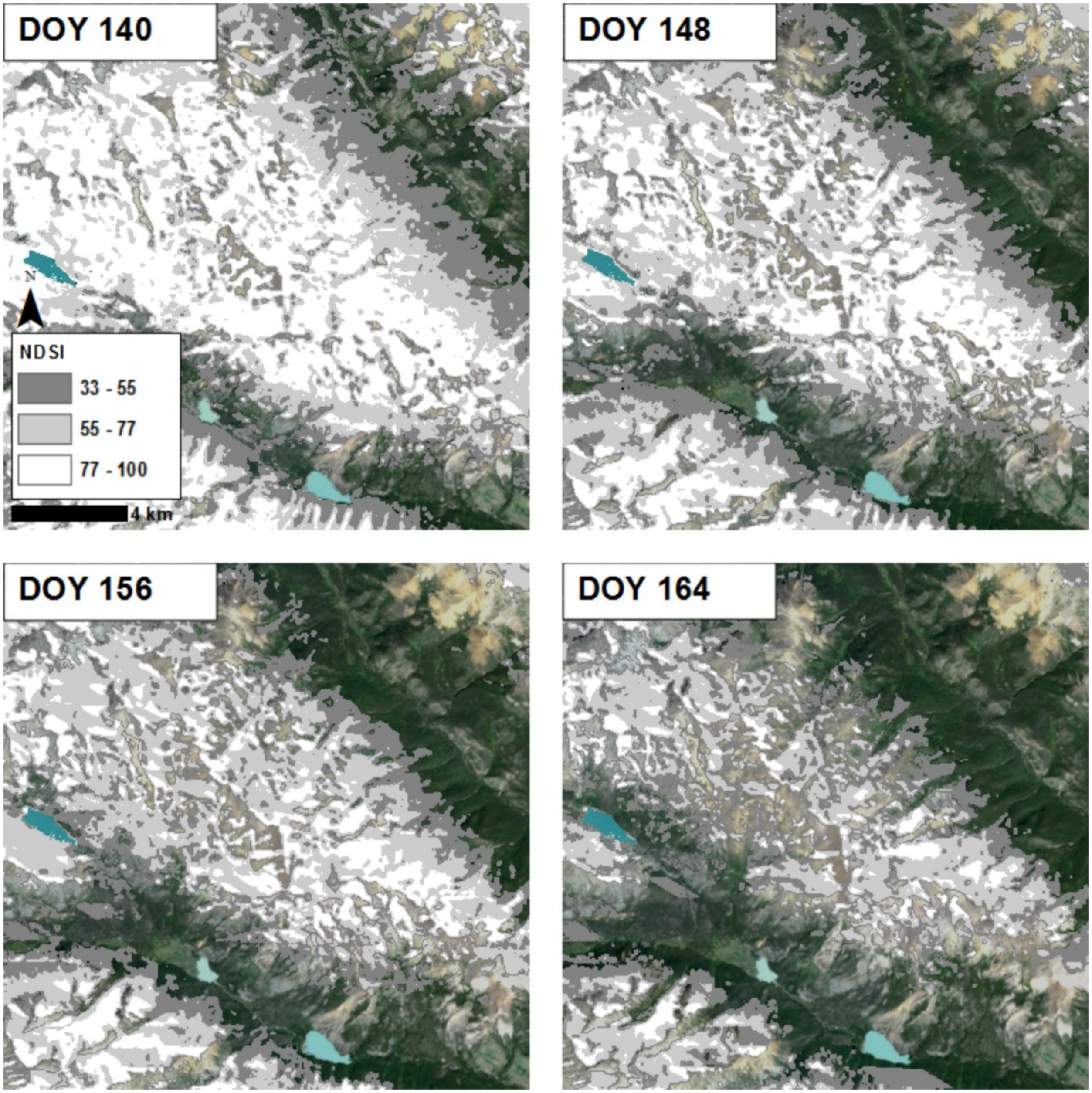

Figure 10: Observed change in snow cover from fusion snow mapping algorithm layers. Note: no color/transparent areas of snow layer indicate NDSI values below the threshold, and therefore classified as snow free. Frames display spatial patterns of the snow melt period for every 8 days, from May 20, 2017 to June 13, 2017.

2.3.4 Inter-annual variability

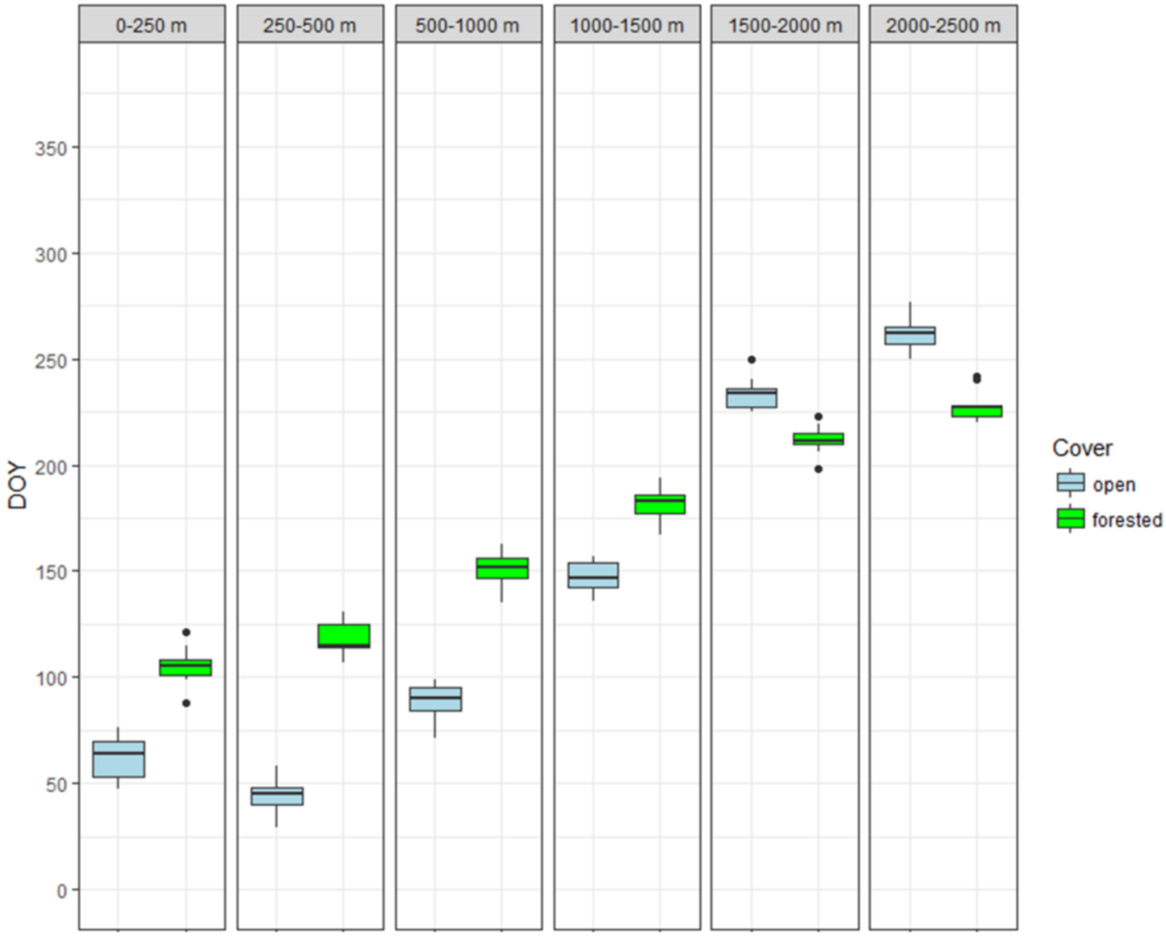

Figure 11: Averaged number of days that 1000 randomly sampled pixels were covered by snow, averaged across all pixels initially. Box plots represent distribution of pixel averages across years 2000 to 2008.

A general linear trend is evident in terms of the number of days with snow cover with increasing elevation resulting in increasing number of snow days (Figure 11). Interestingly, forested areas at lower elevations retain snow cover for longer durations, and this trend is reversed when observing the total number of snow days at the highest elevation bands.

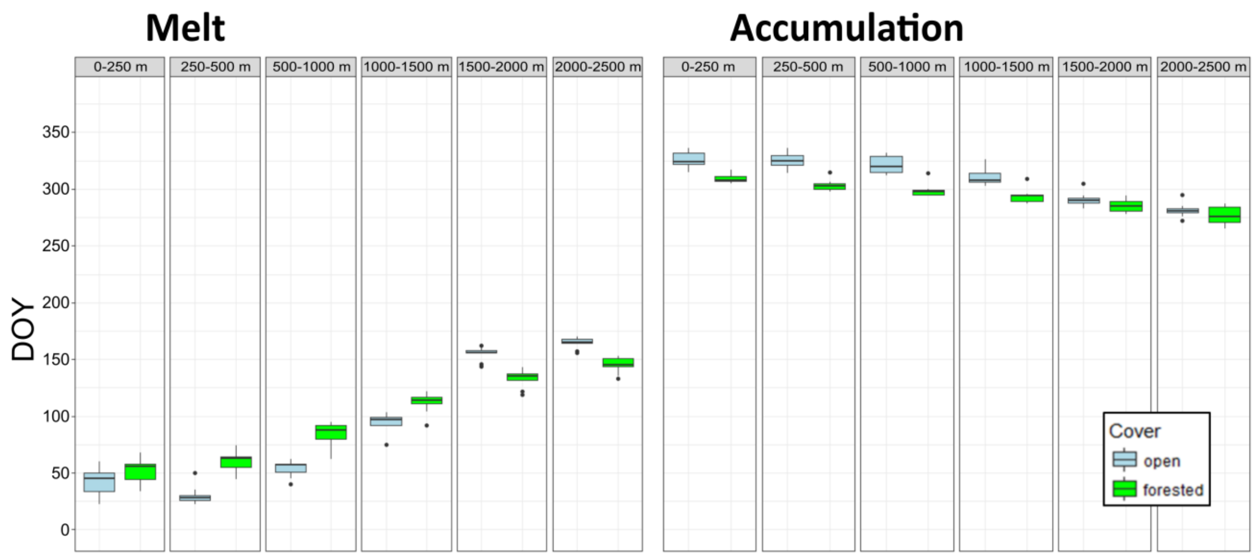

Figure 12: Comparison between transition DOYs within each elevation and land cover class, for the melt and accumulation periods. The 9 averaged transition DOY values from each of the 9 years were used to generate the final inter annual averages summarized in the box plots above.

A similar linear relationship between elevation and the beginning of the melt (lowest median to highest = 45 to 165) and accumulation periods (median range = 325 to 276) is apparent. Within each elevation strata, the same trend appears in the melt period as it does in Figure 11, with forested areas retaining snow cover longer than open areas until 1500 m. The average difference in the median for the first 4 elevation bands is 23.5 DOY. Again, for the two highest elevation bands, the trend is then reversed, the average difference in the median decreasing to 20.5. For the accumulation period, forested areas consistently retain snow cover earlier in the season compared to open areas, with the gap between land cover types gradually decreasing as elevation increases. The lower 3 elevation band's average difference in the median is 20, and the higher 3 is 8.

2.4 Discussion

The MODSAT-NDSI algorithm has been shown to be capable of utilizing a large quantity of data from two spatially and temporally divergent optical remote sensing instruments. Through the relatively simple computation of averaging and deriving difference ratios, the NDSI metric common to both instruments can be used to enable accurate, frequent, and fine-scale snow mapping. The development of a snow cover product that is daily, and 30 m spatial resolution, allows finer detail predictions of snow occurrence. Such predictions can be used for a range of applications, including improved wildlife habitat research (Hamer & Herrero, 1987; Luccarini, Mauri, Apollonio, Lamberti, & Ciuti, 2006; Schwartz et al., 2009) and hydrologic modelling by increasing spatial and/or temporal resolution of snow cover maps (De Lannoy et al., 2010; Flint & Flint, 2012; S. Härer, Bernhardt, & Schulz, 2016; Wood et al., 2011).

The use of publicly available climate data as well as time lapse camera networks has allowed for the validation of the algorithm using over 30 sites. Cameras provide information on snow cover visually, rather than through a calibrated measure of distance, as is the case of sensors which have a known ground level, and then emit an active pulse. Depth, and in turn the presence or absence of snow, is determined by the time taken for the pulse to return to the sensor. The lack of visual confirmation from these sonic sensors can be prone to error, especially when snow pack reaches shallower depths (Lundberg, Granlund, & Gustafsson, 2010; Ryan et al., 2008; Varhola, Wawerla, et al., 2010). The camera method is an economic, efficient alternative (Farinotti, Magnusson, Huss, & Bauder, 2010; Fortin, Jean, Brown, & Payette, 2015) allowing for the monitoring of snow cover and depth using stakes at a particular point in the foreground, while also potentially observing spatio-temporal changes in snow cover over the greater landscape in the background (Parajka et al., 2012a).

The algorithm performs well overall, achieving an accuracy of 90.41 % when accounting for all years, based on the independent validation data. Powers (2011) notes how the method of calculating accuracy should account for both a model's ability to predict true positive cases (i.e., precision) as well as true negative observations, or inverse precision. The model during the accumulation period is able to capture most instances of snow, generating low degrees of noise. However, as the total number of snow free instances decreases during accumulation, it becomes more likely that the few days that are snow free are included in the positive predictions. This does not greatly affect the signal to noise ratio of precision with an increasing sample size, but can greatly lower the signal to noise ratio of inverse precision or decrease inverse recall due to real negatives steadily decreasing in sample size. This effect is reversed during the melt period, as false negative predictions of snow are increasingly included in the growing number of false and true negative predictions.

The highest accuracy achieved using the training data necessitated NDSI thresholds to vary from season to season, and from open to forested areas. I argue therefore, as Stefan Härer, Bernhardt, Siebers, & Schulz, (2017) and others have, that NDSI is a less static snow detection tool, and can be tailored according to how different factors affect reflectance (Burns & Nolin, 2014; S. Härer et al., 2016; Stefan Härer et al., 2017; Maher, Treitz, & Ferguson, 2012; Racoviteanu, Paul, Raup, Khalsa, & Armstrong, 2009; Silverio & Jacquet, 2009; Yin, Cao, Chen, Shao, & Chen, 2013). In one case, land cover can affect the detection of snow by attenuating the signal within the visible or infrared spectrum. In such cases, a number of studies reveal how different combinations of landscape greenness (NDVI) can be used to reduce the threshold in forested areas to as low as 0.1, a threshold which in this instance still signals the presence of snow (Hall & Riggs, 2007; Molotch & Margulis, 2008). Härer et al. (2016) have also found that shadow alters results, and thus they calibrated the NDSI threshold value using shadow masks and camera-derived data for specific focus areas. The brightness, temperature, moisture content and grain structure of snow is also known to change over time, and thus has an effect on radiative reflectance and absorbance (Czyzowska-Wisniewski et al., 2015; Hall & Martinec, 1986; Hall, Riggs, & Barton, 2001; Salomonson & Appel, 2004). For example, when considering melt rates between different elevations, aspects, and degrees of canopy closure, the moisture in snow before melt is known to alter the crystalline structure. The altered structure scatters passive microwave radiation, attenuating the response of a portion of the electromagnetic spectrum often used to detect snow (Hall et al., 2001). Hall et al. (2001) also found that older snow crystalline structure changes from Lambertian to specular, which can result in the visible spectrum in multiband sensors being forward scattered, depending on viewing angle. In view of these considerations, it is important to note that the current MOD10A1 version does not set a binary threshold using the common NDSI > 0.4 method. The product's user guide explicitly states that the data from their algorithm is meant for users to utilize the full range of NDSI values in potentially more flexible modelling approaches, and to adapt thresholds based on locally relevant features/processes (Riggs & Hall, 2015).

For the focus area, the detection of snow based on NDSI thresholds appear to vary in response to season and forest cover. As snow pack develops, the albedo of snow tends to decrease (Amaral, Wake, Dibb, Burakowski, & Stampone, 2017), and this may be the reason for detection accuracies improving with lower NDSI thresholds during the melt period, as it allows the algorithm to be more sensitive to old but still present snowpack. The reason for using greater NDSI thresholds for open sites compared to forested sites was aforementioned, while the highest thresholds used for the accumulation period may be due to weaker signals of ephemeral and/or gradual snow accumulation from snowfall. Seasonally senesced features may also potentially reflect the visible and short-wave bands more similarly to snow during this period compared to spring or summer, and so only stronger NDSI signals may be indicating snow cover.

Based on the NDSI thresholds used, accuracy is shown to be high during the winter season (Figure 5E and 6), and less so in transition periods on average, likely due to the effects of the coast having differing accumulation periods than the interior in the fall. For the melt period, prolonged periods of snow cover persisting as late as June or July in the high elevation interior regions may result in albedo/reflectance changes large enough to warrant further tailoring of NDSI thresholds. There are also permanent ice/snow fields within the study area but they likely did not affect results, as the highest validation site was at 1969 meters above sea level. For winter habitat selection for ungulates, and other terrestrial species active during the peak of winter, the MODSAT-NDSI algorithm is particularly appropriate, for the fact that accuracy remains the highest during this period of time. For example, ongoing research identifying mule deer (*Odocoileus hemionus*) winter habitat identifies snow cover and/or depth as an important variable during the winter season, affecting movement rates and resource selection (Armleder, Waterhouse, Keisker, & Dawson, 1994; Doerr et al., 2005; Gilbert et al., 2017; Parker et al., 1984; Poole & Wright, 2010).

The results show that the MODSAT-NDSI algorithm is able to identify a clear linear trend between total snow cover days and transition periods against elevation (Figure 11 and 12). There is also a clear trend between the number of snow cover days and land cover type. The insulating properties of the forest canopy may be the cause of the significant difference between the timing of melt periods between the two land cover types (Figure 12). Comparatively warmer temperatures at lower elevations facilitate more rapid snowmelt rates as seasonal temperatures increase, while the tree shaded areas within the same elevations retain cooler temperatures, preventing snow from melting sooner (Anderson, 1956). The difference in the average median day of transition between open and forested is more than 3 weeks, resulting in forested areas at lower elevations having many more days of snow cover on average. The highest median difference being as much as 62 DOYs – or more than 2 months – for elevation strata 250 – 500 m. The trend may reverse at the highest elevation bands due to the same reason: temperatures remaining cold at the highest elevations may allow for the persistence of snow in open areas, while tree cover may intercept snow fall and insulate enough heat to promote ablation sooner for snow under the canopy. Otherwise, the presence of generally greater volumes of snow at the highest elevations results in a greater length of time needed for snow to melt completely.

Chapter 3: Will mule deer preferentially select locations with decreased fractional snow cover and of greater canopy interception (i.e., areas providing shelter and forage)?

3.1 Introduction

In recent years, the challenge of adapting habitat management for winter survival in migratory ungulates has driven wildlife researchers to concurrently analyze how local environments may be changing, either due to climate change (Beschta et al., 2013; Wu et al., 2017) habitat loss (Bergman et al, 2014; Sawyer et al., 2006) or seasonality (O'Kane & Macdonald, 2018; Viana et al., 2018). The adaptive behavior of migratory ungulates permits individuals to take advantage of resources available between differing locations (Gilbert et al., 2017; Winkler et al., 2014). The mechanisms of migration and habitat selection form from a broad spectrum of behavioral characteristics, aspects of population ecology, and the constantly changing availability and location of resources and territory (Dingle & Drake, 2007; Messier, 1991; Robinson & Merrill, 2012). Therefore, an improved understanding of migration patterns and how changes in environmental conditions affect these patterns is a critical component in wildlife habitat management and research (Bohrer et al., 2014; Dodge et al., 2013; Gavashelishvili et al., 2012; Gillespie, 2001; Jonsen et al., 2003; Moore, 2011; Puckett et al., 2006; Schick et al., 2013).

The mechanisms involved in migration and habitat selection are noted in the literature to create unique challenges for land management due to continuously dynamic environments being altered by climate change and/or habitat loss (Moore, 2011; Poole & Wright, 2010; Rockwell &

Gormezano, 2009). However, recent advances in remote sensing technology enable land cover information to be updated at an increasing rate, allowing researchers to conduct fine-scale animal movement studies that may better explain how a constantly changing environment can affect daily or even hourly habitat selection decisions. In this study, I addressed the challenge of managing for ungulate winter survival by analyzing telemetry data of mule deer (*Odocoileus hemionus*) with novel, daily, and fine-scaled snow cover maps during both the winter as well as spring and fall "shoulder seasons". I sought to determine the effect that snow cover has on the seasonal selection of habitat, and hope my results will help inform management decisions about protecting winter range.

Mule deer are an economically and culturally important wildlife species, as well as an integral part of many other ecosystem services that are regulatory and supportive in nature (Anthony, 1977; Mackie, 1970; Putman, 1996). For many First Nations communities, including the St'át'imc, mule deer are an essential part of the diet, providing sustenance to those harvesting them as a source of protein. Many communities have also developed a deep reverence and connection to the mule deer, perpetuating both the cultural and recreational values and services attributed to the species (Poole & Wright, 2010; Procter, Bio, & Iredale, 2013).

There are several studies indicating declines in mule deer populations throughout various regions of North America and at different periods of time throughout the last 100 years (Anderson et al., 2012; Bergman et al., 2014; Mackie, 1970; Sawyer et al., 2006). Habitat loss and degradation continue to occur within mule deer range due to industrial development and resource extraction (Poole & Wright, 2010; Procter et al., 2013). Development is often associated with disrupting migratory routes to which mule deer retain a high fidelity (Lendrum, Anderson, Long, Kie, & Bowyer, 2012) and altering mule deer habitat selection to a level where they are likely forced into areas with less food, lower quality food or both. Most importantly for this paper, degraded habitat used in winter is also highly linked to decreases in annual survivorship, as reductions in forest cover allows for deeper snow pack to accumulate, burying potential forage and limiting mobility (Anderson et al., 2012; Armleder, Dawson, & Thomson, 1986; Bergman et al., 2014; Doerr, Degayner, & Ith, 2005; Parker, Robbins, & Hanley, 1984).

For mule deer and many other homeotherms in northern climates, winter has proven to be the seasonal period where a net energy deficit occurs (Armleder and Waterhouse (1994). Energy losses during winter are generally not recovered until later seasons, and if winter range habitat is arduous to traverse while providing little forage and shelter, fatal losses of fat reserves are likely to occur (Armleder et al., 1994; Parker et al., 1984). Therefore, quality winter range habitat that mitigates the effects of exhaustion and starvation is necessary for mule deer survival.

Mule deer winter range (MDWR) is characterized as areas occupied by mule deer during the winter, and the quality of MDWR has been associated with limited snow cover and adequate tree cover (Armleder et al., 1994; Doerr et al., 2005; Gilbert, Hundertmark, Person, Lindberg, & Boyce, 2017; Poole & Wright, 2010). Greater tree canopy closure is believed to ensure greater snow fall interception, resulting in unburied forage and snow that is shallow enough to traverse with limited effort. Knowing where snow cover occurs on the landscape during winter months at the ecologically relevant temporal and spatial scale is therefore important in winter range habitat selection research, since comparisons can then be made between winter ranges of varying proximity to forested and open areas, and snow cover in relation to Global Positioning System (GPS) radio collar point locations.

Previous studies have been hindered when characterizing MDWR habitat selection by inadequate snow data (Armleder et al., 1994; Doerr et al., 2005; Poole & Wright, 2010; Procter & Iredale), due to the disparity between fine spatial resolution snow map data and temporally frequent snow cover information. Therefore, data fusion techniques designed to combine the strengths of coarse and finer spatial resolution satellite instruments have been developed (Berman et al., 2018; as well as discussed in Chapter 2). Such snow cover maps can be especially valuable for wildlife telemetry data analysis, where daily or even hourly relocation frequencies and individual point data may require daily, fine-scale environmental data sets to best capture the conditions of the landscape and how species respond to such conditions (Berman et al., n.d.).

In this study, I integrated spatial and temporal dynamics of snow cover data from a newly developed data fusion algorithm (Mityók et al., 2018) into step selection functions (SSFs). I tested these snow data sets in this paper for the winter and also the spring and fall "shoulder seasons", in order to address the gap in knowledge between mule deer habitat selection and snow cover. I compare SSF model outputs calculating the relative probability of use against core model covariates, and demonstrated how novel data fusion snow maps can be incorporated into wildlife research which often requires finer-scaled environmental data. I subset GPS telemetry data of mule deer locations from three previous studies (Mitchell, Wilton, & Reynolds, 2012; Poole & Wright, 2010; Procter et al., 2013) to first test the efficacy of different types of snow cover information on different periods of the year: if snow cover persistence temporally increases in the shoulder seasons of spring and fall (hereafter spring/fall periods), then the relative probability of mule deer habitat selection decreases. The second hypothesis is: if snow cover spatial extent and distribution increases in an area during the winter, then the relative probability of selection for that area decreases. To compare results between the winter and spring/fall periods, I produced two separate step selection function models for GPS locations observed in the spring/fall periods and those retrieved in the winter. The final hypothesis is: wintering deer will select for greater canopy cover and forest edge and less bare ground and herbaceous areas compared to deer in the spring/fall periods, as the need for cover is greater during the winter where snow cover extent is greatest.

3.2 Materials and methods

An overview of the SSF and environmental data mapping methods is provided in subsequent sections. The SSF model selection steps and environmental covariates were used to develop the relative probability of use figures and maps found in the results section.

3.2.1 Study area for chapter 3

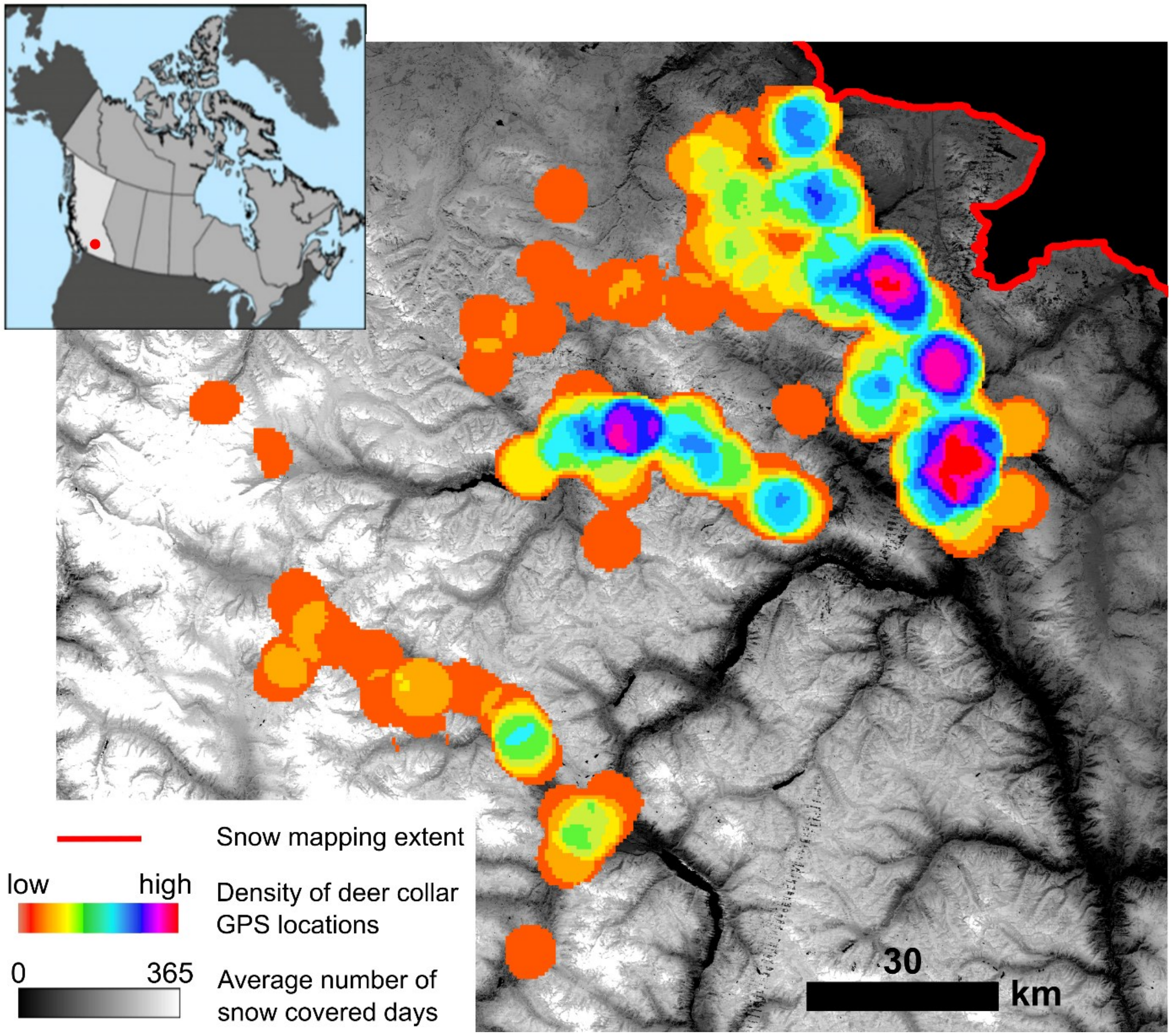

Figure 13: Entirety of the mule deer collar data extent, which includes the Northeastern extent of the St'át'imc territory located in south-central British Columbia, Canada. Total number of deer used in spring/fall periods SSF analysis = 77. Total number of deer used in winter period SSF analysis = 38. Spring/fall periods were from months April 1 – May 31 and September 1 – October 31, and relocation frequency was 1 hour. Winter period was from November 1 – March 31 and relocation frequency was 45 minutes.

This thesis' second study area is smaller than the extent used to develop MODSAT-NDSI, and includes portions of St'át'imc First Nations territory as well as surrounding landscape unit areas linked to Grizzly bear meta-populations, and is approximately 29,000 km^2. The landscape unit areas adjacent to the territory border were previously used to outline the study area extent in a land cover classification and change detection study (Chance, Hermosilla, Coops, Wulder, & White, 2016) (Figure 13). Consequently, this chapter uses the same northeastern boundary as Chance et al. (2016) to develop the environmental covariate maps used in modelling.

The St'át'imc First Nation's northeastern portion of the territory encompasses approximately 75 % of the smaller area used to analyze the mule deer GPS data, and is within prime mule deer habitat. Within the St'át'imc nation, mule deer have been in decline according to elders, with the Ministry of Environment's harvesting population index supporting this claim (Poole & Wright, 2010). The greater frequency and extent of industrial development and clear-cut harvesting is believed to have resulted in less available habitat for wildlife (Anthony, 1977; Mackie, 1970; Poole & Wright, 2010; Procter et al., 2013; Sawyer et al., 2006). Mining activities, road development, and flooding have resulted in cumulative impacts increasing wildlife mortality (Senger et al., 2008). Road networks developed for accessing timber have specifically been linked to increases in hunting pressure on mule deer and other wildlife, facilitating greater access into wildlife habitat (Boulanger, Stenhouse, & Margalida, 2014; Ciarniello, Boyce, Heard, & Seip, 2007).

In light of the archived literature by Mackie (1970, p. 23) and Wood (1949, p. 44), as well as the fact that many First Nations' elders are inciting the impetus to address the decline of mule deer populations, the “shifting baseline syndrome” is likely occurring in relation to mule deer. The syndrome describes how human beings misidentify contemporary population abundance as the baseline for a given species. Current generations are therefore unable to perceive real and potentially dramatic declines, while previous generations who remember healthier ecological conditions from their youth do (Pauly, 1995). Indications of the shifting baseline syndrome occurring for mule deer within the study area is not only supported by elders and government, but also by reviewing archived scientific literature:

“In summer, the deer range as high as the timberline. They are the most plentiful big-game animal. Around Spruce Lake or upper Tyaughton Creek, it is not uncommon to see 30 or 40 deer in the course of a day’s walk. However, Bralorne and Pioneer residents who hunt on the slopes adjacent to the Bridge River Valley claim that the animals are becoming fewer each year” (Wood, 1949, p. 44).

3.2.2 GPS collar data

Table 8: Previous mule deer research conducted within the St’át’imc territory and the sources of this paper’s GPS data.

Study	Number of deer	Sex	Region	Date Range	Minimum and Maximum Distance Travelled During Migration (km)
Poole & Wright (2010)	29	Female	Fraser Valley	2007 – 2009	2 – 94
Procter & Iredale (2013)	42	Male	Carpenter Lake Fraser Valley	2010 – 2013 2010 – 2013	16 – 40

Mitchell, Wilton & Reynolds (2012)	12	Female	Pemberton Valley	2010 – 2012	18 – 96

Migration routes and winter ranges have been recorded using GPS radio collars attached to a subset of the mule deer population within the study area in 2007 to 2009 and 2010 to 2014 (Poole & Wright, 2010; Procter and Iredale, 2013 respectively). Additional GPS data was used from the Pemberton and Upper Lillooet Valleys in 2009 to 2011 (Mitchell et al., 2012) (Table 8). Poole and Wright (2010) incorporated St'át'imc elders' Traditional Ecological Knowledge (TEK) by comparing GPS relocation data with the elders' delineated migration corridors to determine MDWR habitat beyond the area designated by Ministry of Environment (Poole & Wright, 2010). GPS data matched quite well with local TEK, demonstrating that mule deer retain high fidelity to their respective migration routes from year to year. Seasonal migration distances averaged to 50.3 km for the Pemberton Valley mule deer, all of which were migratory (Mitchell et al., 2012). The mule deer does analyzed by Poole and Wright (2010) included resident and migratory deer, where resident deer were identified in all previous studies as those with overlapping summer and winter ranges. Migratory does moved an average of 39 km from spring to summer range. Finally, among the migratory mule deer bucks collared by Procter and Iredale (2013), an average of 29.4 km were covered between summer and winter range. For this paper's analysis, I removed six deer due to having less than 500 observations within the winter or spring/fall period.

I defined the winter period – when mule deer are residing within their winter range – using the previous studies that identified seasonal ranges based on movement rate analysis and visually assessing movement patterns and herd density (Mitchell et al., 2012; Poole & Wright, 2010; Procter, 2013). Poole and Wright (2010) define winter range as between November 1 to late February. However, my study includes a large number of GPS relocation data from September 1 to October 31, as well as from April 1 to the end of May. From a total number of 551,158 GPS points used in this analysis, 55 % were obtained between the September-October and April-May periods. According to the aforementioned research as well as the Kelly & Reynolds (2015) study, spring migration has generally occurred later than March and fall migration begins in September. Therefore, I compared mule deer habitat selection in the spring and fall to selection patterns observed in the winter, with GPS collar telemetry data sets separated into a winter period data set from November 1 to March 31, and a spring/fall period using data from April 1 to May 31, and September 1 to October 31. Of 77 deer used in the spring/fall data set, 15 were resident deer. Of the 42 wintering deer, 5 were residents. In addition, I resampled the GPS locations to a uniform fix rate of 1 hour for the spring/fall GPS data set, and 45 minute intervals for the winter range data set, each having a tolerance of 15 minutes in order to include relocations that were not precisely recorded at the respective intervals. The difference in relocation sampling between the two data sets was the result of the previous studies programming alternate relocation frequencies according to season. For example, Procter and Iredale (2013) attempted locations every 45 minutes from May to June, and September to December in their Carpenter Lake study. Then, between January and April, they altered the relocation frequency to every 3.5 hours.

3.2.3 Satellite data

3.2.3.1 Snow covariates

My first two hypotheses test whether mule deer avoid areas of greater snow cover extent and persistence in both the spring/fall periods and in winter. I described snow cover extent and persistence by producing five different types of snow cover information in order to determine the type of snow cover information that is most significant when testing the first two hypotheses. The five types of snow cover information fall under either the spatial covariate group, or temporal covariate group (Table 9). Two of the five snow covariates are related to the spatial distribution of snow cover, and include snow cover extent and snow pack variability. The second group of snow covariates provide temporal information related to the timing and duration of snow events (Table 9). The five snow covariates were derived from the daily, 30 m resolution snow cover maps recently developed (Chapter 2), named MODSAT- Normalized Difference Snow Index (NDSI). The MODSAT-NDSI data set has values for every day of year (DOY) from 2000 – 2017. Snow covariate values were generated for the years of mule deer GPS observations (annually-derived covariates) and also averaged across the 18 years of available snow cover data (time-averaged covariates) in order to compare univariate models that used either yearly data that matched the GPS observation year or the long term average. I used Akaike's Information Criterion (AIC) to determine whether yearly or long term average snow covariates would be used in subsequent models (Burnham & Anderson, 2002). To differentiate long-term time-averaged snow covariates from annually derived covariates, I denote long-term information as average, and annual data as yearly. For all covariates including snow and other habitat covariates, I tested for collinearity by removing any covariates that were greater than 0.7 and performed worse than the best univariate model, according to AIC (D'Eon & Serrouya, 2005; Gilbert et al., 2017; McKee et al., 2015).

Table 9: The remote sensing environmental data sets used in step selection regressions. All snow related data was derived from MODSAT-NDSI (discussed in Chapter 2). Matasci et al.'s (2018) imputation algorithm generated the canopy cover maps for the study area. The St'át'imc Land Cover Classification and distance to forest edge maps were derived from Chance et al.'s (2016) land cover map.

Map Product	Abbreviated Covariate Name	Snow Covariate Type	Values	Spatial/Temporal Resolution
MODSAT-NDSI	(Ave)SW	Spatial	1 = < 25 % snow cover 2 = 25 – 50 % snow cover 3 = 50 – 75 % snow cover 4 = > 75 % snow cover	30 m daily Low pass filtered (120 m^2 kernel)
Total Snow Covered Days	(Ave)SUM	Temporal	1 – 365 days of the year	30 m yearly Low pass filtered (120 m^2 kernel)
Accumulation Date	(Ave)ACC	Temporal	1 – 365 days of the year	30 m yearly Low pass filtered (120 m^2 kernel)
Melt Date	(Ave)MELT	Temporal	1 – 365 days of the year	30 m yearly Low pass filtered (120 m^2 kernel)
Snowpack Variability Index	(Ave)VAR	Spatial	0 – > 1.4	30 m yearly Calculated using MODSAT-NDSI and applying Shannon's Diversity index on a 120 m^2 kernel
Percent Canopy Cover	CC	n/a	0 – 100 %	30 m yearly Low pass filtered (120 m^2 kernel)

St'át'imc Land Cover Classification	Bare & NTV	n/a	Bare = proportional coverage (%) Non-treed vegetation = proportional coverage (%)	30 m single year Calculated using 120 m^2 kernel
Distance to Forest Edge	DFE	n/a	Meters	Point to polyline distance Single year used
Digital Elevation Model	DEM	n/a	Meters above sea level	30 m

The first spatial snow covariate is snow rank (SW), and was produced using the snow cover classification values from the MODSAT- NDSI. I expected that an increase in the snow rank within a pixel – indicating greater snow cover extent – would decrease deer selection for that pixel area. Ecologically, I also expected that spatial snow covariates would affect mule deer habitat selection more than temporal snow covariates during winter, and therefore spatial snow covariates would replace temporal ones in the top winter model. The MODSAT-NDSI data set consists of pixels ranked for each day of the study period according to the strength of their NDSI signal, which corresponds to snow cover extent, and is therefore a 4-class model with values ranging from 1 to 4 (Table 9). For every pixel and every day associated with a deer GPS point observation, the snow rank ordinal category was appended to each GPS relocation to first obtain daily values. I averaged the daily snow rank values across the 18 years to provide a single time-averaged snow rank for each pixel for each day of deer observations, resulting in a continuous rather than ordinal covariate (i.e., average snow rank, or AveSW). I compared AIC scores for univariate models of the raw MODSAT-NDSI data set and the derived time-averaged daily data set. I generated univariate models separately for the winter and spring/fall period GPS data sets.

For winter and spring/fall periods, the time-averaged snow rank covariate performed better (an AIC difference of 4.3 and 35.1 respectively).

The second spatial snow cover covariate developed was the snow pack variability index (hereafter VAR). VAR was created to capture the degree of evenness of the four snow classes, which was done to quantify the degree of "patchiness" of snow cover across the landscape within a larger 120 m^2 area. The derived VAR snow map data set indicates zero or near zero occurs in regions where snow is not present, and therefore deer I predicted that deer most likely select areas with very low variability, especially at lower elevations where the chance of finding snow free ground is greatest. However, at the highest elevations where snow cover becomes largely unavoidable (i.e., very few areas with a value near zero or snow free ground); I expect deer to select areas with higher snow pack variability. A highly variable, "patchy" environment would be selected for at higher elevations as the chance of finding forage unburied increases with snow pack variability. VAR was calculated using Shannon's Diversity Index (Shannon, 1948):

$$H = -\sum_{j=1}^{z} p_j \ln p_j \tag{8}$$

Where j is the snow rank class and p_j is the relative proportion of the j^{th} snow rank to the total number of snow ranks occurring in each 120 m^2 pixel kernel. The natural logarithm ($\ln p_j$) of p_j is then multiplied against this proportion, summed across each snow rank, and multiplied by -1 to provide a final VAR between zero (indicating complete evenness or no variability) to approximately 1.4 (i.e., the highest degree of snow pack variability, where a given pixel has equal distribution among the 4 snow cover classes across the year). VAR values were calculated for each year of deer observations (yearly VAR), and time-averaged across all 18 years to produce AveVAR. For the spring/fall periods, yearly VAR performed better than AveVAR (Δ *AIC* = 17) while AveVAR was the better covariate for the winter period (Δ *AIC* = 65).

The second group of covariates defined as temporal snow covariates (Table 9). These timing-related measures of persistence are expected to affect habitat selection, where the greatest number of snow covered days, latest melt periods (with consequently the latest forage green up) and earliest start of winter dates all produce increasingly negative selection patterns. Ecologically, I also expected that temporal snow covariates would impact mule deer habitat selection more than spatial snow covariates during spring/fall, since there is much less snow and the timing of melt and accumulation would have the greatest effect on decisions to migrate and forage. Therefore, I expected temporal snow covariates to be in the top spring/fall model. The temporal snow covariates were calculated by first generating a binary daily snow cover map from raw MODSAT-NDSI rank values, where a snow rank value of 1 indicates no snow and rank values 2 – 4 indicates snow cover within a pixel (between 25 and 100 %) (Table 9). For spring/fall dates (i.e., ACC and MELT), I used a 16 day moving window to calculate the day of year (DOY) when there was at least 8 consecutive days of snow or snow free days for each year. Total number of snow-covered days (SUM) is the sum of each year's binary snow cover data set on a pixel-by-pixel basis. I calculated long-term temporal trends by time averaging the DOYs of ACC and MELT, and the snow day totals of SUM across all 18 years. For both the spring/fall and winter periods, yearly ACC, average MELT (AveMELT), and average SUM (AveSUM) performed best when comparing univariate models' AIC.

3.2.3.2 Other habitat covariates

For the third hypothesis, I predicted that deer would avoid areas with high canopy cover during spring and fall, as snow interception is less important at this time, and warmer temperatures facilitate greater forage biomass accumulation in open areas. All models included four core habitat covariates assumed to reflect the degree of snowfall interception or forage availability: canopy cover (as both a linear and squared term), distance to forest edge (hereafter DFE) and the proportional coverage of bare ground and non-treed vegetation (hereafter NTV). Percent canopy cover was a raster data set produced for each year of GPS data observations (2007 to 2014) from the imputation algorithm developed by Matasci et al. (2018) using both Light Detection and Ranging (LIDAR) and Landsat time series imagery. I expected deer to select intermediate canopy cover in winter, given the hypothesis that the optimal winter range habitat will provide tree cover as well as more open foraging space (Gilbert et al., 2017; Prokopenko, Boyce, & Avgar, 2017), and thus I include linear and quadratic terms for percent cover.

The remaining three core habitat covariates were derived from a classification map developed by Chance et al., (2016) for the St'át'imc Government Services Environmental Program. The classification map utilized Landsat Operational Land Imager (OLI) satellite imagery from 2014 and included three classes of non-treed vegetation: grassland, herbaceous land cover and shrub land. I combined the three classes into my single NTV land cover class. To produce a continuous variable from the NTV and bare ground class variables, I used a 120 m^2 kernel to calculate the proportional coverage of each class as a percentage within the larger kernelled area. I expected deer to avoid habitats that are more open during the winter compared to the spring/fall periods, since the winter would have the greatest spatial or temporal persistence of snow cover. Deer were expected to seek shelter and thermal cover more frequently due to increased snowfall that likely buries palatable herbs and shrubs and makes it more difficult to move within non-forested areas.

The “bare ground” class was combined from initially separate land cover classes of ice, urban, and barren/dirt/rock, capturing the types of areas that provide neither cover nor forage for mule deer, and consequently is expected to be avoided. However, with decreasing number of snow cover days or more shallow and uniform snow pack, and I expected that deer would increasingly tolerate and therefore increase selection for bare ground, in their search for forage. A 30 m digital elevation model was also incorporated into core models, but only when snow covariates did not correlate with elevation beyond a threshold of $|r| > 0.7$ (D’Eon & Serrouya, 2005; Gilbert et al., 2017; McKee et al., 2015).

Lastly, deer are believed to increase selection for areas closest to the forest edge during winter in order to balance the amount of cover and forage that they require according to changing conditions in snow pack and weather. The opposite effect is believed to occur during the spring and fall, where deer will avoid areas closest to the forest edge and venture out into much more open environments including alpine meadows and low-lying grasslands. I calculated DFE for each collar GPS relocation point using ArcGIS Pro (ESRI, Redlands, CA, USA) once all forest cover classes from the classification map were reclassified into a single forest class. I defined edge as the interface between areas classified as forested and areas containing bare ground, NTV or water.

3.2.4 Modelling habitat selection

Species distribution models which are explicitly proportional to the probability of use of a resource by a species are defined as resource selection functions (RSF) (Boyce & McDonald, 1999; Lele et al., 2013). The RSF has since been adapted in order to denote types of habitat as the culmination of specific types of resources being used; their relative importance incorporated as any number of independent variables (X_i) in a log-linear model:

$$W(X) = \exp(\beta_0 X_0 + \beta_1 X_1 + \ldots \beta_k X_k) \tag{9}$$

Where $W(X)$ is the relative probability of use. The log linear model is utilized in this thesis by adapting it into an SSF that uses conditional logistic regression to compare used and available locations rather than the steps within each strata. Each GPS point is denoted as a location, while every interval between consecutive locations for a given individual is a step. Each strata was the grouping of a single used and five random locations that were sampled for that single used observation.

I adapted the SSF approach of Gilbert et al. (2017), representing $W(X)$ as the relative probability of a location being selected, and using a 2-step modelling approach consisting of using conditional logistic and mixed-effects regressions. This method takes individual deer behavior into account by using the *survival* and *TwoStepCLogit* packages in R which develops population-level covariate coefficients from the two-step estimation method (Craiu, Duchesne, Fortin, & Baillargeon, 2011; Therneau & Lumley, 2018).

Compared to the relatively consistent directional persistence and greater distances between locations of migrating deer, those that have reached their respective winter ranges have been documented as having circuitous movements and long rest periods (Gilbert et al., 2017). Therefore, for this study, I determined that locations or points are more indicative of utilization distributions compared to steps. I randomly generated available locations for each used location using the exponential distribution of step lengths (i.e., λ^{-1}) and a uniform distribution of turning angles from each individual deer. Lambda (λ) was defined using twice the mean of observed step lengths to account for possible missed relocations to produce five alternative available locations for every used GPS location.

3.2.5 Model selection

I extracted the set of environmental covariates (Table 9) for each mule deer GPS relocation point and its associated five available locations. In cases where correlation between covariates was more than 0.7, univariate models were used to determine the best covariate to use based on AIC. Then, different combinations of covariates were grouped into four groups of models: models with no snow variables, (hereafter "core" models), core model + spatial snow covariates, core model + temporal snow covariates, and core model + both spatial and temporal snow covariates. Within each model group, different candidate models were tested by adding interaction terms for snow covariates. Snow interactions were included with the third hypothesis in mind: that a deer's selection for all other habitat covariates would change according to how much snow cover extent and persistence increases. Concurrently, interactions between different spatial and temporal aspects of snow cover are likely to interact. For example, deer are more likely to avoid areas where snow not only accumulated early, but also melted later in the year, since such areas would have forage buried for a much longer period compared to an area where snow accumulated early but also melted early. Twenty-three models were produced for the spring/fall periods and twenty-eight models for the winter (See Appendix A).

I fit the candidate models to the used and available locations for each individual deer. Models were then ranked using AIC values and weights. For each candidate model, all AIC weights from each individual deer were averaged to give the candidate model a mean AIC weight ($\overline{w}_i$). The model with the highest mean AIC weight was then selected for the winter and spring/fall period data sets (Burnham & Anderson, 2002; Gilbert et al., 2017). After the best candidate models were selected for the winter and spring/fall periods, I used the R package *TwoStepCLogit* (Craiu et al., 2011) to generate the population-level beta coefficients from the top models. The package performs mixed-effects regressions to estimate standard errors and coefficients, the latter used to calculate the relative probability of selection (*W(X))*. Resident deer were included in all modelling steps for both winter and spring/fall periods, while four deer were removed from the population-level winter regression due to the limited variability in snow rank (AveSW) observations, which produces a matrix singularity when using the *TwoStepCLogit* package. For the four deer removed, the standard deviation and variance of AveSW was less than 2 and 3 respectively, while the average of both metrics for all remaining deer were 45 and 2412. Therefore, 77 deer were used in the final spring/fall period population-level model, and 38 deer were used in the final winter period population-level model.

3.3 Results

3.3.1 Model selection

Contrary to expectations, mule deer habitat selection during the spring/fall periods was best explained by the spatial snow covariate: yearly snow pack variability (VAR, Table 10), rather than one of the three temporal snow covariates. For the spring/fall models, the two best performances utilized the yearly snow pack variability (VAR) snow covariate, while the second best model (SP2) included VAR as well as the average snow cover rank (AveSW). For a comparison between the top 3 spring/fall models and the remaining 20, including the model with no snow covariates, see Appendix A. Model SP3 incorporated the temporal snow covariate AveSUM, or the average total number of snow covered days along with AveSW. Only one winter model achieved a $\overline{w}_i$ of 0.10 or more (Table 11), with the remaining candidate models ranging from 0.0027 to 0.084 (see Appendix A). In the top winter model (W1), my hypothesis that mule deer would avoid areas with higher snow cover rank during winter was supported (Table 11). However, temporal snow covariates including the yearly start (ACC) and average end (AveMELT) of winter were also present in W1, with AveMELT also used as the interaction term.

Table 10: Top ranked mule deer model outputs including population-level coefficients (β) and standard errors in parentheses for the spring/fall periods. Interactions are indicated with a "×" symbol. Models with an AIC average ($\overline{w}_i$) of > 0.10 are reported, of which there were 3 out of 23 candidate models (i.e., models SP1, SP2 and SP3). Blank cells indicate that a variable was not used in the model.

Variable	Model SP1	Model SP2	Model SP3
	β (SE)	β (SE)	β (SE)
Yearly snowpack variability (VAR)	0.01 (0.008)	0.02 (0.02)	

Average snow covered days (AveSUM)			-0.004 (0.007)
Bare ground	0.002 (0.004)	0.007 (0.005)	0.001 (0.003)
Bare ground × VAR	-0.0003 (6*e*-5)	-0.0002 (7*e*-5)	
Bare ground × AveSUM			-9*e*-5 (4*e*-5)
Non-treed vegetation (NTV)	-0.006 (0.004)	-0.006 (0.005)	-0.004 (0.003)
NTV × VAR	8*e*-5 (5*e*-5)	-6*e*-5 (-6*e*-5)	
NTV × AveSUM			3*e*-5 (3*e*-5)
Canopy cover (CC)	7.06 (6.84)	1.01 (7.33)	-0.27 (4.96)
CC × VAR	-0.21 (0.08)	-0.16 (0.08)	
CC × AveSUM			-0.11 (0.04)
CC^2	-5.40 (4.88)	-10.06 (5.07)	-4.82 (3.36)
CC^2 × VAR	-0.003 (0.06)	0.06 (0.06)	
CC^2 × AveSUM			0.0008 (0.02)
Distance to forest edge (DFE)	-0.0006 (0.0007)	-0.001 (0.0006)	-0.0007 (0.0007)
DFE × VAR	-2*e*-5 (8*e*-5)	7*e*-6 (7*e*-6)	
DFE × AveSUM			-2*e*-6 (5*e*-6)
Elevation	0.0004 (0.0006)	0.0004 (0.0008)	
Elevation × VAR	-5*e*-5 (6*e*-5)	5*e*-7 (7*e*-6)	
Average snow rank (AveSW)		0.03 (0.01)	-0.02 (0.01)
AveSW × VAR		-0.0003 (0.0001)	
AveSW × AveSUM			9*e*-5 (7*e*-5)
$\bar{w}_i$	**0.162**	**0.158**	**0.103**

Table 11: Top ranked model outputs including population-level coefficients (β) and standard errors in parentheses for the winter period. Interactions are indicated with a "×" symbol. Models with a weighted AIC average ($\bar{w}_i$) of > 0.10 are reported, of which there was one (i.e., model W1). Blank cells indicate that a variable was not used in the model.

Variable	Model W1

	β (SE)
Average winter end date (AveMELT)	-1.66 (0.05)
Bare ground	-0.008 (0.003)
Bare ground × AveMELT	2e-5 (5e-5)
NTV	-0.003 (0.006)
NTV × AveMELT	6e-5 (7e-5)
CC	-3.41 (10.69)
CC × AveMELT	-0.07 (0.10)
CC^2	-2.52 (6.17)
CC^2 × AveMELT	-0.04 (0.06)
DFE	-0.0004 (0.0006)
DFE × AveMELT	1e-6 (1e-6)
Yearly winter start date (ACC)	-0.03 (0.02)
ACC × AveMELT	0.0006 (0.0002)
AveSW	-0.002 (0.001)
AveSW × AveMELT	4e-5 (1e-5)
$\bar{w}_i$	**0.171**

3.3.2 Individual variation

The following table highlights the individual-level variation in selection results (Table 12). The variance for each covariate's population-level coefficient was calculated using all estimated coefficients from each deer, using the top winter and spring/fall model (i.e., W1 and SP1 respectively). Therefore, mule deer individuals that respond similarly to a given environmental covariate, such as distance to forest edge (DFE), will have a very small variance value when the population-level coefficient is estimated (Table 12). Among all individual deer coefficients, the variance of the response to canopy cover (CC variable combinations) is greatest, being many orders of magnitude greater than other covariates.

Table 12: The variance-covariance matrix values of the regression coefficients calculated by the TwoStepCLogit package in R (Craiu et al., 2011). Blank cells indicate variables that were not used in either the top winter (W1) or spring/fall (SP1) model.

Variable	**Variance**	
	SP1	***W1***
Bare	0.0007	0.0001
NTV	0.0006	0.001
CC	2418	3681
CC^2	1137	1158
DFE	$2e$-5	$9e$-6
DEM	$2e$-5	
VAR	0.003	
Bare × VAR	$2e$-7	
NTV × VAR	$1e$-7	
CC × VAR	0.3	
CC^2 × VAR	0.2	
DFE × VAR	$2e$-9	
DEM × VAR	$1e$-9	
AveMELT		0.07
AveSW		$3e$-5
ACC		0.008
Bare × AveMELT		$6e$-8
NTV × AveMELT		$2e$-7
CC × AveMELT		0.3
CC^2 × AveMELT		0.1
DFE × AveMELT		$8e$-10
AveSW × AveMELT		$4e$-9
ACC × AveMELT		$7e$-7

3.3.3 Relative probability of use – spring/fall periods

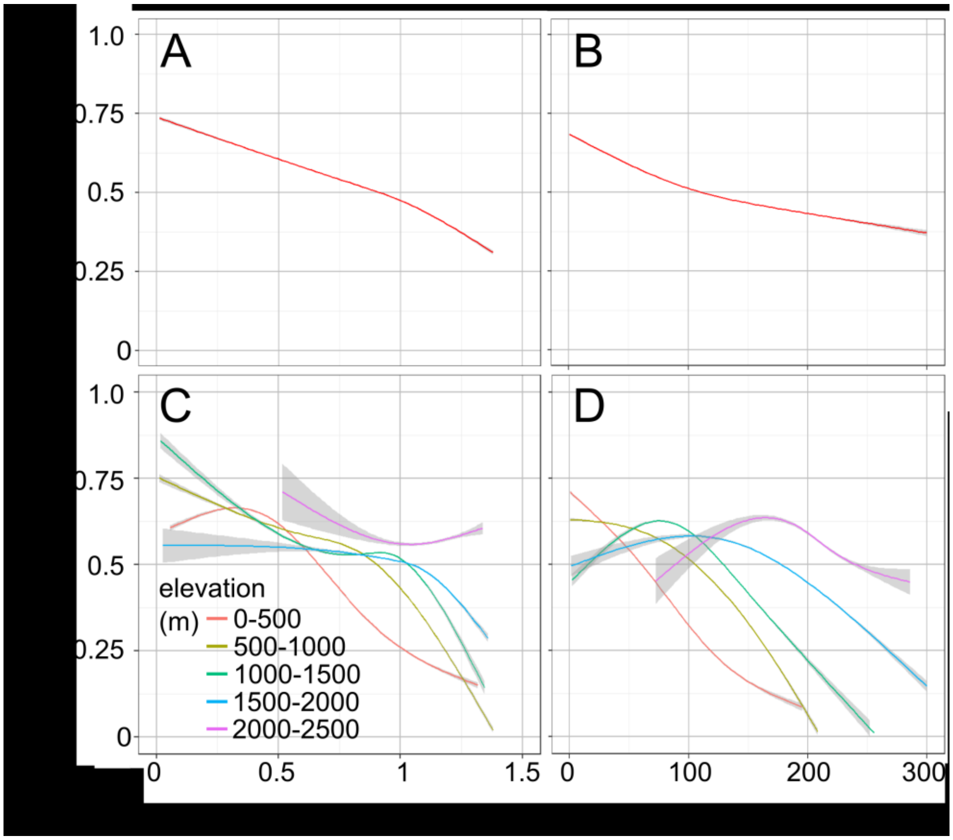

Figure 14: Probability of use plotted against the covariates used in the top population-level spring/fall model (SP1). The model calculated the probability of use for all 77 spring/fall mule deer's available GPS locations using SP1. Figure panels show cubic splines of 4 knots through 250,961 available locations. SP1 model contained the yearly snow pack variability (VAR) covariate (A) which was not correlated more than 0.7 with elevation. Therefore, elevation was also included in the model SP1 (C). The third best model SP3 included average number of snow cover days per pixel (AveSUM), which was plotted here (B and D) to compare selection responses to the covariate to VAR.

As expected, snow pack variability negatively affected deer habitat selection (Figure 14A). However, deer were more likely to select for greater snow pack variability at higher elevations

(Figure 14C), and when the average number of snow-covered days were fewest (Figure 14D). As shown in Table 10, model SP3 included average total number of snow cover days, with Figure 14B indicating how the temporal snow covariate negatively affects selection as the total number of snow cover days increases.

To compare the performance of models with and without the spatial snow covariate VAR, see Appendix B. Averaged AIC weights from all models (see Appendix A) were used to calculate the evidence ratio between models containing each of the snow covariates. The evidence ratio is used to determine how many times more likely a model is the best model compared to the one it is being compared to (Wagenmakers & Farrell, 2004). Appendix B provides an evidence ratio of each snow covariate compared to those models containing both the core covariates and the DEM.

3.3.4 Relative probability of use – winter range

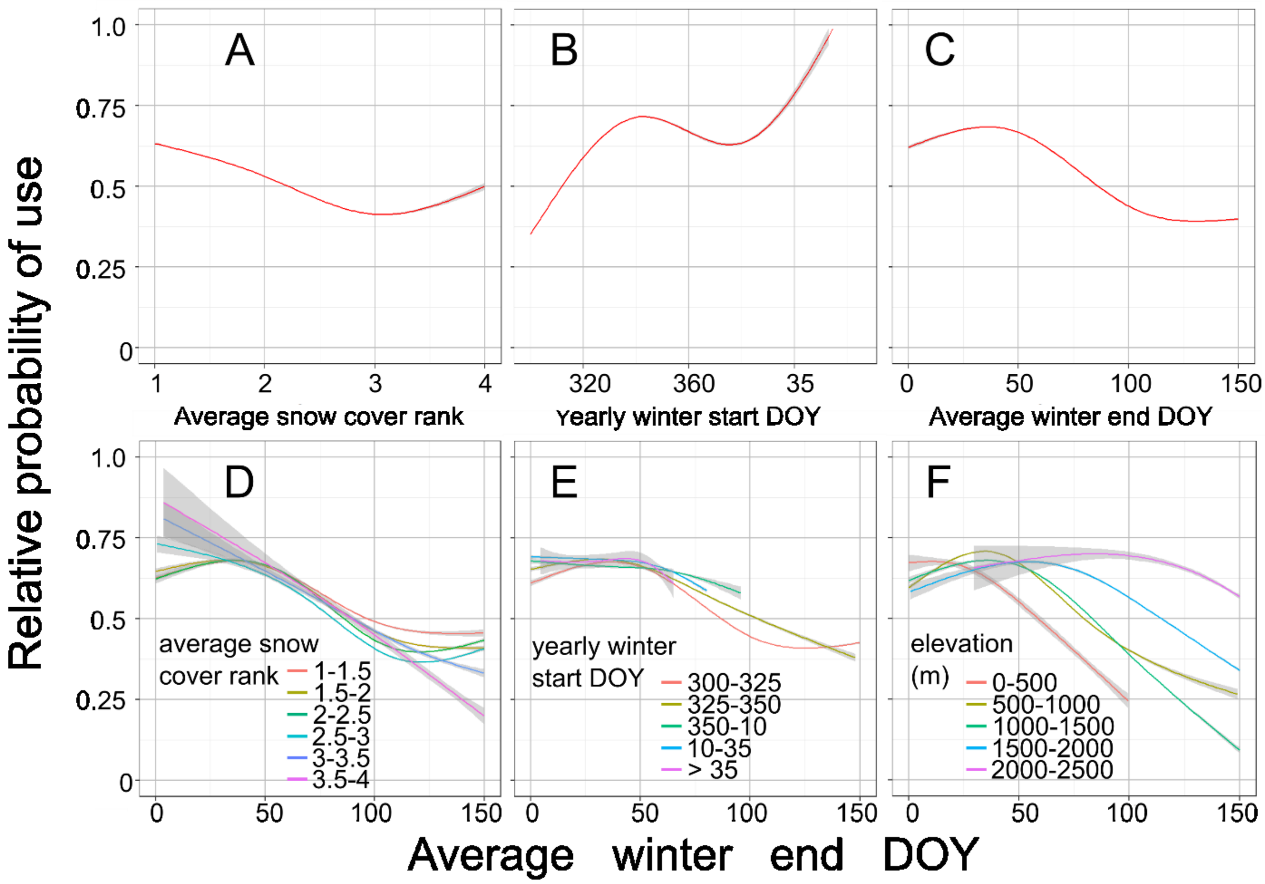

Figure 15: Probability of use plotted against the covariates used in the top population-level winter model (W1), with the exception of elevation. The model calculated the probability of use for all 38 winter mule deer's available GPS locations using W1. Figure panels show cubic splines of 4 knots through 207,580 available locations. The top model containing average winter end (AveMELT) day of the year (DOY) as an interaction term is shown separately (C). The other two snow covariates appearing in the top ranked model were average snow cover rank (AveSW) (A) and yearly winter start (ACC) DOY (B). AveMELT's interaction effects on the two other snow covariates (D and E) and elevation (F) is presented.

During winter, probability of selection decreased with greater snow cover rank (Figure 15A), earlier winter start DOY (Figure 15B) and later winter end DOY (Figure 15C). This combination of spatial and temporal snow covariates within the top model support the second hypothesis, which predicted that greater snow cover extent and persistence would decrease the probability of selection for an area by mule deer. The result also highlights the fact that temporal snow data also affects habitat selection, not just the spatial extent and distribution of snow cover. In locations with later winter end DOY, deer were least likely to select for high snow cover (Figure 15D) and early winter start DOY (Figure 15E). Within different strata of elevation, probability of selection decreases as average winter end DOY increases, but mule deer at higher elevations show to be more tolerant of more persistent snow cover (Figure 15F).

3.3.5 Relative probability of use – other habitat covariates

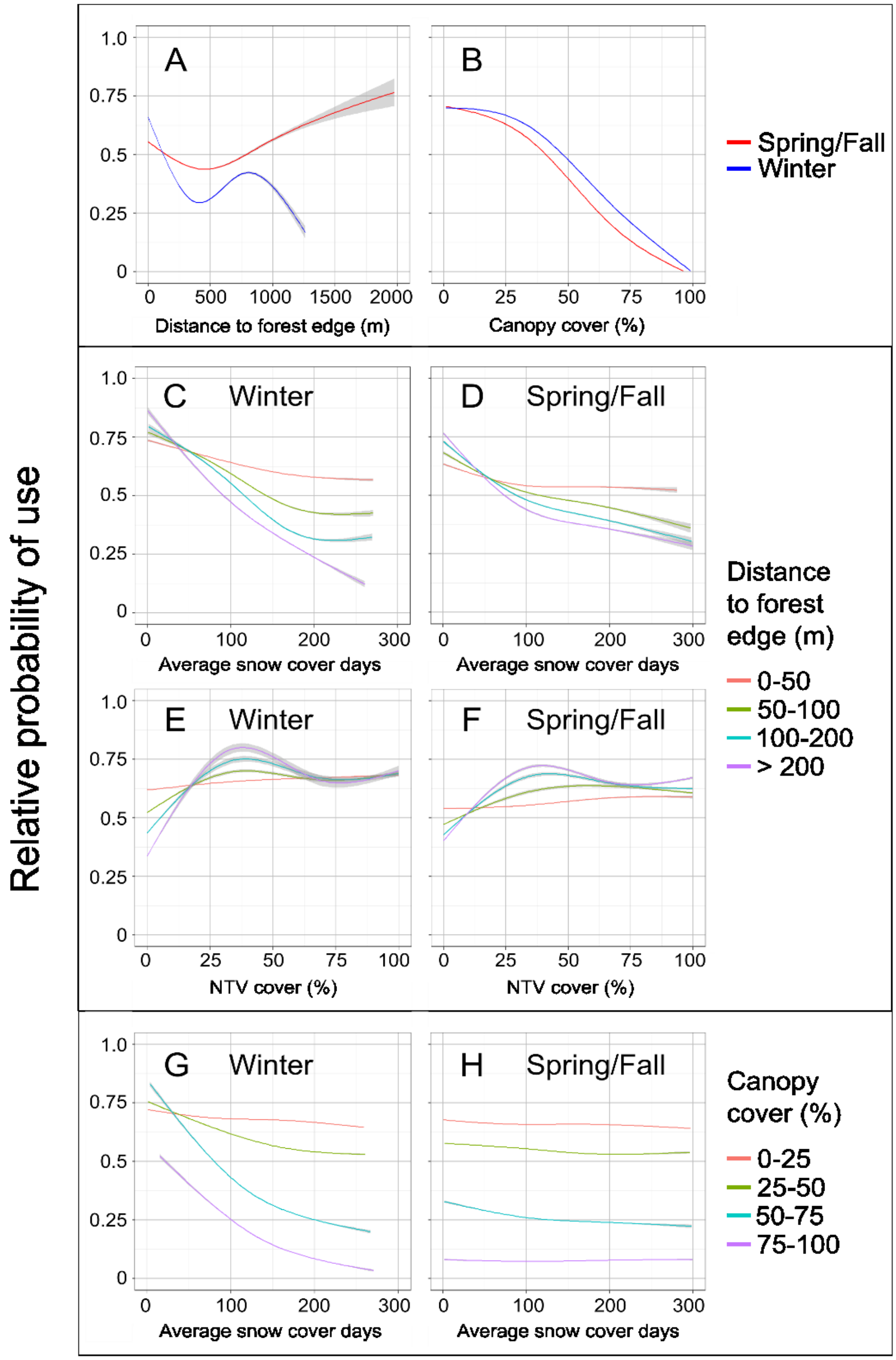

Figure 16: Figure panels A and B display only core forest covariate results, comparing winter to spring/fall. Distance to forest edge (DFE) results show smoothed available locations are also stratified by average number

of snow-covered days (AveSUM, Figures 16C-D) or Non-treed Vegetation (NTV, Figures 16E-F). Canopy cover results plotted against the relative probability of use and stratified by AveSUM are shown in the final two panels G and H.

Figure 16A supports the third and final hypothesis, showing that with increased snow cover and persistence in the winter compared to spring/fall, deer are more likely to remain close to the forest edge. DFE however, also affects mule deer habitat selection depending on the degree of snow cover and persistence. Mule deer will most likely select areas closest to the forest edge as the extent and persistence of snow increases (Figures 16C and D). Canopy cover (Figure 16A, G and H) had little change apart from when locations were also stratified according to the average snow cover days, in which case wintering deer appear to select greater canopy cover in areas with less snow, the opposite of what I expected (Figure 16G). Figure 16E and 16F are displayed in order to note the optimal proportion of NTV selected for according to how far deer are from the forest edge, showing that deer are more likely to use areas with approximately 30 – 40 % NTV cover in both the winter and spring/fall when furthest from the edge.

Not all combinations of plot results are reported here (Figure 16), as several showed no notable trends (for example, proportional coverage of bare ground). Initial data exploration of used deer locations however, showed greater variability of NTV and bare ground land occurrence as a percentage during the spring/fall periods. During winter, deer are more restrictive of their use of the same covariates, particularly with bare ground, which consists of no more than 20 % of the proportional cover at any time on average (See Appendix C).

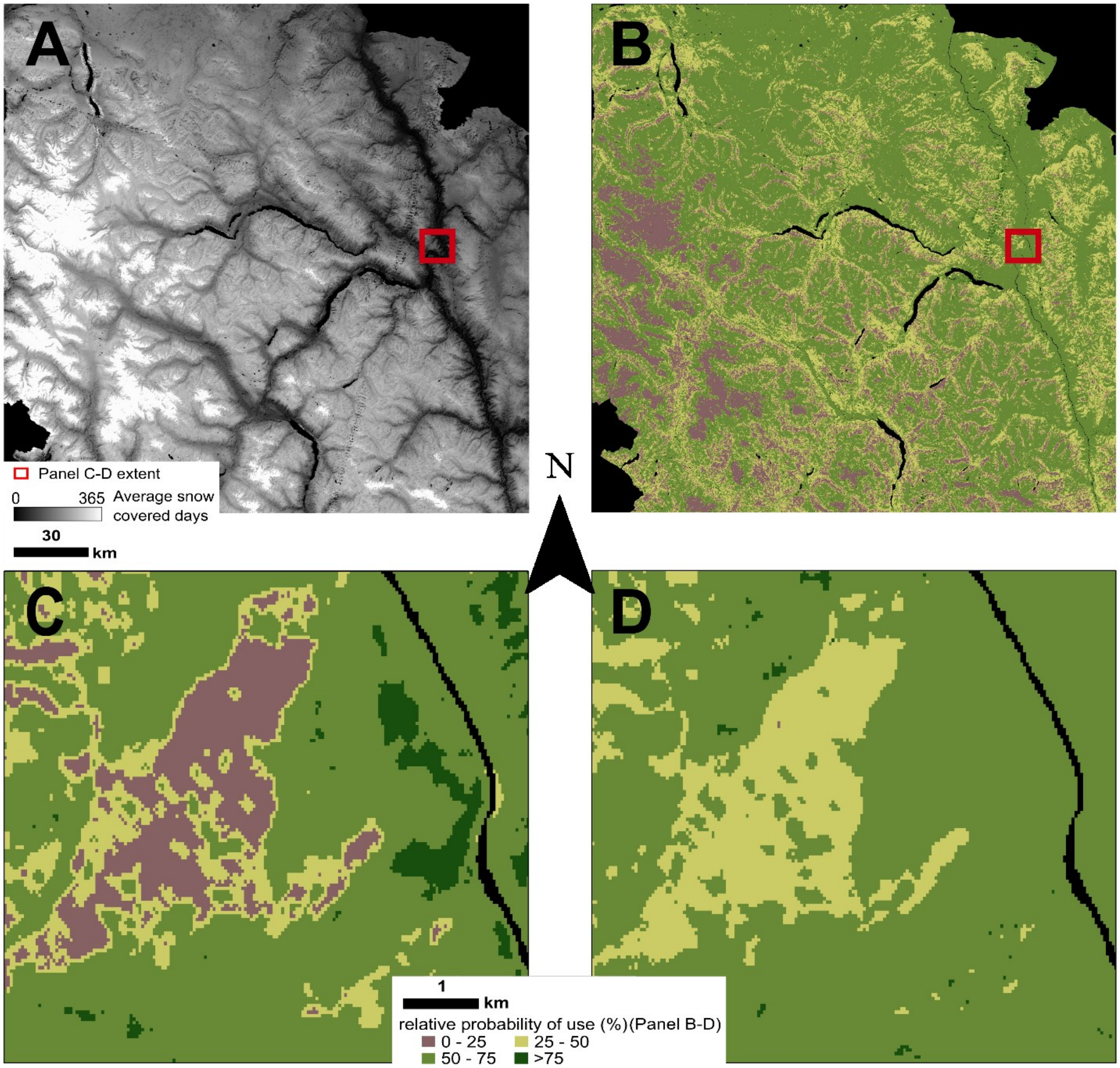

Figure 17: Average number of snow cover days (AveSUM) map for the study area (A) and model-predicted habitat selection probability in winter (B). Habitat selection probability maps were calculated using population-level model coefficients multiplied by each model covariate by using pixel values from the map data sets (see Table 9 and Equation 9). In order to compare finer-scaled predictions of relative probability of use, a smaller geographic area is shown for demonstration, using spring/fall (C) and winter (D) population-level models.

The two top models calculated and mapped the relative probability of habitat selection using their respective beta coefficients across the study area (Figure 17). Deer are shown to be less likely to select particular patches during the spring/fall compared to the winter period, based on top population-level model outputs (Figure 17D, large yellow area compared to the similarly shaped purple area of 17C). During the spring/fall periods, deer are most likely to be in open, low-lying grassland, in this case along the benches of the Fraser River (Figure 17C, darkest green areas).

3.4 Discussion

A 2-step SSF modelling approach has been developed to address information needs associated with potential mule deer winter range habitat requirements using fine temporal and spatial snow cover map information. Herein, I demonstrate the applicability of using such snow cover maps over large areas by presenting relative probability of use results from models developed from two large GPS data sets. The production of more nuanced snow cover information from the daily MODSAT-NDSI maps highlights the inherent flexibility that is now possible when developing habitat selection models. More specified environmental covariates allows researchers and land managers to examine wildlife responses to more precise characteristics of snow cover dynamics.

As indicated in my methods and results, utilizing remote sensing technologies to improve the spatial and temporal resolution of environmental data has many benefits, with snow cover being one of the key sets of information used to model fine-scale wildlife movement and habitat selection (Robinson & Merrill, 2012; Schwartz et al., 2009). I have shown that the resulting outputs from MODSAT-NDSI improves models of mule deer habitat selection for both winter range and periods in the spring and fall (Table 10 and 11, as well as Appendix A and B).

Gilbert et al. (2017) note how the discipline of wildlife habitat selection analysis increasingly recognizes the complexities involved in fine-scale and time dependent movement behavior. Models incorporating estimators that vary through time have captured ecological dynamics in a more intuitive manner (Gilbert et al., 2017; Kie et al., 2010; McLoughlin, Morris, Fortin, Vander Wal, & Contasti, 2010; van Beest, Van Moorter, & Milner, 2012). Individuals of a species can have varying life histories, and adapt and respond to external stimuli in innumerable ways according to resource availability and temporal cues. Such plasticity in selection behavior points to a need for less mechanistic and static models while calling for a greater ability to characterize complex adaptive systems (Levin, 1998; Trifa, Girod, & Collier, 2007) when testing hypotheses. Consequently, I incorporated snow cover dynamic information averaged over 18 years, time-varying predictors updated for each year of deer observations, and average fractional snow cover ranks adjusted for every day of the year when developing step selection function models. These snow covariates have been produced from a daily 30 m resolution snow cover data set in order to utilize the power of data fusion remote sensing technologies while attempting to best capture the temporal and spatial snow cover conditions that wildlife experience on what can now be an hourly or sub-hourly rate.

Gilbert et al. (2017) showed that depth of snow is a key predictor of habitat selection for mule deer in Southeast Alaska. The study found that models incorporating snow depth and any other combination of covariates ubiquitously indicated deer selecting against snow depth. If models incorporated a degree of habitat availability, defined as landscape configuration and composition at a given time, snow cover information could be used to determine the direction and magnitude of selection for these variables, such as old versus second growth forest or shrub biomass. The aforementioned study did not explicitly include canopy cover as a covariate, but rather different degrees of forest stand age and volume. The snow depth model generated in the study also required specialized field equipment and measurements, as well as regionally specific models acquired from previous research (Gilbert et al., 2017). Gaps in knowledge that this paper addressed included the explicit relationship between habitat selection and canopy cover as a percent for populations in south-central British Columbia. The snow cover information that this paper used are from data sets that are more readily available to both scientists and land use managers in the form of thematic maps, which may be generated for any area without field measurements of depth or locally developed linear regression models. Therefore, this paper also sought to evaluate the efficacy of using other metrics related to snow cover besides depth in habitat selection research, and proved that certain types of snow cover information utilized in different combinations for different seasons generate the best performing habitat selection models (Table 10 and 11; Appendix A and B).

3.4.1 Relative probability of use – spring/fall periods

This study also found that the effects of individual snow cover dynamic variables on mule deer habitat selection differ as seasons change (Table 10 and 11), with the core spring/fall periods model producing the highest weighted AIC score once yearly snow pack variability was included and with an interaction term. This result addresses the first question concerning the affect that snow cover dynamics may have on habitat selection during spring/fall periods. Yearly adjusted snow pack variability suggest that during spring/fall periods, snow that remains present on the landscape does continue to have an effect on deer movement and habitat selection, and the relationship between snow pack variability and habitat selection is strongest when accounting for changes in snowpack variability conditions year to year. In addition, Figure 14C and 14D show that when colder temperatures allow snow pack to accumulate sooner or persist during spring longer, the variability of the snow pack becomes an important determinant in finding forage in unburied patches or through varying depths in snow cover.

3.4.2 Relative probability of use – winter range

In addressing the second question: how and what aspect of snow cover dynamics affect winter range habitat selection, the top winter model was found to include the long term or average winter end date while concurrently utilizing yearly changes in winter start date (Figure 15). The reason for one covariate being averaged while one is yearly adjusted may relate to one process being more consistent and gradual than the other. Snow ablation may be a more stable and therefore consistent process through time. Indeed, hydrologic models using parameters such as snow grain size and temperature have been shown to better predict snow melt compared to models using snowfall (Marshall & Oglesby, 1994). Variance in relative changes in snowfall and accumulation however may be best explained by more complex wind field models compared to comparatively static land cover parameters (Varhola, Coops, et al., 2010; Winstral & Marks, 2002). In terms of deer ecology, results from Figure 15 may highlight the fact that deer will select areas where snow melts the earliest in order to locate the earliest greening forage to replenish the negative energy balance incurred during winter (Garrott, White, Bartmann, Carpenter, & Alldredge, 1987). Garrott et al. (1987) also note how harsher winters result in physiologically weaker deer, and therefore Figure 15 supports the idea that mule deer will most likely select areas where the severity of winter is comparatively milder in terms of winter length (i.e., where winter begins later and ends sooner). In addition, the average snow cover rank covariate in the winter range model has selection trends reversing at particular ranges (Figure 15A), suggesting other interactions may begin to affect selection within such areas. For example, snow pack that has allowed to accumulate over the entirety of the winter season may result in a uniformly snow covered landscape by late March – early April, but generally increasing temperatures entice deer to select for or travel through such areas despite them likely having a snow rank of 4. The yearly winter start day of year (DOY) (Figure 15B) also appears to affect selection differently between the 340th DOY (i.e., the second week of December), and the middle of January of the following year. Interactions that were not considered in this analysis that may be affecting selection during this time may include inter species competition, predation and hunting.

From the last three panels (Figures 15D, E and F), it is apparent that the additive effect of having later melt periods, greater fractional snow covered area and earlier winter start dates generates the most negative trends in winter range habitat selection. Although average fractional snow cover describes current snow cover conditions in terms of distribution across the landscape, the inclusion of temporal dynamics in snow cover better describes current conditions. Earlier accumulation and later melt may be a proxy measure for snow pack depth, and may better explain the additional processes that may be occurring at ranges where selection probability trends reverse. If there are many regions for example, where winter begins later but the same areas eventually accumulate much deeper snow packs that persist longer into the spring, then deer habitat selection for such areas may remain less probable compared to other sites.

3.4.3 Relative probability of use – other habitat covariates

Figure 16 characterizes the type of habitat mule deer would be using when avoiding snow cover and persistence. Contrary to my hypothesis, canopy cover selection appears to remain relatively similar in both the spring/fall and winter periods (Figure 16B), while individual variation in response to this covariate was found to be the greatest among both spring/fall and winter deer (Table 12). Differences in the use of forest edges, however, was more pronounced between periods (Figure 16A), where increases in snow cover extent and persistence increased the probability of selection for areas closer and closer to the forest edge. Interestingly, the only identified trend between canopy cover and snow appeared in the winter range data set when the total number of snow covered days would be plotted against relative probability of use (Figure 16G). Although the average number of snow cover days was not a snow covariate appearing in the top winter model, the result is reported here as it shows selection of denser canopy cover is highest within regions of low snow cover and decreases as snow cover days increases. This suggests that deer select for denser canopy cover for reasons other than snowfall interception. Large varying degrees of predation risk between deer may account for this discrepancy, and also may help to explain the large variability in individual responses to canopy cover.

In terms of DFE, all snow covariates for both winter and spring minimally affect the probability of selection when deer are closest to the forest edge, and as the distance increases along with snow cover and/or persistence, selection becomes increasingly more unlikely (Figures 16C-D).

One of Gilbert et al.'s (2017) hypotheses included the prediction that if snow depth increased while both canopy interception and forage would be available, deer would most likely select such an area above one which only provided cover. To some extent, this hypothesis is supported in this paper, since mule deer appear to prefer to remain near both open and forested areas even when snow cover extent and persistence is greatest, rather than retreat further into the forest.

The probability of selection for non-treed vegetation was found to be highest in areas furthest from the forest edge, with NTV comprising 30 – 40 % of a given 120 m^2 area (Figure 16E-F). These last two panels support the notion that deer select for ecologically complex and heterogeneous landscapes when not seeking shelter along the forest edge, but rather preferring habitat that has a mix of both NTV and approximately 25 % canopy cover or less (Figure 16B).

Chapter 4: Conclusions

The aim of this thesis was to establish the feasibility of applying a novel fusion algorithm to snow cover map data sets and use such data sets to analyze mule deer habitat selection patterns within south-central British Columbia. To accomplish this task, I downloaded Landsat and MODIS satellite imagery and used them as inputs in the MODSAT-NDSI data fusion algorithm. I assessed the accuracy of the new maps using 33 validation test sites, and used the original map data output from the validated MODSAT-NDSI algorithm to derive further snow map data sets. These new snow map data sets were used as environmental covariates in a step selection analysis of mule deer GPS relocation points. Finally, I have assessed results from the step selection function to determine biological implications.

4.1 Overview of answer to main research question: How can the understanding of mule deer winter habitat use be improved by remotely sensed snow cover dynamics?

I answer the main research question by first obtaining the aforementioned results from the MODSAT-NDSI distribution layers, which will likely be relevant to a range of potential users, including forestry, conservation and land management groups. I generated daily 30 m snow cover maps for years 2000 – 2017 with an overall accuracy of 90%, using 33 validation sites distributed throughout south-central British Columbia. Analyzed snow cover trends across stratified elevation bands and land cover types reveal that snow cover persists under lower elevation forests for an average of 23.5 days longer than in adjacent open areas during spring. The algorithm itself is a flexible, computationally simple approach that may be applied to any other area of interest, to other metrics (a MODSAT-NDVI algorithm for example) and even to satellite imagery other than MODIS or Landsat, as long as there is a common metric produced between a coarse and fine resolution instrument. The case for improving spatial and temporal resolution simultaneously for snow cover is strengthened by the fact that snow cover is highly variable at scales even finer than 30 m, particularly within more complex and heterogeneous landscapes. Ultimately, this research could provide greater certainty in land use decisions by producing a snow cover maps that can be used to estimate snow meltwater volume and timing, an important piece of information in hydrology, fish and wildlife studies. Emergency preparedness for floods and avalanches would require detailed snow maps to estimate snow meltwater as well, and would additionally use such maps to estimate snow pack depth, extent, and volume. Emergency preparedness for wildfires may also find snow cover maps valuable by using them to determine sites that are driest and wettest as snow cover begins to ablate. Evaluations of road/working conditions for forestry operations and other industrial activities would also require readily updateable snow maps in order to decide where and when harvesting operations should occur.

Secondly, I utilized more than 70 individuals across 8 years of deer telemetry data in the second part of my analysis. Individual variations in responses are accounted for when generating population-level habitat selection trends, and my findings of mule deer responses to forest edge against multiple aspects of snow cover timing and distribution provide support for preserving forested habitats for mule deer. In particular, those forested habitats naturally occurring within the dry interior Douglas Fir (*Pseudotsuga menziesii*) and Ponderosa pine (*Pinus ponderosa*) forest stands, which have characteristically less canopy cover at lower elevations compared to higher elevations (Pojar, Klinka, & Meidinger, 1987). In addition, it also would be important to conserve those forested habitats providing enough variability in land cover to facilitate readily adaptive changes in selection patterns, such as utilizing cover and forage interchangeably. The forest/open area interface facilitates such adaptive behavior in response to current resource needs (Alaback, 2010; Gilbert et al., 2017). In terms of snowmelt and accumulation, the melt and accumulation periods of snow pack differ between open and forested sites within the study area as discussed in chapter 2. However, the forest/open area interface can provide complex microhabitats, integrating characteristics from both forested and open landscapes in terms of moisture regime, shade, precipitation interception, forage, concealment from predators, and snow pack patchiness.

4.2 Significance of research

The main novelty and significance of this work falls in two areas. First, this thesis develops a novel algorithm MODSAT-NDSI to harness the strengths of both coarse and finer spatial resolution imagery by fusing MODIS and Landsat normalized difference snow index (NDSI) data. The MODSAT-NDSI approach captures temporal and spatial advantages of freely available snow cover datasets and can be modified to suit a variety of novel investigations relating to snow cover or other spectral indices. I found notable differences in the timing and duration of snow cover between different land cover types and elevation gradients. This thesis also utilized the MODSAT-NDSI snow maps to produce additional temporal and spatial information concerning snow cover that are new for the region, and included such snow information as variables in step selection analysis to evaluate mule deer habitat selection behavior.

The second area concerns habitat modelling. I demonstrate how novel snow maps produced from data fusion algorithms could be incorporated into wildlife telemetry research that often requires environmental data to be at finer temporal and spatial scales than is typically available. It is now shown that mule deer negatively selected for all variables associated with increased snow cover and longer snow cover duration. Mule deer selected areas nearest to forested habitats during the winter while the selection pattern reversed during the spring and fall. In addition, the relative probability of selection of canopy cover as a percentage did not notably change from fall to spring, highlighting the fact that habitats with greater heterogeneity in terms of snow cover distribution and land cover types within the forest/herb/shrub/grassland interface are a more significant factor in selection during the winter seasons.

4.3 Implications

This research is a partnered effort between SGS, the MITACS organization, and the University of British Columbia to help recover and maintain the health of regional mule deer populations. An improved understanding of how snow cover and timing has been affecting where mule deer migrate and seek shelter in the winter will allow St'át'imc Government Services (SGS) and other organizations to better predict where shelter habitat needs to be conserved and improved. Priority winter range areas could then be identified and protected from deforestation and degradation. In addition, annual snowpack data is typically summarized at a regional scale and used to make forecasts for spring melt conditions and flooding. However, the spatial pattern of snow, its accumulation and melting across the land base, also directly influences the movement and habitat selection for many wildlife species, which in turn affects forest harvesting, and resource management decisions. By examining the spatial distribution of snow on the finer temporal and spatial scale that is now available via MODSAT-NDSI, and incorporating existing wildlife data, better models can be created for wildlife habitat management and climate change impacts. Such data and modelling becomes a valuable service opportunity for SGS and others to use in the creation of partnerships for forest harvesting, wildlife management, conservation, tourism, and heritage projects. It also becomes the leverage for climate change adaptation projects, which will influence future economic opportunities.

In this research, I show that mule deer selected forest edges and avoided areas with greater snow cover. This research thus helps to provide greater certainty in land use decisions regarding winter-season-mortality of mule deer. Mortality could be mitigated by assuring that adequate tree cover is provided while diverse microhabitats are facilitated by land use practices within winter range. The dry interior Douglas fir forest stands within my study area include vast spaces of sparsely distributed stems, fragmented by sagebrush grasslands which may provide enough of the snowfall interception necessary for survival without being further thinned by the selection system currently recommended by management prescriptions (Armleder et al., 1986). Because the mule deer species inhabits lands from California to Alaska (Anderson et al., 2012; Bergman et al., 2014; Doerr et al., 2005; Gilbert et al., 2017; Lomas & Bender, 2007; Mackie, 1970; Sawyer et al., 2006; Woods, Schumaker, Pesavento, Crossley, & Swift, 2018), the effect of canopy cover on habitat selection in one region – such as the Cariboo region highlighted in the Armleder et al. (1986) handbook – may likely differ from another. Bergman et al. (2014) empirically demonstrated how increasing mule deer habitat range (i.e., increasing the coverage of brush vegetation cover) has improved the survivorship of the species in their study site within Colorado, U.S.A. In western Wyoming, U.S.A, Sawyer et al. (2006) were able to detect abrupt and altered patterns in behavior associated with oil and gas development. Wildlife management should be encouraged to remain flexible and take changing landscapes and conditions into account in conservation management decisions, especially in the current age of big data where large volumes of spatial information can now be integrated into ecological models and summarized faster than ever before.

4.4 Limitations

Limitations within this study include the availability of GPS data points for the winter range data set. For the spring/fall periods, I used 77 individuals in the development of models, while 38 deer provided enough GPS relocation data during the winter to develop the 2-step population-level model results. Although all of the 38 winter range deer were included in the spring/fall period models, the greater sample size and added variability in deer habitat selection in the spring/fall period model strengthens the confidence in the model's results compared to the winter range model. In addition, a single year (2014) of land cover data was used to generate the NTV, bare ground and DFE land cover classes, a temporal resolution which removes the context-dependent effect of habitat selection for changing stand productivity, forest succession and/or disturbances from potentially impacting results (Gilbert et al., 2017; Sawyer et al., 2006). Along with anthropogenic and natural stand-replacing disturbances, several other factors can play a role in mule deer habitat selection that were not included in this research, including predators (Altendorf, Laundré, López González, & Brown, 2001; Benson, Sikich, & Riley, 2016), resource competition (Wielgus, 2017) and the sex and age of cohorts observed (Long, Kie, Terry Bowyer, & Hurley, 2009). Finally, in the specific case of Poole and Wright's (2010) study, distinctive differences were found between migratory and resident populations, the latter groups identified as having overlapping winter, spring and summer ranges, occupied the same area year-round, and/or occupied a much larger proportion of agricultural lands (in this case, 18% more than migratory populations). Future research can and should involve identifying the proportion of resident and migratory mule deer within a broader context, as well as determine whether mule deer switch between strategies on an individual scale, as these are additional factors to consider in future MDWR habitat management decisions.

A major strength of this thesis is the derivation of dynamic snow maps derived from robust and rigorous validation tests using ground-truth data. However, additional environmental data sets used in this thesis did not undergo the same degree of accuracy assessment, particularly the canopy cover rasters. The canopy cover estimating algorithm used and applied to my study area has been validated by Matasci et al. (2018) using the Canadian boreal zone, but greater confidence in the canopy cover algorithm's accuracy within this study's region could be assured by acquiring field validation data in the future. Such future validation may be especially helpful when updating MODSAT-NDSI for future winter years since canopy cover is the metric used in the data fusion algorithm to determine the final NDSI thresholds in forested and open areas. The canopy cover data set was also included in the mule deer step selection functions, and therefore any conclusions drawn from my movement model results concerning canopy cover use would also be strengthened by further ground truthing.

Lastly, the habitat selection analysis conducted in this thesis focused on third-order selection, which is the finest spatial scale of selection observing differences between each individual's telemetry locations and the randomly sampled available locations (Johnson, 1980). The two-step conditional logistic regression used in this thesis accounts for individual variations in covariate coefficients, thereby allowing for population-level extrapolation. However, Gilbert et al. (2017) note how studies focusing explicitly on second or first-orders of selection (i.e., studies comparing individual or population-level home ranges to available ranges of the equivalent scale respectively) are also important to consider when determining habitat selection. An example of such complimentary and augmenting research would include designing resource selection functions that compare the three herd populations used in this thesis (i.e., Pemberton Valley, Carpenter Lake and Fraser Valley mule deer herds). Comparing resource selection patterns between the three herd populations would be described by Manly, McDonald, Thomas, McDonald, & Erickson, (2002) as a type 1 experimental design, where selection patterns can be drawn by comparing resource availability found within the total study area to the used resources within each of the three separate herd populations' home ranges. Considering multiple selection scales in this way can help to draw further conclusions regarding responses to snow timing and distribution and forest habitat types, as sub regions included in this thesis such as Pemberton Valley likely experiences very different climatic and hydrologic processes compared to the drier mid-Fraser valley. A type 1 experimental design can account for differing snow dynamics found within differing regions, while testing for whether deer still select for the lowest degree of snow cover and persistence according to their regionally specific extrema.

4.5 Directions for future research

Temporal and spatial dynamics of snow cover is critical for hydrological modelling, aquatic environment assessment and wildlife survival and habitat selection. With the newly developed data fusion snow maps, a comparison between snow dynamics and forest fire footprints can be conducted, as well as further data analysis of the snow map to derive potentially changing snow cover trends that may be utilized in land management strategies addressing future climate change scenarios. This thesis also provides a new technique for mapping snow cover into the future, which can be input into new models, designed to provide insights for other terrestrial wildlife management decisions for species including grizzly bears, wolverines, salmon and other ungulate species.

The data fusion algorithm produced can be applied to any remote sensing spectral indices or metric, as long as it is common to the two satellite instruments used in the data fusion algorithm. This includes finer spatial and temporal resolution products of NDVI estimates, burn ratios, wetness and productivity indices, and geology indices such as the ferrous minerals ratio. The aforementioned list is by no means exhaustive, and the final application of this thesis that paves the way for future research is the snow depth data. With daily 30 m MODSAT-NDSI imagery and more than 20 field sites measuring depth from 2016 to 2017, future researchers can develop models relating snow cover, depth and any combination of other environmental variables (air temperature, aspect, NDVI, etc.,) to predict snow depth using remote sensing. Such models can then be calibrated and validated using the now available snow depth field data. Predicting snow depth is a difficult task that would non-the-less greatly improve all models related to snow pack measurements, hydrological modelling of meltwater runoff, and wildlife movement research as well.

Bibliography

Alaback, P. B. (2010). An evaluation of canopy gaps in restoring wildlife habitat in second growth forests of southeastern Alaska. *The Nature Conservancy-Alaska and the US Forest Service, Juneau*.

Altendorf, K. B., Laundré, J. W., López González, C. A., & Brown, J. S. (2001). ASSESSING EFFECTS OF PREDATION RISK ON FORAGING BEHAVIOR OF MULE DEER. *Journal of Mammalogy*, *82*(2), 430–439. https://doi.org/10.1644/1545-1542(2001)082<0430:AEOPRO>2.0.CO;2

Amaral, T., Wake, C. P., Dibb, J. E., Burakowski, E. A., & Stampone, M. (2017). A simple model of snow albedo decay using observations from the Community Collaborative Rain, Hail, and Snow-Albedo (CoCoRaHS-Albedo) Network. *Journal of Glaciology*, *63*(241), 877–887. https://doi.org/10.1017/jog.2017.54

Anderson, E. D., Long, R. A., Atwood, M. P., Kie, J. G., Thomas, T. R., Zager, P., & Bowyer, R. T. (2012). Winter resource selection by female mule deer Odocoileus hemionus : functional response to spatio-temporal changes in habitat. *Wildlife Biology*, *18*(2), 153–163. https://doi.org/10.2981/11-048

Anderson, H. W. (1956). Forest cover effects on snowpack accumulation and melt, Central Sierra Snow Laboratory. *Eos, Transactions American Geophysical Union*, *37*(3), 307–312. https://doi.org/10.1029/TR037i003p00307

Anthony, R. G. (1977). Ecological Relationships between Mule Deer and White-Tailed Deer in Southeastern Arizona. *Ecological Monographs*, *47*(3), 255. https://doi.org/10.2307/1942517

Armleder, H., Dawson, R., & Thomson, R. (1986). Handbook for Timber and Mule Deer Management Co-ordination on Winter Ranges in the Cariboo Forest Region BC Handbook for Timber and Mule Deer Management Co-ordination on Winter Ranges in the Cariboo Forest Region. BC Ministry of Forests. Retrieved from https://www.for.gov.bc.ca/hfd/pubs/docs/Lmh/Lmh13.pdf

Armleder, H. M., Waterhouse, M. J., Keisker, D. G., & Dawson, R. J. (1994a). Winter habitat use by mule deer in the central interior of British Columbia. *Canadian Journal of Zoology*, *72*(10), 1721–1725. https://doi.org/10.1139/z94-232

Armleder, H. M., Waterhouse, M. J., Keisker, D. G., & Dawson, R. J. (1994b). Winter habitat use by mule deer in the central interior of British Columbia. *Canadian Journal of Zoology*, *72*(10), 1721–1725. https://doi.org/10.1139/z94-232

Arthur, S. M., Manly, B. F. J., Mcdonald, L. L., & Garner, G. W. (1996). Assessing habitat selection when availability changes. *Ecology*, *77*(1), 215–227. https://doi.org/10.2307/2265671

Austin, M. P. (2002). Spatial prediction of species distribution: An interface between ecological theory and statistical modelling. *Ecological Modelling*, *157*(2–3), 101–118. https://doi.org/10.1016/S0304-3800(02)00205-3

Avgar, T., Potts, J. R., Lewis, M. A., & Boyce, M. S. (2016). Integrated step selection analysis: Bridging the gap between resource selection and animal movement. *Methods in Ecology and Evolution*, *7*(5), 619–630. https://doi.org/10.1111/2041-210X.12528

Barnes, W., Xiong, X., Guenther, B., Salomonson, V., Cox, S., Goetz, A., … Murphy, R. (2003). Development , characterization , and performance of the EOS MODIS sensors. *Earth*, *5151*(May 2012), 337–345. https://doi.org/10.1117/12.504818

Baumann, M., Ozdogan, M., Richardson, A. D., & Radeloff, V. C. (2017). Phenology from Landsat when data is scarce: Using MODIS and Dynamic Time-Warping to combine multi-year Landsat imagery to derive annual phenology curves. *International Journal of Applied Earth Observation and Geoinformation*, *54*, 72–83. https://doi.org/10.1016/j.jag.2016.09.005

BCWF- Southern Interior Mule Deer Project. (n.d.). Retrieved March 7, 2019, from http://www.huntingbc.ca/forum/showthread.php?145219-BCWF-Southern-Interior-Mule-Deer-Project

Beck, P. S. A., Atzberger, C., Høgda, K. A., Johansen, B., & Skidmore, A. K. (2006). Improved monitoring of vegetation dynamics at very high latitudes: A new method using MODIS NDVI. *Remote Sensing of Environment*, *100*(3), 321–334. https://doi.org/10.1016/j.rse.2005.10.021

Beniston, M., & Stoffel, M. (2016). Rain-on-snow events, floods and climate change in the Alps: Events may increase with warming up to 4 °C and decrease thereafter. *Science of the Total Environment*, *571*, 228–236. https://doi.org/10.1016/j.scitotenv.2016.07.146

Bennett, E. M., Peterson, G. D., & Gordon, L. J. (2009). Understanding relationships among multiple ecosystem services. *Ecology Letters*, *12*(12), 1394–1404. https://doi.org/10.1111/j.1461-0248.2009.01387.x

Benson, J. F., Sikich, J. A., & Riley, S. P. D. (2016). Individual and Population Level Resource Selection Patterns of Mountain Lions Preying on Mule Deer along an Urban-Wildland Gradient. *PLOS ONE*, *11*(7), e0158006. https://doi.org/10.1371/journal.pone.0158006

Bergman, E. J., Bishop, C. J., Freddy, D. J., White, G. C., & Doherty, P. F. (2014). Habitat management influences overwinter survival of mule deer fawns in Colorado. *Journal of Wildlife Management*, *78*(3), 448–455. https://doi.org/10.1002/jwmg.683

Berman, E. E., Bolton, D. K., Coops, N. C., Mityok, Z. K., Stenhouse, G. B., & Moore, R. D. (Dan). (2018). Daily estimates of Landsat fractional snow cover driven by MODIS and dynamic time-warping. *Remote Sensing of Environment*, *216*, 635–646. https://doi.org/10.1016/J.RSE.2018.07.029

Beschta, R. L., Donahue, D. L., Dellasala, D. A., Rhodes, J. J., Karr, J. R., O'Brien, M. H., … Deacon Williams, C. (2013). Adapting to climate change on western public lands: Addressing the ecological effects of domestic, wild, and feral ungulates. *Environmental Management*, *51*(2), 474–491. https://doi.org/10.1007/s00267-012-9964-9

Bohrer, G., Beck, P. S., Ngene, S. M., Skidmore, A. K., & Douglas-Hamilton, I. (2014). Elephant movement closely tracks precipitation-driven vegetation dynamics in a Kenyan forest-savanna landscape. *Movement Ecology*, *2*(1), 2. https://doi.org/10.1186/2051-3933-2-2

Bokhorst, S., Pedersen, S. H., Brucker, L., Anisimov, O., Bjerke, J. W., Brown, R. D., … Callaghan, T. V. (2016, September 17). Changing Arctic snow cover: A review of recent developments and assessment of future needs for observations, modelling, and impacts. *Ambio*. Springer Netherlands. https://doi.org/10.1007/s13280-016-0770-0

Boulanger, J., Stenhouse, G. B., & Margalida, A. (2014). The impact of roads on the demography of grizzly bears in Alberta. *PLoS ONE*, *9*(12), e115535. https://doi.org/10.1371/journal.pone.0115535

Boyce, M. S., & McDonald, L. L. (1999, July 1). Relating populations to habitats using resource selection functions. *Trends in Ecology and Evolution*. Elsevier Current Trends. https://doi.org/10.1016/S0169-5347(99)01593-1

Boyce, M. S., Meyer, J. S., & Irwin, L. (1994). Habitat-based PVA for the Northern Spotted Owl. In *Statistics in Ecology and Environmental Monitoring* (p. 23). Retrieved from https://scholar.google.ca/scholar?hl=en&as_sdt=0%2C5&q=Boyce%2C+M.+S.%2C+Meyer%2C+J.+S.%2C+%26+Irwin%2C+L.+L.+%281994%29.+Habitat-based+PVA+for+the+northern+spotted+owl.+Statistics+in+Ecology+and+Environmental+Monitoring%2C+63-85.&btnG=

British Columbia Ministry of Forests Lands and Natural Resource Operations. (2017). Automated Snow Weather Station Data. Retrieved May 5, 2018, from https://www2.gov.bc.ca/gov/content/environment/air-land-water/water/water-science-data/water-data-tools/snow-survey-data/automated-snow-weather-station-data

Burnham, K. P., & Anderson, D. R. (2002). *Model Selection and Multi-Model Inference: A Practical Information-Theoretical\rApproach*. https://doi.org/10.1016/j.ecolmodel.2003.11.004

Burns, P., & Nolin, A. (2014). Using atmospherically-corrected Landsat imagery to measure glacier area change in the Cordillera Blanca, Peru from 1987 to 2010. *Remote Sensing of Environment*, *140*, 165–178. https://doi.org/10.1016/j.rse.2013.08.026

Byers, C. R., Steinhorst, R. K., & Krausman, P. R. (1984). Clarification of a technique for analysis of utilization-availiability data. *Journal of Wildlife Management*, *48*(3), 1050–1053. https://doi.org/10.2307/3801467

Carpenter, S. R., DeFries, R., Dietz, T., Mooney, H. A., Polasky, S., Reid, W. V., & Scholes, R. J. (2006). Millennium ecosystem assessment: Research needs. *Science*. American Association for the Advancement of Science (AAAS). https://doi.org/10.1126/science.1131946

Casey, J. A., & Kelly, R. E. J. (2010). Estimating the equilibrium line of Devon Ice Cap, Nunavut, from RADARSAT-1 ScanSAR wide imagery. *Canadian Journal of Remote Sensing*, *36*(sup1), S41–S55. https://doi.org/10.5589/m10-013

Chance, C. M., Hermosilla, T., Coops, N. C., Wulder, M. A., & White, J. C. (2016a). Effect of topographic correction on forest change detection using spectral trend analysis of Landsat pixel-based composites. *International Journal of Applied Earth Observation and Geoinformation*, *44*, 186–194. https://doi.org/10.1016/j.jag.2015.09.003

Chance, C. M., Hermosilla, T., Coops, N. C., Wulder, M. A., & White, J. C. (2016b). Effect of topographic correction on forest change detection using spectral trend analysis of Landsat pixel-based composites. *International Journal of Applied Earth Observation and Geoinformation*, *44*, 186–194. https://doi.org/10.1016/j.jag.2015.09.003

Ciarniello, L. M., Boyce, M. S., Heard, D. C., & Seip, D. R. (2007). Components of Grizzly Bear Habitat Selection: Density, Habitats, Roads, and Mortality Risk. *Journal of Wildlife Management*, *71*(5), 1446–1457. https://doi.org/10.2193/2006-229

Cohen, S., Koshida, G., & Mortsch, L. (2015). Climate and water availability indicators in Canada: Challenges and a way forward. Part III – Future scenarios. *Canadian Water Resources Journal*, *40*(2), 160–172. https://doi.org/10.1080/07011784.2015.1006021

Collins, S. L., Carpenter, S. R., Swinton, S. M., Orenstein, D. E., Childers, D. L., Gragson, T. L.,

… Whitmer, A. C. (2011). An integrated conceptual framework for long-term social-ecological research. *Frontiers in Ecology and the Environment*, *9*(6), 351–357. https://doi.org/10.1890/100068

Coops, N. C., Hilker, T., Bater, C. W., Wulder, M. A., Nielsen, S. E., McDermid, G., & Stenhouse, G. (2012). Linking ground-based to satellite-derived phenological metrics in support of habitat assessment. *Remote Sensing Letters*, *3*(3), 191–200. https://doi.org/10.1080/01431161.2010.550330

Copeland, J. P., McKelvey, K. S., Aubry, K. B., Landa, A., Persson, J., Inman, R. M., … May, R. (2010). The bioclimatic envelope of the wolverine (Gulo gulo): do climatic constraints limit its geographic distribution? *Canadian Journal of Zoology*, *88*(3), 233–246. https://doi.org/10.1139/Z09-136

Cortés, G., Girotto, M., & Margulis, S. A. (2014). Analysis of sub-pixel snow and ice extent over the extratropical Andes using spectral unmixing of historical Landsat imagery. *Remote Sensing of Environment*, *141*, 64–78. https://doi.org/10.1016/j.rse.2013.10.023

Craiu, R. V., Duchesne, T., Fortin, D., & Baillargeon, S. (2011). Conditional logistic regression with longitudinal follow-up and individual-level random coefficients: A stable and efficient two-step estimation method. *Journal of Computational and Graphical Statistics*, *20*(3), 767–784. https://doi.org/10.1198/jcgs.2011.09189

Crawford, C. J. (2015). MODIS Terra Collection 6 fractional snow cover validation in mountainous terrain during spring snowmelt using Landsat TM and ETM+. *Hydrological Processes*, *29*(1), 128–138. https://doi.org/10.1002/hyp.10134

Cullingham, C. I., Nakada, S. M., Merrill, E. H., Bollinger, T. K., Pybus, M. J., & Coltman, D.

W. (2011). Multiscale population genetic analysis of mule deer (Odocoileus hemionus hemionus) in western Canada sheds new light on the spread of chronic wasting disease. *Canadian Journal of Zoology*, *89*(2), 134–147. https://doi.org/10.1139/Z10-104

Czyzowska-Wisniewski, E. H., van Leeuwen, W. J. D., Hirschboeck, K. K., Marsh, S. E., & Wisniewski, W. T. (2015). Fractional snow cover estimation in complex alpine-forested environments using an artificial neural network. *Remote Sensing of Environment*, *156*, 403–417. https://doi.org/10.1016/j.rse.2014.09.026

D'Eon, R. G., & Serrouya, R. (2005, August 22). Mule deer seasonal movements and multiscale resource selction using global postioning system radiotelemetry. *Journal of Mammalogy*. Oxford University Press. https://doi.org/10.1644/1545-1542(2005)086[0736:MDSMAM]2.0.CO;2

De Lannoy, G. J. M., Reichle, R. H., Houser, P. R., Arsenault, K. R., Verhoest, N. E. C., & Pauwels, V. R. N. (2010). Satellite-Scale Snow Water Equivalent Assimilation into a High-Resolution Land Surface Model. *Journal of Hydrometeorology*, *11*(2), 352–369. https://doi.org/10.1175/2009JHM1192.1

Derksen, C., & Brown, R. (2012). Spring snow cover extent reductions in the 2008-2012 period exceeding climate model projections. *Geophysical Research Letters*, *39*(19), n/a-n/a. https://doi.org/10.1029/2012GL053387

Dingle, H., & Drake, V. A. (2007). What Is Migration? *BioScience*, *57*(2), 113–121. https://doi.org/10.1641/B570206

Dodge, S., Bohrer, G., Weinzierl, R., Davidson, S. C., Kays, R., Douglas, D., … Wikelski, M. (2013). The environmental-data automated track annotation (Env-DATA) system: Linking animal tracks with environmental data. *Movement Ecology*, *1*(1), 3. https://doi.org/10.1186/2051-3933-1-3

Doerr, J. G., Degayner, E. J., & Ith, G. (2005). WINTER HABITAT SELECTION BY SITKA BLACK-TAILED DEER. *Journal of Wildlife Management*, *69*(1), 322–331. https://doi.org/10.2193/0022-541X(2005)069<0322:WHSBSB>2.0.CO;2

Dozier, J. (1989). Spectral signature of alpine snow cover from the landsat thematic mapper. *Remote Sensing of Environment*, *28*(C), 9–22. https://doi.org/10.1016/0034-4257(89)90101-6

Dozier, J., Painter, T. H., Rittger, K., & Frew, J. E. (2008). Time-space continuity of daily maps of fractional snow cover and albedo from MODIS. *Advances in Water Resources*, *31*(11), 1515–1526. https://doi.org/10.1016/j.advwatres.2008.08.011

Elith, J., & Leathwick, J. R. (2009). Species Distribution Models: Ecological Explanation and Prediction Across Space and Time. *Annual Review of Ecology, Evolution, and Systematics*, *40*(1), 677–697. https://doi.org/10.1146/annurev.ecolsys.110308.120159

Erran Seaman, D., & Powell, R. A. (1996). An evaluation of the accuracy of kernel density estimators for home range analysis. *Ecology*, *77*(7), 2075–2085. https://doi.org/10.2307/2265701

Farinotti, D., Magnusson, J., Huss, M., & Bauder, A. (2010). Snow accumulation distribution inferred from time-lapse photography and simple modelling. *Hydrological Processes*, *24*(15), 2087–2097. https://doi.org/10.1002/hyp.7629

Fisher, B., Turner, R. K., & Morling, P. (2009). Defining and classifying ecosystem services for decision making. *Ecological Economics*, *68*(3), 643–653. https://doi.org/10.1016/j.ecolecon.2008.09.014

Fisher, J. I., Mustard, J. F., & Vadeboncoeur, M. A. (2006). Green leaf phenology at Landsat resolution: Scaling from the field to the satellite. *Remote Sensing of Environment*, *100*(2), 265–279. https://doi.org/10.1016/j.rse.2005.10.022

Flint, L. E., & Flint, A. L. (2012). Downscaling future climate scenarios to fine scales for hydrologic and ecological modeling and analysis. *Ecological Processes*, *1*(1), 1–15. https://doi.org/10.1186/2192-1709-1-2

Foley, J. A., DeFries, R., Asner, G. P., Barford, C., Bonan, G., Carpenter, S. R., … Snyder, P. K. (2005, July 22). Global consequences of land use. *Science*. American Association for the Advancement of Science. https://doi.org/10.1126/science.1111772

Fortin, V., Jean, M., Brown, R., & Payette, S. (2015). Predicting Snow Depth in a Forest-Tundra Landscape using a Conceptual Model Allowing for Snow Redistribution and Constrained by Observations from a Digital Camera. *Atmosphere - Ocean*, *53*(2), 200–211. https://doi.org/10.1080/07055900.2015.1022708

Gao, F., Masek, J., Schwaller, M., & Hall, F. (2006). On the blending of the landsat and MODIS surface reflectance: Predicting daily landsat surface reflectance. *IEEE Transactions on Geoscience and Remote Sensing*, *44*(8), 2207–2218. https://doi.org/10.1109/TGRS.2006.872081

Gao, X., Xu, Y., Zhao, Z., Pal, J. S., & Giorgi, F. (2006). On the role of resolution and topography in the simulation of East Asia precipitation. *Theoretical and Applied Climatology*, *86*(1–4), 173–185. https://doi.org/10.1007/s00704-005-0214-4

Garrott, R. A., White, G. C., Bartmann, R. M., Carpenter, L. H., & Alldredge, A. W. (1987). Movements of Female Mule Deer in Northwest Colorado. *The Journal of Wildlife Management*, *51*(3), 634. https://doi.org/10.2307/3801282

Garvelmann, J., Pohl, S., & Weiler, M. (2013). From observation to the quantification of snow processes with a time-lapse camera network. *Hydrology and Earth System Sciences*, *17*(4), 1415–1429. https://doi.org/10.5194/hess-17-1415-2013

Gavashelishvili, A., McGrady, M., Ghasabian, M., & Bildstein, K. L. (2012). Movements and habitat use by immature Cinereous Vultures (Aegypius monachus) from the Caucasus. *Bird Study*, *59*(4), 449–462. https://doi.org/10.1080/00063657.2012.728194

Gilbert, S. L., Hundertmark, K. J., Person, D. K., Lindberg, M. S., & Boyce, M. S. (2017). Behavioral plasticity in a variable environment: Snow depth and habitat interactions drive deer movement in winter. *Journal of Mammalogy*, *98*(1), 246–259. https://doi.org/10.1093/jmammal/gyw167

Gillespie, T. W. (2001). Progress in Physical Geography Remote sensing of animals Remote sensing of animals. *Progress in Physical Geography*, *25*(3), 355–362. https://doi.org/10.1177/030913330102500303

Government of British Columbia. (2004). *GOVERNMENT ACTIONS REGULATION Consolidated Regulations of British Columbia*. Victoria: Queen's Printer. Retrieved from www.bclaws.ca.

Government of Canada. (n.d.). Historical Data - Climate - Environment and Climate Change Canada. Retrieved May 2, 2018, from http://climate.weather.gc.ca/historical_data/search_historic_data_e.html

Graham, E. A., Hamilton, M. P., Mishler, B. D., Rundel, P. W., & Hansen, M. H. (2006). Use of a Networked Digital Camera to Estimate Net CO2 Uptake of a Desiccation-Tolerant Moss. *International Journal of Plant Sciences*, *167*(4), 751–758. https://doi.org/10.1086/503786

Graham, E. A., Riordan, E. C., Yuen, E. M., Estrin, D., & Rundel, P. W. (2010). Public Internet-connected cameras used as a cross-continental ground-based plant phenology monitoring system. *Global Change Biology*, *16*(11), 3014–3023. https://doi.org/10.1111/j.1365-2486.2010.02164.x

Gustafsson, K. M. (2013). Environmental discourses and biodiversity: The construction of a storyline in understanding and managing an environmental issue. *Journal of Integrative Environmental Sciences*, *10*(1), 39–54. https://doi.org/10.1080/1943815X.2013.769455

Haila, Y. (1999). Biodiversity and the divide between culture and nature. *Biodiversity and Conservation*, *8*(1), 165–181. https://doi.org/10.1023/A:1008877628720

Hall, D. K., Foster, J. L., Verbyla, D. L., Klein, A. G., & Benson, C. S. (1998). Assessment of snow-cover mapping accuracy in a variety of vegetation-cover densities in central Alaska. *Remote Sensing of Environment*, *66*(2), 129–137. https://doi.org/10.1016/S0034-4257(98)00051-0

Hall, D. K., & Martinec, J. (1986). Remote sensing of ice and snow. Retrieved from https://books.google.ca/books?hl=en&lr=&id=mt0sBAAAQBAJ&oi=fnd&pg=PA1&dq=Hall,+D.+K.,+%26+Martinec,+J.+(1985).+Snow+cover.+In+Remote+Sensing+of+Ice+and+Snow+&ots=qRCIUBBU2h&sig=pYATF6G2Y5fWQwtICZqtL8pqWuE

Hall, D. K., & Riggs, G. A. (2007). Accuracy assessment of the MODIS snow products. In *Hydrological Processes* (Vol. 21, pp. 1534–1547). Wiley-Blackwell.

https://doi.org/10.1002/hyp.6715

Hall, D. K., Riggs, G. A., & Barton, J. S. (2001). MODIS Snow and Sea Ice-Mapping Algorithms. *Modis Atbd*, *the MODIS*(September), 45. Retrieved from https://eospso.gsfc.nasa.gov/sites/default/files/atbd/atbd_mod10.pdf

Hall, D. K., Riggs, G. A., & Salomonson, V. V. (1995). Development of methods for mapping global snow cover using moderate resolution imaging spectroradiometer data. *Remote Sensing of Environment*, *54*(2), 127–140. https://doi.org/10.1016/0034-4257(95)00137-P

Hamer, D., & Herrero, S. (1987). Grizzly bear food and habitat in the front ranges of Banff National Park, Alberta. *International Conference on Bear Research and Management*, *7*, 199–213. https://doi.org/10.2307/3872626

Hansen, M. C., DeFries, R. S., Townshend, J. R. G., Carroll, M., Dimiceli, C., & Sohlberg, R. A. (2003). Global Percent Tree Cover at a Spatial Resolution of 500 Meters: First Results of the MODIS Vegetation Continuous Fields Algorithm. *Earth Interactions*, *7*(10), 1–15. https://doi.org/10.1175/1087-3562(2003)007<0001:GPTCAA>2.0.CO;2

Härer, S., Bernhardt, M., & Schulz, K. (2016). PRACTISE - Photo Rectification and ClassificaTIon SoftwarE (V.2.1). *Geoscientific Model Development*, *9*(1), 307–321. https://doi.org/10.5194/gmd-9-307-2016

Härer, S., Bernhardt, M., Siebers, M., & Schulz, K. (2017). On the need of a time and location dependent estimation of the NDSI threshold value for reducing existing uncertainties in snow cover maps at different scales. *The Cryosphere*, (under review), 1–27. https://doi.org/10.5194/tc-2017-177

Hermosilla, T., Wulder, M. A., White, J. C., Coops, N. C., & Hobart, G. W. (2018, January 2). Disturbance-Informed Annual Land Cover Classification Maps of Canada's Forested Ecosystems for a 29-Year Landsat Time Series. *Canadian Journal of Remote Sensing*, pp. 1–21. https://doi.org/10.1080/07038992.2018.1437719

Hilker, T., Wulder, M. A., Coops, N. C., Linke, J., McDermid, G., Masek, J. G., … White, J. C. (2009). A new data fusion model for high spatial- and temporal-resolution mapping of forest disturbance based on Landsat and MODIS. *Remote Sensing of Environment*, *113*(8), 1613–1627. https://doi.org/10.1016/j.rse.2009.03.007

Horne, J. S., Garton, E. O., Krone, S. M., & Lewis, J. S. (2007). Analyzing animal movements using Brownian bridges. *Ecology*, *88*(9), 2354–2363. https://doi.org/10.1890/06-0957.1

Huang, X., Liang, T., Zhang, X., & Guo, Z. (2011). Validation of MODIS snow cover products using landsat and ground measurements during the 2001-2005 snow seasons over northern Xinjiang, China. *International Journal of Remote Sensing*, *32*(1), 133–152. https://doi.org/10.1080/01431160903439924

Hwang, T., Song, C., Bolstad, P. V., & Band, L. E. (2011). Downscaling real-time vegetation dynamics by fusing multi-temporal MODIS and Landsat NDVI in topographically complex terrain. *Remote Sensing of Environment*, *115*(10), 2499–2512. https://doi.org/10.1016/j.rse.2011.05.010

Johansson, Ö., Simms, A., & McCarthy, T. (2016). From VHF to Satellite GPS Collars: Advancements in Snow Leopard Telemetry. In *Snow Leopards: Biodiversity of the World: Conservation from Genes to Landscapes* (pp. 355–365). Academic Press. https://doi.org/10.1016/B978-0-12-802213-9.00026-2

Johnson, D. H. (1980). The Comparison of Usage and Availability Measurements for Evaluating Resource Preference. *Ecology*, *61*(1), 65–71. https://doi.org/10.2307/1937156

Jonsen, I. D., Myers, R. A., & Flemming, J. M. (2003). META-ANALYSIS OF ANIMAL MOVEMENT USING STATE-SPACE MODELS. *Ecology*, *84*(11), 3055–3063. https://doi.org/10.1890/02-0670

Jönsson, P., & Eklundh, L. (2004). TIMESAT - A program for analyzing time-series of satellite sensor data. *Computers and Geosciences*, *30*(8), 833–845. https://doi.org/10.1016/j.cageo.2004.05.006

Jost, G., & Weber, F. (2012). Potential Impacts of Climate Change on Bc Hydro’S Water Resources, 1–28. Retrieved from https://www.bchydro.com/content/dam/hydro/medialib/internet/documents/about/climate_change_report_2012.pdf

Justice, C. O., Townshend, J. R. G., Vermote, E. F., Masuoka, E., Wolfe, R. E., Saleous, N., … Morisette, J. T. (2002, November 1). An overview of MODIS Land data processing and product status. *Remote Sensing of Environment*. Elsevier. https://doi.org/10.1016/S0034-4257(02)00084-6

Kelly, J. V, & Reynolds, D. (2015a). Mackenzie-Wolverine Deer Winter Range: calibrating an index. Retrieved from http://www.pembertonwildlifeassociation.com/media/21072/mackenzie wolverine dwr_calibrating an index.pdf

Kelly, J. V, & Reynolds, D. (2015b). Mackenzie-Wolverine Deer Winter Range: calibrating an index. Retrieved from http://www.pembertonwildlifeassociation.com/media/21072/mackenzie wolverine dwr_calibrating an index.pdf

Keshri, A. K., Shukla, A., & Gupta, R. P. (2009). ASTER ratio indices for supraglacial terrain mapping. *International Journal of Remote Sensing*, *30*(2), 519–524. https://doi.org/10.1080/01431160802385459

Khadka Mishra, S., Hayse, J., Veselka, T., Yan, E., Kayastha, R. B., McDonald, K., … Lagory, K. (2017). Economic Analysis of the Impacts of Climate-Induced Changes in River Flow on Hydropower and Fisheries in Himalayan region. *American Geophysical Union, Fall Meeting 2017, Abstract #GC51D-0825*. Retrieved from http://adsabs.harvard.edu/abs/2017AGUFMGC51D0825K

Kie, J. G., Matthiopoulos, J., Fieberg, J., Powell, R. A., Cagnacci, F., Mitchell, M. S., … Moorcroft, P. R. (2010). The home-range concept: are traditional estimators still relevant with modern telemetry technology? *Philosophical Transactions of the Royal Society of London. Series B, Biological Sciences*, *365*(1550), 2221–2231. https://doi.org/10.1098/rstb.2010.0093

Kostadinov, T. S., & Lookingbill, T. R. (2015). Snow cover variability in a forest ecotone of the Oregon Cascades via MODIS Terra products. *Remote Sensing of Environment*, *164*, 155–169. https://doi.org/10.1016/j.rse.2015.04.002

Lauer, D. T., Morain, S. A., & Salomonson, V. V. (1997). The Landsat Program : Its Origins, Evolution, and Impacts. *Photogrammetric Engineering & Remote Sensing*, *63*(7), 831–838. Retrieved from http://citeseerx.ist.psu.edu/viewdoc/download?doi=10.1.1.472.5192&rep=rep1&type=pdf

Lele, S. R., Merrill, E. H., Keim, J., & Boyce, M. S. (2013). Selection, use, choice and occupancy: Clarifying concepts in resource selection studies. *Journal of Animal Ecology*, *82*(6), 1183–1191. https://doi.org/10.1111/1365-2656.12141

Lemke, P., Ren, J., Alley, R. B., Allison, I., Carrasco, J., Flato, G., … Zhang, T. (2007). Observations: Changes in snow, ice and frozen ground. *Climate Change 2007: The Physical Science Basis. Contribution of Working Group I to the Fourth Assessment Report of the Intergovernmental Panel on Climate Change*, 337–383. https://doi.org/10.1016/j.jmb.2004.10.032

Lendrum, P. E., Anderson, C. R., Long, R. A., Kie, J. G., & Bowyer, R. T. (2012). Habitat selection by mule deer during migration: effects of landscape structure and natural-gas development. *Ecosphere*, *3*(September), art82. https://doi.org/10.1890/ES12-00165.1

Levin, S. A. (1998). Ecosystems and the biosphere as complex adaptive systems. *Ecosystems*, *1*(5), 431–436. https://doi.org/10.1007/s100219900037

Lieth, H. (2013). *Phenology and seasonality modeling*. Retrieved from https://books.google.ca/books?hl=en&lr=&id=_ajtCAAAQBAJ&oi=fnd&pg=PR7&dq=Lieth+H,+editor.+Phenology+and+seasonality+modeling.+Springer+Science+%26+Business+Media%3B+2013+Mar+9.&ots=UgztxOzH_S&sig=8P--PXBQkJnhFFPIk7fLlh8fh0c

Liston, G. E. (1999). Interrelationships among Snow Distribution, Snowmelt, and Snow Cover Depletion: Implications for Atmospheric, Hydrologic, and Ecologic Modeling. *Journal of Applied Meteorology*, *38*(10), 1474–1487. https://doi.org/10.1175/1520-0450(1999)038<1474:IASDSA>2.0.CO;2

Liu, J., Woodcock, C. E., Melloh, R. A., Davis, R. E., McKenzie, C., & Painter, T. H. (2008).

Modeling the View Angle Dependence of Gap Fractions in Forest Canopies: Implications for Mapping Fractional Snow Cover Using Optical Remote Sensing. *Journal of Hydrometeorology*, *9*(5), 1005–1019. https://doi.org/10.1175/2008JHM866.1

Lomas, L. A., & Bender, L. C. (2007). Survival and Cause-Specific Mortality of Neonatal Mule Deer Fawns, North-Central New Mexico. *Journal of Wildlife Management*, *71*(3), 884–894. https://doi.org/10.2193/2006-203

Long, R. A., Kie, J. G., Terry Bowyer, R., & Hurley, M. A. (2009). Resource Selection and Movements by Female Mule Deer *Odocoileus hemionus* : Effects of Reproductive Stage. *Wildlife Biology*, *15*(3), 288–298. https://doi.org/10.2981/09-003

Lowe, T. (2018). New study looking into restoring some of B.C.'s declining mule deer populations - Okanagan | Globalnews.ca. Retrieved March 7, 2019, from https://globalnews.ca/news/4337012/new-study-looking-into-restoring-some-of-b-c-s-declining-mule-deer-populations/

Luccarini, S., Mauri, L., Apollonio, M., Lamberti, P., & Ciuti, S. (2006). Red Deer ("Cervus elaphus") Spatial Use in the Italian Alps : Home Range Patterns, Seasonal Migrations, and Effect of Snow and Winter Feeding. *Ethology Ecology & Evolution. JULY, 2006*, *JULY*(2), 1000–1019. https://doi.org/10.1400/53712

Lundberg, A., Granlund, N., & Gustafsson, D. (2010). Towards automated "ground truth" snow measurements-a review of operational and new measurement methods for Sweden, Norway, and Finland. *Hydrological Processes*, *24*(14), 1955–1970. https://doi.org/10.1002/hyp.7658

Macdonald, D. W. (1978). Radio-tracking: some applications and limitations. In *Animal Marking* (pp. 192–204). London: Macmillan Education UK. https://doi.org/10.1007/978-1-349-

03711-7_20

Mackie, R. J. (1970). Range Ecology and Relations of Mule Deer, Elk, and Cattle in the Missouri River Breaks, Montana. *Wildlife Monographs*, *20*, 3–79. https://doi.org/10.2307/3830629

Maher, A. I., Treitz, P. M., & Ferguson, M. A. . (2012). Can Landsat data detect variations in snow cover within habitats of arctic ungulates? *Wildlife Biology*, *18*(1), 75–87. https://doi.org/10.2981/11-055

Manly, B. F. J., McDonald, L. L., Thomas, D. A., McDonald, T. L., & Erickson, W. E. (2002). *Resource selection by animals: statistical design and analysis for field studies*. Retrieved from https://books.google.ca/books?hl=en&lr=&id=rBXnBwAAQBAJ&oi=fnd&pg=PR9&dq=Manly,+B.+F.+L.,+McDonald,+L.,+Thomas,+D.,+McDonald,+T.+L.,+%26+Erickson,+W.+P.+(2007).+Resource+selection+by+animals:+statistical+design+and+analysis+for+field+studies.+Springer+Sci

Manning, J. A., & Garton, E. O. (2012). Reconstructing historical snow depth surfaces to evaluate changes in critical demographic rates and habitat components of snow-dependent and snow-restricted species. *Methods in Ecology and Evolution*, *3*(1), 71–80. https://doi.org/10.1111/j.2041-210X.2011.00144.x

Markham, B. L., Storey, J. C., Williams, D. L., & Irons, J. R. (2004, December). Landsat sensor performance: History and current status. *IEEE Transactions on Geoscience and Remote Sensing*. https://doi.org/10.1109/TGRS.2004.840720

Marshall, S., & Oglesby, R. J. (1994). An improved snow hydrology for GCMs. Part 1: snow cover fraction, albedo, grain size, and age. *Climate Dynamics*, *10*(1–2), 21–37.

https://doi.org/10.1007/BF00210334

Marty, C., & Meister, R. (2012). Long-term snow and weather observations at Weissfluhjoch and its relation to other high-altitude observatories in the Alps. *Theoretical and Applied Climatology*, *110*(4), 573–583. https://doi.org/10.1007/s00704-012-0584-3

Matasci, G., Hermosilla, T., Wulder, M. A., White, J. C., Coops, N. C., Hobart, G. W., & Zald, H. S. J. (2018). Large-area mapping of Canadian boreal forest cover, height, biomass and other structural attributes using Landsat composites and lidar plots. *Remote Sensing of Environment*, *209*, 90–106. https://doi.org/10.1016/J.RSE.2017.12.020

McKee, C. J., Stewart, K. M., Sedinger, J. S., Bush, A. P., Darby, N. W., Hughson, D. L., & Bleich, V. C. (2015). Spatial distributions and resource selection by mule deer in an arid environment: Responses to provision of water. *Journal of Arid Environments*, *122*, 76–84. https://doi.org/10.1016/j.jaridenv.2015.06.008

McLoughlin, P. D., Morris, D. W., Fortin, D., Vander Wal, E., & Contasti, A. L. (2010). Considering ecological dynamics in resource selection functions. *Journal of Animal Ecology*, *79*(1), 4–12. https://doi.org/10.1111/j.1365-2656.2009.01613.x

Melaas, E. K., Friedl, M. A., & Zhu, Z. (2013). Detecting interannual variation in deciduous broadleaf forest phenology using Landsat TM/ETM+ data. *Remote Sensing of Environment*, *132*, 176–185. https://doi.org/10.1016/j.rse.2013.01.011

Messier, F. (1991). The Significance of Limiting and Regulating Factors on the Demography of Moose and White-Tailed Deer. *The Journal of Animal Ecology*, *60*(2), 377. https://doi.org/10.2307/5285

Mitchell, A., Wilton, W., & Reynolds, D. (2012). *Pemberton Valley Black-tailed Deer Monitoring Project*.

Mityók, Z. K., Bolton, D. K., Coops, N. C., Berman, E. E., & Senger, S. (2018). Snow cover mapped daily at 30 meters resolution using a fusion of multi-temporal MODIS NDSI data and Landsat surface reflectance. *Canadian Journal of Remote Sensing*, 1–22. https://doi.org/10.1080/07038992.2018.1538775

Mladenoff, D. J., & Sickley, T. A. (1998). Assessing Potential Gray Wolf Restoration in the Northeastern United States: A Spatial Prediction of Favorable Habitat and Potential Population Levels. *The Journal of Wildlife Management*, *62*(1), 1. https://doi.org/10.2307/3802259

Moen, R., Pastor, J., & Cohen, Y. (1997). Accuracy of GPS Telemetry Collar Locations with Differential Correction. *The Journal of Wildlife Management*, *61*(2), 530. https://doi.org/10.2307/3802612

Molotch, N. P., & Margulis, S. A. (2008). Estimating the distribution of snow water equivalent using remotely sensed snow cover data and a spatially distributed snowmelt model: A multi-resolution, multi-sensor comparison. *Advances in Water Resources*, *31*(11), 1503–1514. https://doi.org/10.1016/j.advwatres.2008.07.017

Moore, T. T. (2011a). Climate Change and Animal Migration. *Environmental Law*, *41*, 393–405. https://doi.org/10.2307/43267496

Moore, T. T. (2011b). CLIMATE CHANGE AND ANIMAL MIGRATION. *Environmental Law*. Lewis & Clark Law School. https://doi.org/10.2307/43267496

Neumann, W., Martinuzzi, S., Estes, A. B., Pidgeon, A. M., Dettki, H., Ericsson, G., & Radeloff, V. C. (2015). Opportunities for the application of advanced remotely-sensed data in ecological studies of terrestrial animal movement. *Movement Ecology*, *3*(1), 8. https://doi.org/10.1186/s40462-015-0036-7

Nijland, W., Bolton, D. K., Coops, N. C., & Stenhouse, G. (2016). Imaging phenology; scaling from camera plots to landscapes. *Remote Sensing of Environment*, *177*, 13–20. https://doi.org/10.1016/j.rse.2016.02.018

Nobert, B. R., Merrill, E. H., Pybus, M. J., Bollinger, T. K., & Hwang, Y. Ten. (2016). Landscape connectivity predicts chronic wasting disease risk in Canada. *Journal of Applied Ecology*, *53*(5), 1450–1459. https://doi.org/10.1111/1365-2664.12677

Nolin, A. W. (2011, September 8). Recent advances in remote sensing of seasonal snow. *Journal of Glaciology*. Cambridge University Press. https://doi.org/10.3189/002214311796406077

O'Kane, C. A. J., & Macdonald, D. W. (2018). Seasonal influences on ungulate movement within a fenced South African reserve. *Journal of Tropical Ecology*, *34*(03), 200–203. https://doi.org/10.1017/S0266467418000160

Olivas-Sánchez, M. P., Vital-García, C., Flores-Margez, J. P., Mora-Covarrubias, A. D. La, & Clemente-Sánchez, F. (2018). Mule deer forage availability and quality at the Chihuahuan Desert rangelands, Mexico after a severe 3-year drought. *Cogent Biology*, *4*(1). https://doi.org/10.1080/23312025.2018.1536315

Onstott, R. G. (1997). Results of satellite and in-situ remote sensing measurement and modeling studies of Arctic sea ice which support the monitoring of changes in the global climate. *Geoscience and Remote Sensing, 1997. IGARSS '97. Remote Sensing - A Scientific Vision* *for Sustainable Development., 1997 IEEE International*. IEEE. https://doi.org/10.1109/IGARSS.1997.606427

Painter, T. H., Rittger, K., McKenzie, C., Slaughter, P., Davis, R. E., & Dozier, J. (2009). Retrieval of subpixel snow covered area, grain size, and albedo from MODIS. *Remote Sensing of Environment*, *113*(4), 868–879. https://doi.org/10.1016/j.rse.2009.01.001

Parajka, J., & Blöschl, G. (2008). Spatio-temporal combination of MODIS images - Potential for snow cover mapping. *Water Resources Research*, *44*(3). https://doi.org/10.1029/2007WR006204

Parajka, J., Haas, P., Kirnbauer, R., Jansa, J., & Blöschl, G. (2012). Potential of time-lapse photography of snow for hydrological purposes at the small catchment scale. *Hydrological Processes*, *26*(22), 3327–3337. https://doi.org/10.1002/hyp.8389

Parajka, J., Holko, L., Kostka, Z., & Blöschl, G. (2012). MODIS snow cover mapping accuracy in a small mountain catchment - Comparison between open and forest sites. *Hydrology and Earth System Sciences*, *16*(7), 2365–2377. https://doi.org/10.5194/hess-16-2365-2012

Parker, K. L., Robbins, C. T., & Hanley, T. A. (1984). Energy expenditures for locomotion by mule deer and elk. *Journal of Wildlife Management*, *48*(2), 474–488. https://doi.org/10.2307/3801180

Pauly, D. (1995). Anecdotes and the shifting baseline syndrome of fisheries. *Trends in Ecology & Evolution*. https://doi.org/10.1016/S0169-5347(00)89171-5

Pettorelli, N., Laurance, W. F., O'Brien, T. G., Wegmann, M., Nagendra, H., & Turner, W. (2014, August 1). Satellite remote sensing for applied ecologists: Opportunities and challenges. (E. J. Milner-Gulland, Ed.), *Journal of Applied Ecology*. Wiley/Blackwell (10.1111). https://doi.org/10.1111/1365-2664.12261

Pierce, B. M., Bowyer, R. T., Bleich, V. C., The, S., Management, W., & Jul, N. (2009). Habitat selection by mule deer : Forage benefits or risk of predation? *The Journal of Wildlife Management*, *68*(3), 533–541. Retrieved from https://onlinelibrary.wiley.com/doi/abs/10.2193/0022-541X(2004)068[0533:HSBMDF]2.0.CO;2

Pigeon, K. E., Côté, S. D., & Stenhouse, G. B. (2016). Assessing den selection and den characteristics of grizzly bears. *Journal of Wildlife Management*, *80*(5), 884–893. https://doi.org/10.1002/jwmg.1069

Pigeon, K. E., Stenhouse, G., & Côté, S. D. (2016). Drivers of hibernation: linking food and weather to denning behaviour of grizzly bears. *Behavioral Ecology and Sociobiology*, *70*(10), 1745–1754. https://doi.org/10.1007/s00265-016-2180-5

Pojar, J., Klinka, K., & Meidinger, D. V. (1987). Biogeoclimatic ecosystem classification in British Columbia. *Forest Ecology and Management*, *22*(1–2), 119–154. https://doi.org/10.1016/0378-1127(87)90100-9

Poole, K. G., & Wright, K. (2010). Mule deer migration and seasonal ranges within the St ' at ' imc Nation Territory , southwestern British Columbia, (October).

Powers, M. W. (2011). Archived at the Flinders Academic Commons : This is the author ' s post-print version of this article . The published article is available at : © 2011 Bioinfo Publications Please note that any alterations made during the publishing process may not appear, *2*(1), 37–63.

Procter, C. (2013). HABITAT USE & MIGRATIONS OF MULE DEER BUCKS IN THE FRASER RIVER BASIN OF THE SOUTHERN INTERIOR OF BRITISH COLUMBIA.

Procter, C., Bio, R. P., & Iredale, F. (2013). *Mule Deer Buck Migrations and Habitat Use in the Bridge River, British Columbia: Preliminary Results*. Retrieved from http://a100.gov.bc.ca/appsdata/acat/documents/r37960/12.W.BRG.03_finalreport2012_13_mule_1378215957484_4304516039bb99bff7c79c07312a33c1dfa0e26f480ada9ac9cf542ce2f02e69.pdf

Prokopenko, C. M., Boyce, M. S., & Avgar, T. (2017). Characterizing wildlife behavioural responses to roads using integrated step selection analysis. *Journal of Applied Ecology*, *54*(2), 470–479. https://doi.org/10.1111/1365-2664.12768

Puckett, C., Delaney, J., & Antonios, P. (2006). Satellites Help Scientists Track Migratory Birds: GPS the Latest Tool in Fight Against Avian Influenza. Retrieved May 16, 2018, from https://soundwaves.er.usgs.gov/2006/11/SW200611-100.pdf

Qin, D. H., Liu, S. Y., & Li, P. J. (2006). Snow cover distribution, variability, and response to climate change in western China. *Journal of Climate*, *19*(9), 1820–1833. https://doi.org/10.1175/JCLI3694.1

Racoviteanu, A. E., Paul, F., Raup, B., Khalsa, S. J. S., & Armstrong, R. (2009). Challenges and recommendations in mapping of glacier parameters from space: Results of the 2008 global land ice measurements from space (GLIMS) workshop, Boulder, Colorado, USA. In *Annals of Glaciology* (Vol. 50, pp. 53–69). Cambridge University Press. https://doi.org/10.3189/172756410790595804

Raleigh, M. S., Rittger, K., Moore, C. E., Henn, B., Lutz, J. A., & Lundquist, J. D. (2013).

Ground-based testing of MODIS fractional snow cover in subalpine meadows and forests of the Sierra Nevada. *Remote Sensing of Environment*, *128*, 44–57. https://doi.org/10.1016/j.rse.2012.09.016

Rickbeil, G. J. M., Coops, N. C., & Adamczewski, J. (2015). The grazing impacts of four barren ground caribou herds (Rangifer tarandus groenlandicus) on their summer ranges: An application of archived remotely sensed vegetation productivity data. *Remote Sensing of Environment*, *164*, 314–323. https://doi.org/10.1016/j.rse.2015.04.006

Riggs, G. A., & Hall, D. K. (2015). MODIS Snow Products Collection 6 User Guide. Retrieved from https://nsidc.org/sites/nsidc.org/files/files/MODIS-snow-user-guide-C6.pdf

Rittger, K., Painter, T. H., & Dozier, J. (2013). Assessment of methods for mapping snow cover from MODIS. *Advances in Water Resources*, *51*, 367–380. https://doi.org/10.1016/j.advwatres.2012.03.002

Robinson, B. G., & Merrill, E. H. (2012). The influence of snow on the functional response of grazing ungulates. *Oikos*, *121*(1), 28–34. https://doi.org/10.1111/j.1600-0706.2011.19408.x

Rockwell, R. F., & Gormezano, L. J. (2009). The early bear gets the goose: Climate change, polar bears and lesser snow geese in western Hudson Bay. *Polar Biology*, *32*(4), 539–547. https://doi.org/10.1007/s00300-008-0548-3

Russell, R. E., Gude, J. A., Anderson, N. J., & Ramsey, J. M. (2015). Identifying priority chronic wasting disease surveillance areas for mule deer in Montana. *Journal of Wildlife Management*, *79*(6), 989–997. https://doi.org/10.1002/jwmg.914

Ryan, W. A., Doesken, N. J., & Fassnacht, S. R. (2008). Evaluation of ultrasonic snow depth sensors for U.S. snow measurements. *Journal of Atmospheric and Oceanic Technology*, *25*(5), 667–684. https://doi.org/10.1175/2007JTECHA947.1

Sachs, J. D., & Reid, W. V. (2006, May 19). Investments toward sustainable development. *Science*. American Association for the Advancement of Science. https://doi.org/10.1126/science.1124822

Salazar, M. F. M., Waldner, C., Stookey, J., & Bollinger, T. K. (2016). Infectious disease and grouping patterns in mule deer. *PLoS ONE*, *11*(3), e0150830. https://doi.org/10.1371/journal.pone.0150830

Salomonson, V. V., & Appel, I. (2004). Estimating fractional snow cover from MODIS using the normalized difference snow index. *Remote Sensing of Environment*, *89*(3), 351–360. https://doi.org/10.1016/j.rse.2003.10.016

Salomonson, V. V., & Appel, I. (2006). Development of the aqua MODIS NDSI fractional snow cover algorithm and validation results. *IEEE Transactions on Geoscience and Remote Sensing*, *44*(7), 1747–1756. https://doi.org/10.1109/TGRS.2006.876029

Sawyer, H., Nielson, R. M., Lindzey, F., & Mcdonald, L. L. (2006). Winter Habitat Selection of Mule Deer Before and During Development of a Natural Gas Field Winter Habitat Selection of Mule Deer Before and During Development of a Natural Gas Field. *Http://Dx.Doi.Org/10.2193/0022-541X(2006)70[396:WHSOMD]2.0.CO;2*, *70*(2), 396–403. https://doi.org/10.2193/0022-541X(2006)70

Schick, R. S., Roberts, J. J., Eckert, S. A., Halpin, P. N., Bailey, H., Chai, F., … Clark, J. S. (2013). Pelagic movements of pacific leatherback turtles (dermochelys coriacea) highlight the role of prey and ocean currents. *Movement Ecology*, *1*(1), 11.

https://doi.org/10.1186/2051-3933-1-11

Schwartz, M. K., Copeland, J. P., Anderson, N. J., Squires, J. R., Inman, R. M., McKelvey, K. S., … Cushman, S. A. (2009). Wolverine gene flow across a narrow climatic niche. *Ecology*, *90*(11), 3222–3232. https://doi.org/10.1890/08-1287.1

Selkowitz, D., & Forster, R. (2015). An Automated Approach for Mapping Persistent Ice and Snow Cover over High Latitude Regions. *Remote Sensing*, *8*(1), 16. https://doi.org/10.3390/rs8010016

Senger, S., Hamiton, T., & McLellan, M. (2008). Ecological relationships between grizzly bears and forest management in the coast-interior transition of British Columbia, 2007 Year End Report. *Report Prepared for The Lillooet TSA Association*, 12 pp. Retrieved from http://a100.gov.bc.ca/appsdata/acat/documents/r37442/Ecological_Grizzly_Transition_2007_1375973096902_b12b5213c3ca94a0bfec74fcd625fcda9d696dcda6ea4b18bdcda43760269e85.pdf

Shannon, C. E. (1948). A Mathematical Theory of Communication. *Bell System Technical Journal*, *27*(3), 379–423. https://doi.org/10.1002/j.1538-7305.1948.tb01338.x

Shimamura, Y., Izumi, T., & Matsuyama, H. (2006). Evaluation of a useful method to identify snow-covered areas under vegetation - Comparisons among a newly proposed snow index, normalized difference snow index, and visible reflectance. *International Journal of Remote Sensing*, *27*(21), 4867–4884. https://doi.org/10.1080/01431160600639693

Shuai, Y., Masek, J. G., Gao, F., & Schaaf, C. B. (2011). An algorithm for the retrieval of 30-m snow-free albedo from Landsat surface reflectance and MODIS BRDF. *Remote Sensing of Environment*, *115*(9), 2204–2216. https://doi.org/10.1016/j.rse.2011.04.019

Silverio, W., & Jacquet, J.-M. (2009). Prototype land-cover mapping of the Huascara´n Biosphere Reserve (Peru) using a digital elevation model, and the NDSI and NDVI indices. *Journal of Applied Remote Sensing*, *3*(1), 033516. https://doi.org/10.1117/1.3106599

Singh, K. K., Datt, P., Sharma, V., Ganju, A., Mishra, V. D., Parashar, A., & Chauhan, R. (2011). Snow depth and snow layer interface estimation using Ground Penetrating Radar. *Current Science*, *100*, 1532–1539. https://doi.org/10.2307/24076673

Sirén, A. P. K., Somos-valenzuela, M., Callahan, C., & Kilborn, J. R. (2018). Looking beyond wildlife : Using remote cameras to evaluate accuracy of gridded snow data. *Remote Sensing in Ecology and Conservation*, 1–42. https://doi.org/10.1002/rse2.85

Sproles, E. A., Roth, T. R., & Nolin, A. W. (2017). Future snow? A spatial-probabilistic assessment of the extraordinarily low snowpacks of 2014 and 2015 in the Oregon Cascades. *Cryosphere*, *11*(1), 331–341. https://doi.org/10.5194/tc-11-331-2017

Stahl, K., Moore, R. D., Shea, J. M., Hutchinson, D., & Cannon, A. J. (2008). Coupled modelling of glacier and streamflow response to future climate scenarios. *Water Resources Research*, *44*(2). https://doi.org/10.1029/2007WR005956

Stroeve, J. C., Box, J. E., & Haran, T. (2006). Evaluation of the MODIS (MOD10A1) daily snow albedo product over the Greenland ice sheet. *Remote Sensing of Environment*, *105*(2), 155–171. https://doi.org/10.1016/j.rse.2006.06.009

Therneau, T. M., & Lumley, T. (2018). Package “survival”. Survival Analysis. R package version 2.42-3. Comprehensive R Archive Network (CRAN). Retrieved from https://cran.r-project.org/web/packages/survival/index.html

Thurfjell, H., Ciuti, S., & Boyce, M. S. (2014, February 7). Applications of step-selection functions in ecology and conservation. *Movement Ecology*. BioMed Central. https://doi.org/10.1186/2051-3933-2-4

Trifa, V., Girod, L., & Collier, T. (2007). Automated wildlife monitoring using self-configuring sensor networks deployed in natural habitats. *Proc. of the 12th …*, 1–4. Retrieved from https://escholarship.org/uc/item/2059b99k

van Beest, F. M., Van Moorter, B., & Milner, J. M. (2012). Temperature-mediated habitat use and selection by a heat-sensitive northern ungulate. *Animal Behaviour*, *84*(3), 723–735. https://doi.org/10.1016/j.anbehav.2012.06.032

Varhola, A., Coops, N. C., Weiler, M., & Moore, R. D. (2010). Forest canopy effects on snow accumulation and ablation: An integrative review of empirical results. *Journal of Hydrology*, *392*(3–4), 219–233. https://doi.org/10.1016/J.JHYDROL.2010.08.009

Varhola, A., Wawerla, J., Weiler, M., Coops, N. C., Bewley, D., & Alila, Y. (2010). A new low-cost, stand-alone sensor system for snow monitoring. *Journal of Atmospheric and Oceanic Technology*, *27*(12), 1973–1978. https://doi.org/10.1175/2010JTECHA1508.1

Viana, D. S., Granados, J. E., Fandos, P., Pérez, J. M., Cano-Manuel, F. J., Burón, D., … Soriguer, R. C. (2018). Linking seasonal home range size with habitat selection and movement in a mountain ungulate. *Movement Ecology*, *6*(1), 1. https://doi.org/10.1186/s40462-017-0119-8

Wagenmakers, E. J., & Farrell, S. (2004). AIC model selection using Akaike weights. *Psychonomic Bulletin and Review*. https://doi.org/10.3758/BF03206482

Walker, J. J., De Beurs, K. M., Wynne, R. H., & Gao, F. (2012). Evaluation of Landsat and MODIS data fusion products for analysis of dryland forest phenology. *Remote Sensing of Environment*, *117*, 381–393. https://doi.org/10.1016/j.rse.2011.10.014

Walters, R. D., Watson, K. A., Marshall, H. P., McNamara, J. P., & Flores, A. N. (2014). A physiographic approach to downscaling fractional snow cover data in mountainous regions. *Remote Sensing of Environment*, *152*, 413–425. https://doi.org/10.1016/j.rse.2014.07.001

Wegmann, M., Orsolini, Y., Vázquez, M., Gimeno, L., Nieto, R., Bulygina, O., … Brönnimann, S. (2015). Arctic moisture source for Eurasian snow cover variations in autumn. *Environmental Research Letters*, *10*(5), 054015. https://doi.org/10.1088/1748-9326/10/5/054015

Whetton, P. H., Haylock, M. R., & Galloway, R. (1996). Climate change and snow-cover duration in the Australian Alps. *Climatic Change*, *32*(4), 447–479. https://doi.org/10.1007/BF00140356

Wielgus, R. B. (2017). Resource competition and apparent competition in declining mule deer (*Odocoileus hemionus*). *Canadian Journal of Zoology*, *95*(7), 499–504. https://doi.org/10.1139/cjz-2016-0109

Winkler, D. W., Jørgensen, C., Both, C., Houston, A. I., McNamara, J. M., Levey, D. J., … Piersma, T. (2014, May 29). Cues, strategies, and outcomes: How migrating vertebrates track environmental change. *Movement Ecology*. BioMed Central. https://doi.org/10.1186/2051-3933-2-10

Winstral, A., & Marks, D. (2002). Simulating wind fields and snow redistribution using terrain-based parameters to model snow accumulation and melt over a semi-arid mountain catchment. *Hydrological Processes*, *16*(18), 3585–3603. https://doi.org/10.1002/hyp.1238

Wood, E. F., Roundy, J. K., Troy, T. J., van Beek, L. P. H., Bierkens, M. F. P., Blyth, E., … Whitehead, P. (2011). Hyperresolution global land surface modeling: Meeting a grand challenge for monitoring Earth's terrestrial water. *Water Resources Research*, *47*(5). https://doi.org/10.1029/2010WR010090

Wood, G. A. (1949). The Bridge River region a geographical study. https://doi.org/10.14288/1.0106711

Woods, L. W., Schumaker, B. A., Pesavento, P. A., Crossley, B. M., & Swift, P. K. (2018). Adenoviral hemorrhagic disease in California mule deer, 1990–2014. *Journal of Veterinary Diagnostic Investigation*, *30*(4), 530–537. https://doi.org/10.1177/1040638718766036

Wu, Mingquan, Niu, Zheng, Wang, Changyao, Wu, Chaoyang, Li, W. (2012). Use of MODIS and Landsat time series data to generate high-resolution temporal synthetic Landsat data using a spatial and temporal reflectance fusion model. *Journal of Applied Remote Sensing*, *6*(1), 063507. https://doi.org/10.1117/1.JRS.6.063507

Wu, X., Dong, S., Liu, S., Su, X., Han, Y., Shi, J., … Xu, D. (2017). Predicting the shift of threatened ungulates' habitats with climate change in Altun Mountain National Nature Reserve of the Northwestern Qinghai-Tibetan Plateau. *Climatic Change*, *142*(3–4), 331–344. https://doi.org/10.1007/s10584-017-1939-7

Wulder, M. A., Masek, J. G., Cohen, W. B., Loveland, T. R., & Woodcock, C. E. (2012). Opening the archive: How free data has enabled the science and monitoring promise of Landsat. *Remote Sensing of Environment*, *122*, 2–10. https://doi.org/10.1016/j.rse.2012.01.010

Xiao, X., Shen, Z., & Qin, X. (2001). Assessing the potential of vegetation sensor data for mapping snow and ice cover: A normalized difference snow and ice index. *International Journal of Remote Sensing*, *22*(13), 2479–2487. https://doi.org/10.1080/01431160119766

Yin, D., Cao, X., Chen, X., Shao, Y., & Chen, J. (2013). Comparison of automatic thresholding methods for snow-cover mapping using Landsat TM imagery. *International Journal of Remote Sensing*, *34*(19), 6529–6538. https://doi.org/10.1080/01431161.2013.803631

Zeman, J. (n.d.). BC Interior Mule Deer Project. Retrieved March 7, 2019, from http://bcwf.net/index.php/southern-bc-mule-deer-project

Zschille, J., Stier, N., & Roth, M. (2008). Radio tagging American mink (Mustela vison)-experience with collar and intraperitoneal-implanted transmitters. *European Journal of Wildlife Research*, *54*(2), 263–268. https://doi.org/10.1007/s10344-007-0139-6

Appendices

Appendix A

Appendix A: All candidate models used in model selection. "Core" includes all of the non-snow related habitat covariates, with the exception of elevation (DEM) as DEM was found to be collinear with most snow covariates. * Indicates that a covariate's interaction terms were included in the candidate model. Note: "Ave" before variable name indicates time-averaged covariate; otherwise, it is the yearly value. ACC = accumulation date, MELT = ablation date, SUM = total snow covered days, SW = snow rank, and VAR = snow pack variability. Bold values indicate top ranked models with an AIC weight greater than 0.10.

Model Group	Variables	Average AIC Weight	Tally
	Core + AveACC	0.0088	0
Spring/fall	Core + AveACC + AveSW	0.0157	1
	Core + AveACC + AveSW*	0.0419	3
	Core + AveACC*	0.0683	7
	Core + AveMELT	0.0079	1
	Core + AveMELT + AveSW	0.0068	0
	Core + AveMELT + AveSW*	0.0077	0
	Core + AveMELT*	0.0377	4
	Core + AveSUM	0.0063	0
	Core + AveSUM + AveSW	0.0205	3
	Core + AveSUM + AveSW*	0.0132	1
	Core + AveSUM*	0.0539	3
	Core + AveSW + AveACC*	0.0935	7
	Core + AveSW + AveMELT*	0.0706	5
	Core + AveSW + AveSUM*	**0.1031**	**8**
	Core + DEM	0.0228	2
	Core + DEM + AveSW	0.0143	0
	Core + DEM + AveSW + VAR*	**0.1584**	**12**
	Core + DEM + AveSW*	0.0329	2
	Core + DEM + VAR	0.0234	1
	Core + DEM + VAR + AveSW*	0.0457	3
	Core + DEM + VAR + AveSW	0.0094	0
	Core + DEM + VAR*	**0.1617**	**14**

			TOTAL = 77
Winter	Core + ACC + AveMELT	0.0055	0
	Core + ACC + AveMELT + AveSW	0.0028	0
	Core + ACC + AveMELT + AveSW*	0.0349	1
	Core + ACC + AveMELT*	0.0482	2
	Core + ACC + AveVAR + AveSW	0.0044	0
	Core + ACC + AveVAR + AveSW*	0.0771	4
	Core + AveMELT	0.0083	0
	Core + AveMELT + ACC*	0.0644	3
	Core + AveMELT*	0.0253	1
	Core + AveSUM	0.0097	0
	Core + AveSUM + AveSW	0.0041	0
	Core + AveSUM + AveSW*	0.0205	1
	Core + AveSUM*	0.0254	1
	Core + AveSW + ACC + AveMELT*	**0.1711**	**7**
	Core + AveSW + ACC + AveVAR*	0.0804	3
	Core + AveSW + AveMELT + ACC*	0.0871	3
	Core + AveSW + AveSUM*	0.0524	2
	Core + AveSW + AveVAR + ACC*	0.0495	3
	Core + AveSW + AveVAR*	0.0292	0
	Core + AveVAR	0.0129	1
	Core + AveVAR + AveSW	0.0075	0
	Core + AveVAR + AveSW*	0.0312	1
	Core + AveVAR*	0.0340	3
	Core + DEM	0.0110	1
	Core + DEM + ACC	0.0126	0
	Core + DEM + AveSW	0.0066	0
	Core + DEM + AveSW*	0.0300	1
	Core + DEM +ACC*	0.0870	4
			TOTAL = 42

Appendix B

Appendix B: AIC weights from all models shown in Appendix A that were averaged based on the presence of each covariate listed below. "Core" includes all of the non-snow related habitat covariates, with the exception of elevation (DEM) as DEM was found to be collinear with most snow covariates. Evidence Ratio calculated by dividing each snow covariate models' average AIC weight with the average AIC weight of Core + DEM models' average. This produces a numerical value for how many times more likely a given model is the best one over the other (Wagenmakers & Farrell, 2004). Note: "Ave" before variable name indicates time-averaged covariate; otherwise, it is the yearly value. ACC = accumulation date, MELT = ablation date, SUM = total snow covered days, SW = snow rank, and VAR = snow pack variability. Bold values indicate top ranked covariates, based on their averaged AIC weight.

Model Group	Variables	Average AIC Weight	Evidence Ratio compared to Core + DEM models' average
Spring/fall	AveACC	0.0456	0.7782
	AveMELT	0.0261	0.4454
	AveSUM	0.0394	0.6724
	VAR	**0.0863**	**1.47**
	AveSW	0.0453	0.7730
	Core + DEM	0.0586	n/a
Winter	**ACC**	**0.0558**	**1.8980**
	AveMELT	0.0497	1.6905
	AveSUM	0.0224	0.7619
	AveVAR	0.0325	1.1054
	AveMELT	0.0431	1.4660
	Core + DEM	0.0294	n/a

Appendix C

Initial data exploration of used deer locations showed greater variability of NTV and bare ground land occurrence as a percentage during the spring/fall periods. During winter, deer are more restrictive of their use of the same covariates, particularly with bare ground, which consists of no more than 20 % of the proportional cover at any time on average:

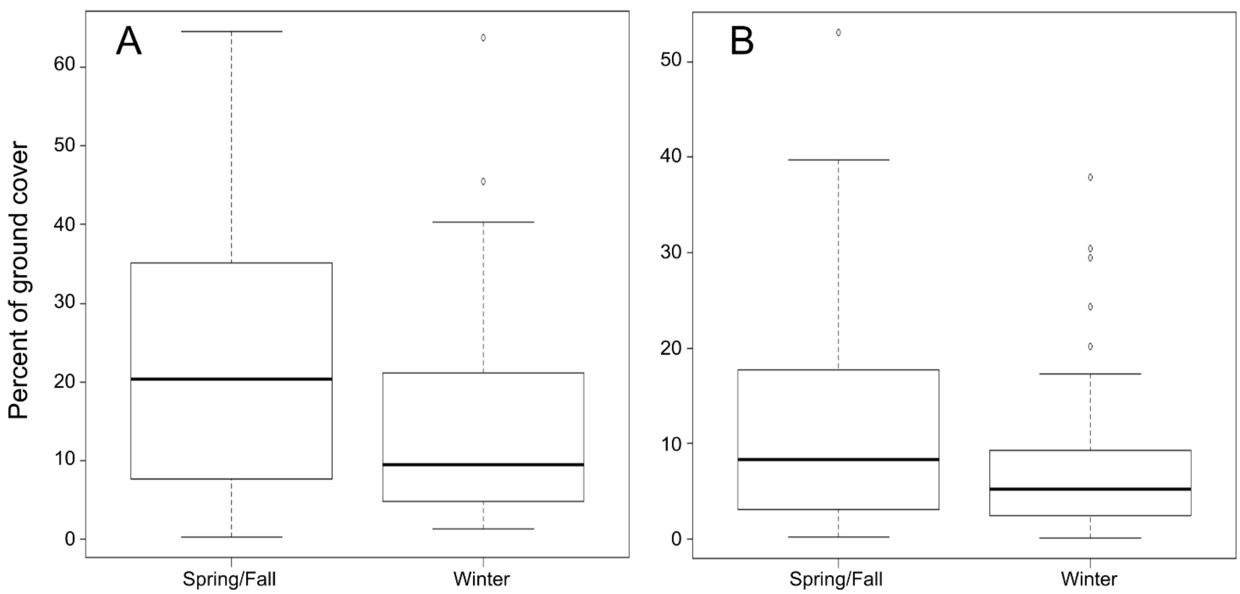

Appendix C: Variability in the percent of ground cover for (A) non-treed vegetation (NTV) and (B) bare ground, according to used mule deer GPS locations. Spring/Fall (n) = 77, Winter (n) = 42.